# DEFORMATION ANALYSIS OF FOAM-ENCAPSULATED APPLES UNDER IMPACT LOADING

Dissertation for the Degree of Ph. D.
MICHIGAN STATE UNIVERSITY
YOAV SARIG
1976

This is to certify that the

thesis entitled

DEFORMATION ANALYSIS OF FOAM-ENCAPSULATED APPLES
UNDER IMPACT LOADING

presented by

YOAV SARIG

has been accepted towards fulfillment
of the requirements for

Ph.D. degree in Agricultural Engineering

Larry J. Segerlind
Major professor

Date 30 January 1976

O-7639

ABSTRACT

DEFORMATION ANALYSIS OF FOAM-ENCAPSULATED APPLES UNDER IMPACT LOADING

By

Yoav Sarig

The objective of this work was to ascertain the feasibility of a method to reduce impact damage induced in apples during mechanical harvesting. The method investigated consisted of spraying the tree with a Urea-Formaldehyde foam prior to harvesting thereby encapsulating the apple and branches in a layer of foam which absorbs the impact energy.

The apparent elastic modulus and Poisson's ratio of the foam were obtained through experimentation and were subsequently incorporated in a numerical evaluation of the apple's deformation based on a theoretical analysis.

Two analytical methods were presented and compared for predicting the apple deformation under given boundary conditions. The first utilized the axi-symmetric Boussinesq's method whereby the foam-encapsulated apple was modeled as an elastic layer (the foam), lying on an elastic subspace (the limb). In the second approach the domain was modeled as an elastic sphere embedded in an elastic shell subjected to a flat plate loading and solved using the finite element method. The objective in both analyses was to obtain an approximation of the deformation that would occur if the real foam-apple domain was indented by a limb. Good agreement was obtained between the two solutions, and the optimal parameters of the encapsulation for an accepted level of apple deformation were obtained.

Foam density of 0.0112 gr/cm$^3$ and thickness of 15 mm is recommended. Although a lower value for the foam thickness may have provided the needed protection, it has generally been unattainable in field experiments.

Experimental and field studies showed that when fruit was harvested that had been covered with the foam, no indentation occurred and the fruit was rated at prime quality. However, application difficulties in the field resulted in only part of the fruit being covered (50% on the average). It is conceivable, however, that a perfection of the method of application would improve the percent.

Approved Larry J. Segerlind
Major Professor

Approved D. R. Heldman
Department Chairman

# DEFORMATION ANALYSIS OF FOAM-ENCAPSULATED APPLES UNDER IMPACT LOADING

By

Yoav Sarig

A DISSERTATION

Submitted to
Michigan State University
in partial fulfillment of the requirements
for the degree of

DOCTOR OF PHILOSOPHY

Department of Agricultural Engineering

1976

## ACKNOWLEDGMENTS

The author wishes to express his thanks to Dr. L. J. Segerlind, Associate Professor, Department of Agricultural Engineering, for his guidance and advice throughout this research and for the friendly atmosphere that typified his direction. Also the author would like to recognize the entiree committee members, Dr. R. L. Little, Professor and Chairman, Department of Mechanical Engineering, Dr. D. R. Heldman, Professor and Chairman, Department of Agricultural Engineering, Dr. D. H. Dewey, Professor, Department of Horticulture and Dr. B. A. Stout, Professor, Department of Agricultural Engineering. The author is grateful to all the committee members not only for their contributions to this thesis but also for the more specific benefits acquired from their classes, their published work, and the pleasure of their acquaintance.

The author would like to thank J. H. Levin, ARS, USDA Research Leader, a colleague and true friend, for his direction, encouragement and support throughout this research. In addition, the author wishes to thank the entire ARS, USDA research group for their hospitality and assistance. In particular he would like to thank R. J. Wolthuis, Mechanical Engineering Technician, for his assistance in equipment construction and field experiments, and to Mrs. Judy Powell for typing not only the rough drafts of this manuscript but the numerous typing jobs associated with his graduate work.

The author also acknowledges thc assistance from Mr. Kramer of Rapperswill Co., N.Y., and Dr. Straus of Rapco Chemical Co., South Carolina, who expressed their interest in this study and provided the hardware for the experiments. During his Ph.D. studies the author was the recipient of a fellowship from the 'Baron De Hirsh Fund,' to whom he would like to express his thanks at this time. Partial support was also provided through scholarships from the Hebrew Technical Institute and the 'Loeb Foundation' to whom the author is grateful.

The author also acknowledges the Assistantship provided by the Department of Agricultural Engineering. He is also indebted to Mr. D. Nahir, Director, The Agricultural Engineering Institute, Bet-Dagan, Israel, for his constant help and encouragement that made this work possible.

Finally, to his wife Bina, son Ido and daughter Noa, the author expresses his deep gratitude for their patience, sacrifice and encouragement.

The author dedicates this work to his parents who instilled in him the desire to study.

TABLE OF CONTENTS

Page

# LIST OF FIGURES

| Figure | | Page |
|---|---|---|

LIST OF TABLES

Table Page

LIST OF APPENDICES

## LIST OF SYMBOLS

| | |
|---|---|
| { } | - A column vector |
| [ ] | - A square matrix |
| $[\ ]^T$ | - Transpose of a matrix |
| A | - An arbitrary function or constant, also an area |
| a | - Radius of a flat circular punch |
| B | - Strain-displacement matrix, $\{\varepsilon\} = [B]\{U\}$ |
| | - Also an arbitrary function or constant |
| b | - A constant, also body force |
| C | - Arbitrary function or constant, also temperature centigrade |
| $C_{ijkl}$ | - A constant relating the stress and strain in the generalized Hooke's law |
| cm | - Centimeter(s) |
| D | - Stress-strain matrix, $\{\sigma\} = [D]\{\varepsilon\}$. Also an arbitrary function or constant, also diameter. |
| E | - The Lagrangian strain tensor, also elastic modulus of an isotropic material, also an arbitrary function or constant |
| $E_f$ | - Apparent elastic modulus |
| e | - Base of the Natural Logarithm |
| F | - Harmonic function, also a compressive force or body force |
| f | - Function |
| G | - Harmonic function, also modulus of rigidity, $G = \frac{E}{2(1+\mu)}$ |
| gr | - Gram(s) |
| H | - Ratio of foam thickness to punch radius (h/a) |
| $H_n$ | - Hankel transform of order n |

$h$ - Foam layer thickness

$i$ - Index

$\hat{i}_r$, $\hat{i}_e$, $\hat{i}_z$ - Unit vectors in polar cylindrical coordinates

$J_n$ - Bessel function of the first kind of order n

$j$ - Index

$[K]$ - Stiffness matrix

$K$ - Kernel of an equation, also a constant

$K_1$, $K_2$, $K_3$, $K_4$ - Constants

kg - Kilogram(s)

$L$ - Length

l - Liter(s)

m - Meter(s)

mm - Millimeter(s)

min - Minute

$N$ - Shape function matrix, also an arbitrary function, also Newtons

$n$ - Index

$P$ - Compressive Force

$P^*$ - A function of the indenting force, $P^* = \frac{P}{\mu_1 \delta}$

$q$ - Load pressure

$R$ - Radius

$r$ - Radial coordinate, also radius

$S$ - Surface area

$t$ - A dummy variable

$U$ - Displacement, also strain energy

U-F - Urea-Formaldehyde

$V$ - Volume

$x$ - Cartesian coordinate

$\overline{x}$ - Average value

$W$ - Total external loads on a structure

$y$ - Cartesian coordinate

$z$ - Vertical coordinate

$\delta$ - Indentation induced by a punch

| | |
|---|---|
| $\delta_{ij}$ | - Kronecker delta, $\begin{cases} 1 & \text{if } i=j \\ 0 & \text{if } i \neq j \end{cases}$ |
| $\varepsilon$ | - Compressive strain |
| $\varepsilon_{ij}$ | - Strain tensor |
| $\theta$ | - Cylindrical coordinate |
| $\lambda$ | - Lamé constant, $\lambda = \frac{E\nu}{(1+\nu)(1-2\nu)}$ |
| $\mu$ | - Lamé constant, $\mu = \frac{E}{2(1+\nu)}$, modulus of rigidity |
| $\nu$ | - Poisson's ratio |
| $\Pi$ | - Total strain energy |
| $\xi$ | - Hankel transformed variable |
| $\rho$ | - Mass density |
| $\sigma$ | - Stress, also standard deviation |
| $\sigma_{ij}$ | - Stress tensor |
| $\Sigma$ | - The sum of |
| $\phi$ | - Cylindrical coordinate, also arbitrary function |
| $\chi$ | - Arbitrary function, also a functional that denotes the total potential energy |
| $\Psi$ | - Arbitrary function |
| $\Psi(\varepsilon)$ | - A dimensionless function of the compressive strain |
| $\overline{\nabla}$ | - Vector operator (del operator), $\overline{\nabla} = \hat{1}_{(k)}\frac{\partial}{\partial x_k}$ |
| $\overleftarrow{\nabla}$ | - Post-gradient of a vector, $\overline{U}\overleftarrow{\nabla} = \hat{1}_{(i)}\frac{\partial U_i}{\partial x_j}\hat{1}_{(j)}$ |
| $\overrightarrow{\nabla}$ | - Pre-gradient of a vector, $\overline{\nabla}\overrightarrow{U} = \hat{1}_{(i)}\frac{\partial U_j}{\partial x_i}\hat{1}_{(j)}$ |
| — | - Vector quantity |
| ▬ | - Second-order tensor quantity |
| $\partial$ | - Partial derivative |
| · (dot) | - Indicates differentiation with respect to time |
| > | - Greater than |

# 1. INTRODUCTION

## 1.1 Historical Background and Problem Assessment

Lack of satisfactory seasonal labor availability for fruit picking characterizes the conditions prevailing in most fruit-growing regions. Not only is the number of farm workers decreasing, but the quality of their work is becoming less adequate each year (Levin 1970). This makes it mandatory to mechanize the harvesting which will reduce the dependency on manpower in the future.

Attempts to mechanize the harvesting of fruit started with the development of man positioners that replaced the ladder. Picking was still done by hand with little savings in manpower. Where labor is scarce this approach is not feasible, especially for large apple orchards. This led to the advent of mass removal systems utilizing the shake and catch method (Levin 1970, Rehkugler 1968, Tennes and Levin 1972) which have the capacity for mass harvesting and hence a great savings in manual labor. The major factor associated with mechanical harvesting, apart from the obvious economic consideration, is the increased damage induced in the fruit. Mechanical harvesting systems have been successfully applied to prunes, cherries and cling peaches destined for processing because processed fruit can tolerate more bruising than fresh market fruits. In addition the interval between harvest and consumption, which affects the quality, is shorter for fruit destined for processing. Regardless of the end use, excessive damage reduces the quality of the product, slows packing house operations and increases processing costs.

The quality problem is accentuated in apples destined for fresh market because many apples are placed in expensive long-term controlled atmosphere storage in an effort to preserve a premium product and to provide a year-around supply. Many investigations (Burt 1959, Wennergren and Lee 1961, Gillesphe 1950, Tennes *et al.* 1974) have shown that a bruised apple has a shorter storage potential than a bruise-free apple.

The problem of apple bruising associated with mechanical harvesting could basically be approached in two ways. One approach suggests that mechanical harvesting will always be associated with a significant level of bruising and efforts should be directed at developing a method of bruise detection followed by removal of damaged fruit to be channeled to processing utilization. This approach, apart from not being presently available commercially (Rehkugler and Throop 1973), can be considered only as a supplementary method after some attempts have been made to reduce the overall damage.

A second approach is to attempt to minimize the fruit damage. Fruit bruising in the process of mechanical harvesting is a result of three major factors (Fig. 1): pre-detachment damage induced to the fruit as a result of the fruit's impact with limbs while falling through the tree, and bruising due to impact with the catching surface (Fridley *et al.* 1964, Schomer 1957, Levin 1970, Tennes and Levin 1972).

Predetachment damage can be attenuated by using abscission chemicals which loosen the bond between the fruit and the stem, thus reducing the probability of the fruit impinging against an obstacle, or by optimal use of stroke-frequency relationship in the shaking mechanism. Proper padding of the catching surface can eliminate most of the damage resulting from impact with the catching frame. The primary source of fruit damage occurs during the impact with limbs within the tree and as yet this problem has not been successfully solved. (Although some fruit damage reduction was achieved with various experimental systems, the total damage was of sufficient magnitude to discourage further development for commercial application.)

Tree training can minimize the problem (Levin 1970, Tennes and Levin 1972) but may result in some loss of yield and methods have not been developed that eliminate the damage.

The various research studies attempting to solve the bruising problem have been aimed at reducing the impact energy imparted to the fruit. This could be accomplished

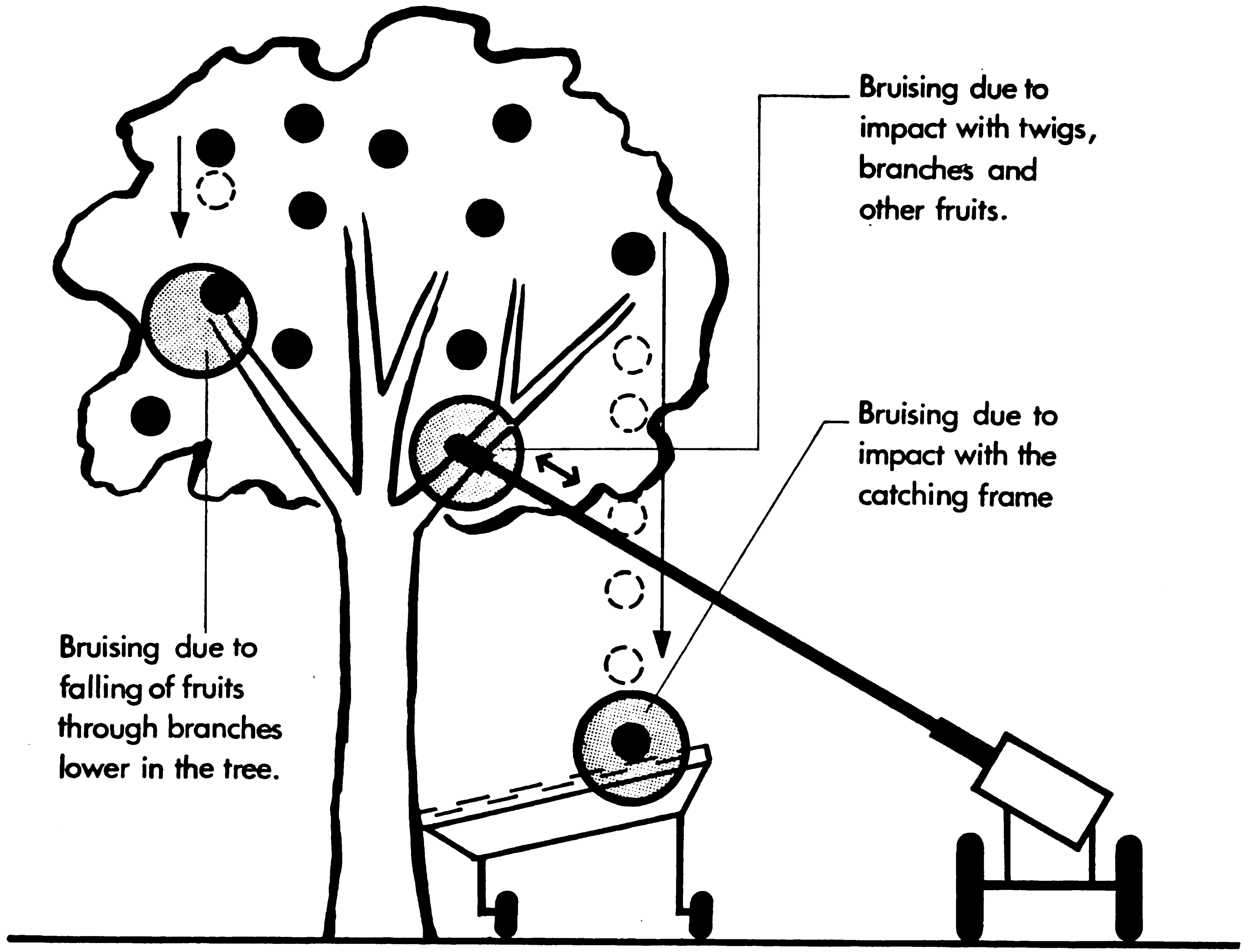


Fig. 1.1 Potential sources of damage to fruit harvested mechanically.

either by reducing the fruit's energy at impact, or absorbing the energy of impact through cushioning. The first approach was taken by many investigators such as Millier *et al.* (1973), at Cornell University, who developed an insertable multi-level catching system which "intercepts and removes fruit from the tree at any level without requiring specific tree modification." The in-tree catching surface consisted of a set of inflatable tines which, when inflated, provided a seal. The conclusion of this experiment was that results were encouraging but inadequate. Another approach was developed by Schertz and Brown (1966) who developed an intermediate-level collection device made of a rigid cylindrical trough to be used in citrus harvesting. The drawbacks of this device were difficulty in penetrating the tree and foliage blockage.

Rehkugler and Markwardt (1971) proposed the use of horizontal padded tines placed in the tree to decelerate fruit and minimize high-velocity impacts of the fruit on the limbs. A similar approach was taken by Fridley *et al.* (1973) who tested a collector-decelerator which combined the decelerating arms with a device for directing the fruit out of the tree. A unique implementation of the impact energy attenuation approach is the space-fill concept. This procedure, conceived and patented by Joe Perrelli of California (1970) and tested experimentally by Fridley *et al.* (1973), utilized an enclosure, supported around the fruit-bearing portion of a tree. The enclosure is filled with lightweight plastic balls to completely enclose the fruit and branches. The fruit is then separated from the branches by shaking, and progressively moved downwardly through the mass of balls to the bottom of the enclosure for collection and transfer to a desired point. A similar system is described in a patent by Bernshausen (1970). The concept was tested in California on apples, pears and peaches and the quality compared with hand-picked samples. The results indicated that the space-fill approach reduced both the amount and severity of bruising. Poor fruit removal was observed, however, because of the damping of the shaking action. The same system was subsequently studied in Washington by Berlage and Langmo (1974) with the conclusion that the slight reduction in fruit bruising was not sufficient to justify the reduction in the system capacity. Independently, this concept was conceived and tested on apples in Denmark and Israel with variation of the medium used (Tene *et al.* 1973). Evaluation of the various methods tested pertaining to the feasibility of the concept indicate that although a significant reduction of bruise damage was achieved, it is not considered sufficient to warrant the increased harvesting time and the expense of the machine.

These rather disappointing results utilizing the energy attenuation approach for solving the bruising problem leave the option of trying to absorb rather than reduce the impact energy. Conceptually, absorbing the impact-energy could be accomplished either by padding the limb or through encapsulating of fruits, or by both.

The use of limb padding was tested by spraying a polyurethane foam on the major limbs of the tree (Fridley *et al.* 1973). Drop tests with apples and peaches indicated that the polyurethane padding greatly reduced impact damage. However the amount of fruit hitting padded limbs was found to be low, making the net benefit of the padding marginal. The same method had been reported by Rehkugler (1968), indicating the potential but with no further exploration.

The feasibility of encapsulating apples with a sprayable coating before shake harvesting has been studied on a limited scale by Whitney and Lord (1970) and by Whitney (1971, 1975) although originally proposed by Despain (1968). The idea consisted of coating the apple in-situ on the tree with a cushioning material, followed by mechanically shaking and collecting the fallen fruit. Although two formulations of a suitable foam were claimed to be tried successfully on a primitive scale, no trace of continued work was found. Judging from the suggested formulation it seems unlikely to be both feasible and practical.

Whitney and Lord (1970) studied the encapsulation of mature fruit on the tree prior to the shake and catch harvesting operation by using a spray-on plastic foam material. This is a material resulting from a chemical reaction of polymeric isocyanate and Polygol which contains aminols and fluorocarbons. The two liquid chemicals are combined within a mixing chamber of the spray gun, and as it is applied to a surface, an instantaneous expansion of 30:1 occurs with a corresponding instantaneous set. The reported work comprised of laboratory models of encapsulated fruit made by foaming thin shells of the material and filled with silicone rubber to simulate the apple. Energy methods of analysis were utilized to predict deformation and bruise damage. Ling and Whitney (1975) analyzed theoretically the same problem using the model of a spherical shell acted on by two concentric forces. In addition, limited field studies were conducted on 'McIntosh' apple trees to determine the feasibility of such a procedure. A significant reduction of bruises as determined by bruise analysis was observed, pointing the way to procedures which may lead to a feasible solution reducing fruit damage significantly. The method, though serving as a useful model, was useless as a field practice due to the nature of the material being used.

A suggestion utilizing encapsulation was made also by Rehkugler and Markwardt (1971) who visualized a coating on the apples before harvest to enhance resistance to bruising. More significant and promising results were reported by Sarig *et al.* (1975) who independently explored the potential of a method for reducing bruise damage utilizing the foam-encapsulating technique. The unique application of such a technique demands several prerequisites regarding the nature of the foam. This led, after evaluating various possibilities, to the choice of Urea-Formaldehyde (U-F) foam, favored because of its lack of toxicity and non-polluting character--being a biodegradable material--and the relatively low price of the raw material. The studies were carried out on grapefruit trees where both the fruit and the limbs were sprayed by the foam made within a special mixing chamber and ejected by air pressure. After a period of foam curing, the trees were shaken using a commercial shake and catch system followed by bruise evaluation. The results clearly indicated that a significant reduction in bruise damage was observed. It is evident that the padding effect of U-F foam is beneficial to mechanical harvested fruit and it is conceivable that with appropriate refinement, the encapsulation could become a part of the mechanical harvesting process.

## 1.2 Objectives of the Study

The objective of this work was to determine the foam properties and encapsulation thickness necessary to reduce bruise damage in mechanically harvested apples.

The specific objectives required to complete the overall objectives were:

1) to derive the mechanical properties of the encapsulation (foam), and to predict desired characteristics for maximum energy absorption,

2) to perform an analytical analysis of the response of the encapsulated apple to impact conditions,

3) to compare various foam densities and thicknesses for possible future application, and

4) in addition to the primary objectives, to conduct limited field studies utilizing the proposed method.

# 2. LITERATURE REVIEW

The subject of mechanical properties of agricultural products, especially those associated with fruit behavior during harvesting and handling, has become a major research area (Mohsenin 1970). This research involves the application of the principles and laws of classical mechanics to the study of the mechanical behavior of biological systems. Thus, an analysis in the solid mechanics domain should precede any analysis pertaining to mechanical behavior of agricultural products.

## 2.1 The Behavior of Colliding Solids

It is beyond the scope of this work to mention the imposing list of contributions to the field of impact. A rather extensive account has been compiled by Goldsmith (1960), who indicates that the early theories based on the behavior of colliding objects as rigid bodies, remains essentially unchanged.

The collision of two or more objects is conventionally termed impact (Goldsmith 1960). This process develops high-magnitude forces which are exerted and removed on a microsecond scale and which usually initiate stress waves emanating from the contact region, and subsequently propagating throughout the entire domain of the impinging bodies. In addition, the impact is usually accompanied by a local contact phenomena which differs from the response of the objects at points remote from the collision region. The contact phenomenon is manifested by a local indentation of one or both of the colliding members and is accompanied either by the embedment or rebound of the striker.

The complicated process of energy transfer under impact conditions leads to serious difficulties in the mathematical analysis. As a consequence, no general impact theory has been developed (Goldsmith 1960), although many different approaches to the same problem have been recorded. Complete solutions have been obtained only for simple geometrical configurations, utilizing the laws of conservation of mass, conservation of momentum, and a mechanical energy balance.

Elastic wave propagation effects and local indentation at the contact point are of significance in the general case of impact. In reality the disturbance generated at the contact point propagates into the interior of the bodies with a finite velocity, and its reflection at bounding surfaces produces oscillations or vibrations in the solid. The energy converted into vibrations would be very small when the duration of contact is large compared to the period of the lowest natural frequency of either of the colliding bodies. In this event it was shown that when only the local contact phenomenon is considered, the bodies may be considered to be in a state of quasi-equilibrium, and the effect of wave propagation may be ignored without loss of accuracy (Timoshenko and Goodier 1970).

Previous work (Hamman 1967) has shown, that for impact associated with the free drop of apples, the effect of the pulse propagating in the apple is negligible due to the fast decaying of the propagated wave. Therefore, we may conclude that for the cited problem only the contact phenomenon should be considered.

## 2.2 The Contact Problem

The contact problem belongs to the broad class of problems concerned with the determination of the state of stress in elastic bodies which are pressed against each other. This problem involves a mixed specification of boundary conditions: the surface displacement is prescribed over a region $S_1$ of the surface and tractions stresses over the remaining region $S_2$. Usually the size of the area of contact is small in comparison with the radius of curvature of the bodies in contact, therefore, it is frequently assumed that one of the bodies can be replaced by a semi-infinite space.

The first three-dimensional contact problem was posed and solved by Hertz (1896). He considered the contact of two elastic bodies which are bounded by surfaces of the second order (elliptical cylinders and elliptical paraboloids) and gave formulae for the determinations of the pressure distribution over the contact region, the size of this region and the "relative approach" of the contacting bodies. Experimental verifications of Hertz's theory, as well as calculations which arise during the determination of the stress and displacement distributions in the contacting bodies, have been carried out by a number of authors. An account of this work is given by Luré (1964).

The simplest case of a contact problem occurs when one of the bodies can be regarded as absolutely rigid, i.e., when it is a rigid punch, while the other is an elastic half space. An early contribution to this problem was made by Boussinesq (1885) who considered the problem of a concentrated force (a punch) on an elastic semi-infinite body. Following Boussinesq's publication alternative solutions have been derived, to include three-dimensional considerations (Galin 1961 and Muki 1960). A systematic treatment of the punch problem (Boussinesq's method) of a half-space indented by a rigid punch is available (Sneddon 1951).

An outline of the development of the work on contact problems and their detailed bibliography has been given by Galin (1961) which consists primarily of the work done by Soviet scientists. A more complicated case, the indentation of an elastic layer, resting on a rigid immovable base, by a rigid die of circular cross section, was considered by Lebedev and Ufliand (1958). They utilized the harmonic functions of Papkovich and Neuber (Galin 1961) for the representation of the components of the displacement vector, and reduced the formulated problem to dual integral equations which are solved by the use of some relations between the Hankel and Fourier transforms (Sneddon 1951).

An analogous problem was solved by Keer (1964) who considered the case of an elastic sphere (elastic die) indenting an elastic layer. The problem is reduced to a similar set of dual integral equations and, in fact, one is able to obtain all the significant information from the asymptotic solution of Lebedev and Ufliand (1958).

Although both punch problems for an elastic half-space and an elastic layer have been treated separately for various punch configurations, the punch problem for an elastic layer resting on an elastic subspace, has been barely considered. An elastic analysis of stresses and displacement in a layered medium has been presented by Burmister (1945). He considered the situation of an elastic half-space bonded to one or two elastic layers and subjected to an axi-symmetric surface loading. His analytical results are limited to the top plane surface, where the pressure load has been prescribed. Chen (1971) presented an exact analysis of stresses and displacements in a linear elastic half-space composed of one or two layers bonded to another homogeneous half-space. He solved the problem for the axi-symmetric loading case using the Fourier transform method but has shown that the analysis is applicable to a general shape of a loaded region and arbitrary pressure distribution. His analysis, like Burmister, was aimed at the surface of the top layer and was formulated for the case where surface tractions are prescribed within and outside the region of loading. Dhaliwal (1970), Dhaliwal and Rau (1970) and Rau and Dhaliwal (1972) obtained general analytical results for the Boussinesq problem of an elastic layer lying over an elastic half-space for a punch of arbitrary profile. This is a more general form of solution from which the half-space problem or the case of an elastic layer lying over a rigid foundation can easily be derived.

The theoretical formulation of our problem is based on the Dhaliwal (1970) derivation for the case of a flat-ended cylindrical punch.

## 2.3 Mechanical Behavior of Apple Under Impact Loading

One of the major causes of mechanical damage to agricultural products is attributed to frequent impacts they receive in harvesting and handling. Apples, in particular, experience numerous collisions from the time they are harvested until they are processed or consumed.

The frequency and severity of impacts that apples experience increased with the advent of mechanical harvesters and bulk handling systems. Research has shown that stresses induced in apples under impact loading may reach very high levels even for short drop heights, resulting in severe damage not experienced in static loading. Fridley *et al.* (1964) reported a three-fold increase in damage for dynamic conditions. Mohsenin and Göehlich (1962) found that both forces and energy associated with bruising of apples under impact loading were twice the magnitude of forces and energy levels which cause bruising under static loading. The main objective in studying apple behavior under impact loading was to determine the parameters associated with the resulting damage. Nelson and Mohsenin (1968) found correlations of absorbed energy with bruise volume. Fridley and Adrian (1966) and Horsfield *et al.* (1972) also attribute bruising to energy since they found that multiple impacts, with less energy per impact, cause the same injury as do fewer impacts with more energy per impact. In addition they state that the material's dimensions are also involved in initiating bruising.

In one of the early studies on bruises caused from vertical drops, Gaston and Levin (1951) concluded that apples are highly susceptible to bruising resulting from vertical drops. The larger the apple the more liable it is to be bruised. For large apples (> 6.35 cm diameter) even a drop from a height of 2.54 cm resulted in a bruise which disqualified the apple for top quality (according to U.S. grading scale). Green (1962) conducted impact tests on apples by dropping the fruit from four heights onto a smooth solid block of wood. He found that the diameter of the resulting bruises could be used as a convenient measure of the degree of injury. According to Green the damage threshold is a drop from a height of about 5.08 cm. The weight of the apples had no apparent effect on the size of the bruise. This result seems rather debatable since numerous investigators (Hammerle and Mohsenin 1965, Fluck and Ahmed 1973) have shown that increasing the mass increases impact damage in agricultural products. Green concluded that the velocity of impact was apparently the main factor influencing injury.

Fluck and Ahmed (1973) investigated both the theoretical and experimental aspects of impacts for fruits and vegetables. They report that increasing either drop height or falling mass increases the likelihood of damage. Since only one measured parameter, peak force, increased with both increasing drop height and mass, they concluded that peak force and resulting internal stresses are critical elements in the incidence of impact damage. Increasing drop height or mass results in an increase of the potential energy of the fruit, which can potentially be dissipated within the fruit with resultant damage. However, Fluck and Ahmed could not resolve the question whether energy or force is the more important parameter associated with the damage. Likewise, Mohsenin (1971) in a review of a decade of research pertaining to mechanical properties of fruits and vegetables, stated that thus far there is no satisfactory answer as to what causes impact damage in fruit tissue.

In studying the mechanics of impact of a falling fruit, several investigators used the Hertz contact theory. Hamann (1967) treated the apple as a viscoelastic solid and solved the Hertz contact problem for impacting visco-elastic bodies, and predicted internal stress levels for apples. The material properties as derived in his study were used in a study of an impact of a viscoelastic sphere (representing an apple) by Rumsey and Fridley (1974) who used a finite-element formulation for calculating indentations and principle contact stresses that occur under impact loading. The Hertz contact theory was also used by Horsfield *et al.* (1972) relating it to a harvest-ing situation.

## 2.4 Experimental Techniques for Impact Testing of Apple

The experimental study of agricultural products is similar to experimental investigation of non-biological materials which have been studied extensively (Goldsmith 1960). Since impact of fruits is usually characterized by impingement at low impact velocities (in the order of

1.5-3.0m/sec), the production of collision phenomena under controlled laboratory conditions is relatively simple and the actual testing procedure is dictated by availability of equipment and the nature of the problem studied. The various techniques employed in impact testing of agricultural products can be categorized basically into two methods; a drop test and a pendulum test.

During a drop test, either the product is dropped upon a rigid surface, or a mass is dropped upon the product. A transducer is mounted on the dropping head so that a complete acceleration-time curve is obtained with the aid of an oscillograph or other recording device.

Falling masses instrumented with accelerometers were developed by several investigators. Hammerle and Mohsenin (1966) developed a drop test apparatus for impact testing of food and agricultural products, incorporating piezoelectric accelerometers and load cells, which offered means by which impact force and displacement could be measured. In a later experiment Mohsenin *et al.*(1974) used a drop test device incorporating a force transducer, sandwiched between two aluminum plates, to sense the impact force and the duration of impact. The lower plate of the transducer was embedded into a rigid concrete block to minimize the energy losses. The dropping mechanism also included a magnetic holder, which could slide on a vertical channel frame to vary the object drop height. Schmidt (1962) developed an apparatus for the dynamic evaluation of cushioning materials simulating conditions that exist in any catching frame. His cushioning material evaluator consisted of a 7-m drop chute simulating the maximum height the fruit would fall when shaken from a tree. A set of strain gages applied to an impact beam was used to sense the impact of a falling object and a system of phototubes for recording the velocity. Whitney (1971) performed impact tests on various sizes of plastic foam wafers related to the energy of impact by fruit, using a test apparatus similar to that developed by Wright and Splinter (1967). The apparatus consisted of a wire guided drop weight released by a magnet onto a test specimen which rested directly upon a force transducer with a direct readout through an oscilloscope. The same apparatus was also used by Fluck and Ahmed (1973) in conducting impact testing of apples. Other researchers have used the drop test technique for documenting impact in a variety of agricultural products. A comprehensive list of related studies has been compiled by Mohsenin (1970).

The drop testing apparatus lacks the requirements of absolute rigidity and frictionless guide tracks which are essential in an energy balance analysis of any impact study. To overcome these shortcomings many investigators preferred the use of a pendulum apparatus. Here the impact is achieved through the swing of a ballistically suspended body, and the sensing transducers and recording devices are basically the same as with the drop tests. Bittner *et al.* (1967) used the pendulum apparatus for measuring height of drop and height of rebound when either a fruit or a rigid ball was allowed to impact a piece of cushioning material affixed to a rigid impacting surface on a wall. Simpson (1971) used the pendulum arrangement in measuring forces and apple damage during cushioned impact. The impact bodies--half of an apple, or half of a cast aluminum sphere--were suspended from two linen threads of negligible mass and the accelerometers for measuring peak acceleration were mounted at their center. By covering the impact body with a thin layer of Prussian blue he was able to also measure the contact diameter. The pendulum method has been used by many other investigators, primarily for studying impact of fruits or testing of cushioning materials (Stern 1958, Fridley *et al.* 1954, Mohsenin and Göhlich 1962, Nelson and Mohsenin 1968).

Both drop tests and pendulums have initial loading velocities limited by drop height. Impacts at higher velocity were attained by pneumatic impact devices (Fletcher *et al.* 1965), spring loaded arms (Fridley and Adrian 1966) and arms rotated by electric motors (Burkhardt and Stout 1971). Still higher velocity can be attained by the firing of projectiles from air guns, or specially designed ultra-speed devices utilizing the reaction of a compressed gas. The latter, however, is usually beyond the range desired in agricultural products. In addition to the two basic techniques some special methods for incrementing impact have also been reported including high-speed photography (Davis and Rehkugler 1971) and the use of simulated fruitlike objects encapsulating the sensing transducers (Rider *et al.* 1973). Thus the information pertaining to the impact is transmitted to the recording equipment on a continuous basis, a desired technique, especially in studying handling effects.

The variety of methods recorded in the literature indicates that no single technique is superior and universally used. Therefore, the final selection of an experimental procedure is governed by the specific problem, and availability of suitable equipment.

## 2.5 Analysis of Apple Bruising

There is general agreement that bruising is the most common apple defect seen on the fresh market. The symptoms of injury are flattened areas or indentations on the side of the fruit with the flesh browned beneath. Its significance is manifested as being the major criterion in evaluating the suitability of experimental and existing machines and methods for fruit harvesting and handling. The measurement of bruise severity was approached differently by numerous investigators. Several have used the diameter of the bruised area as the sole criterion of severity of damage (Gaston and Levin 1951, Gillepshe and Scott 1950, Schomer 1957). Burt (1959) considered depth as well as diameter in a study of bruises on 'McIntosh' apples, classifying bruises as either slight, moderate or severe following the U.S. grading standards. Wennergren and Lee (1961) used trimming losses to assess bruise damage. This procedure was also used by Tennes *et al.* (1974) who defined bruising loss as the weight loss that occurs as a result of the damage sustained by the fruit during harvesting and handling. Dedolph and Austin (1961) related the diameter of the surface area damaged by bruising to the depth of the flesh damage and ascertained the influence of fruit variety and location of the damage on the fruit to this relationship. They concluded that simple diameter measurements of the bruised area are sufficient for prudent estimation of the total damage to the fruit caused by impact bruising. Furthermore, they report changes in the diameter of depth ratio of bruises at different locations on the fruit which may imply differences in the physical properties of the apple flesh at different areas within a fruit in some varieties. In addition, this can also be attributed to the variation of density of apple tissue with location within the apple as shown by Megilley *et al.* (1968).

The location probabilities of surface injuries for mechanically harvested apples were studied by Brown and Segerlind (1975) who suggest that 98 percent of the injuries are located at a particular portion of the fruit surface. They also report that the probability of the injuries increased as fruit size increased. Their results are valuable because they indicate where the encapsulating material should be applied.

The exact nature of bruising is still subject to discussion and interpretation. It is conceivable, however, to visualize the apple as a biological structure made up of cells, thus amenable to an engineering structural analysis, possibly linking the apple bruising to one of the common theories of failure. However, a general acceptable failure criterion associated with bruising has not been established although some suggestions have been made. Fridley *et al.* (1964), deducing from compression tests on peaches and pears, concluded that bruising is probably caused by excessive shearing stresses. Hamman (1967) suggested that compressive stresses might be the critical factor in bruise occurrence. Miles (1971) reported that the most important parameter in determination of apple failure is shear stress, although the actual limiting value is heavily dependent on the axial strain and dependent to a lesser degree on the mean normal stress. The results obtained by Apaclla (1973) seem to substantiate Miles' observations. The criterion of maximum shear stress as a possible failure parameter was suggested also by Fridley and Adrian (1966).

Fluck and Ahmed (1973) studied impact bruising of whole fruits and concluded from their experiments that it was impossible to say whether energy or force is more important parameter in bruising. DeBaerdermaker (1975) suggested that tensile strength of apple flesh should be investigated in view of the resulting bruise at a point of maximum tensile and shear stress. Attempts have also been made to relate energy of impact to the actual damage. Nelson and Mohsenin (1968) found correlations of absorbed energy with bruise volume. Fridley and Adrian (1966) and Horsfield *et al.* (1972) found that multiple impacts with less energy per impact cause the same injury as do fewer impacts with more energy per impact. Bittner *et al.* (1967) indicates that initiation of definite bruising encountered in falling apples is associated with a change of energy level absorbed by the apple. Thus energy, at least, when some threshold stress is exceeded, is a direct cause of injury. From these diversified suggestions one may conclude that there is apparently no clear-cut criterion applicable to all loading conditions. Moreover, it seems that in many cases the conclusions were based on the specific measurement technique. It follows that more work is needed to sort out the exact failure mechanism associated with initiation of a bruise.

# 3. THE MECHANICAL CHARACTERISTICS OF THE ENCAPSULATING FOAM

The analysis of the response of foam-encapsulated apples to impact loading requires analyzing the mechanical behavior of both media. In recent years both quasi-static and dynamic properties of apples have been extensively explored under various loading conditions (Hamann 1967, Clevenger and Hamann 1968, Miles 1971, DeBaerdemaker 1975). On the other hand, information pertaining to the mechanical behavior of the specific foam in our study--the Urea-Formaldehyde foam--is very limited. This foam is used almost exclusively as an insulating material rather than a cushioning material and all the available technical data pertains to its thermal properties. Nevertheless, the mechanical behavior of other polymeric foams has been explored and documented and numerous testing techniques have been established. Since many of the cellular foams share the same typical characteristics, basing our analysis on previous studies would enable us to estimate the dynamic properties of U-F foam.

## 3.1 Impact Behavior of Polymeric Foams

Polymeric foams designed for impact applications must exhibit a specific stress-strain behavior as well as an ability to dissipate energy. It is important for an impacting object to be compressed at a constant stress for maximum efficiency of energy absorption. A foam which exhibits a plateau region in its stress-strain curve, resembling yielding, will absorb impact energy at a relatively constant stress (Rusch 1969).

The foam should also dissipate most of the energy it absorbs during impact to avoid the transmission of the undissipated energy to the object. The rebound effect is undesirable in our application.

Polymeric foams have been utilized commercially in the design of energy-absorbing structures. The ability to control load-compression response through variation of cell geometry, density and the matrix polymer, make foamed polymers ideal for such applications. This advantageous diversity, however, complicates the prediction of various parameters of the foam behavior. Empirical or trial and error procedures rather than analytic techniques have been adopted for selecting the suitable material for a particular application (Meinecke and Schwaber 1970). An optimal design for a specific problem requires understanding quantitatively the mechanics of the material and the structural details that govern its behavior.

A simplified model was proposed by Gent and Thomas (1963) to relate polymeric foam properties to the foam structure. Their model, developed first for open-celled foam and extended subsequently to incorporate closed-cell foam consists of thin threads whose unstrained length is designated by $l_o$ and whose cross-sectional area by $D^2$. The threads are joined together to form a cubical lattice, as shown in Fig. 3.1. The intersections are cubical regions each of whose volume is $D^3$, and are assumed rigid, or substantially undeformable. When a compression force is applied parallel to a set of threads, they buckle. This buckling effect is demonstrated in a load-deformation diagram, Fig. 3.2. The load and deformation are linearly related at a low strain level until a critical value is reached at which buckling is initiated. The modulus then decreases due to an increase in the bending moments of the columns within the foam (Schwaber 1973). The modulus increases at larger deformations because the struts start to touch and interfere with each other's movement. The modulus of the foam then approaches the compressive modulus of the solid material. Gent and Thomas (1963) developed an equation in which the compressive force is related to the bending moments of the buckling struts and established a relation between the compressive stress and the compressive strain in terms of the density of the foam.

The dependence of stress on the foam structure was also observed by Skochdopole and Rubens (1965). At low values of strain the stress is dominated by the compressive modulus of the cell walls. The modulus value levels off as the cell walls reach a critical buckling stress and

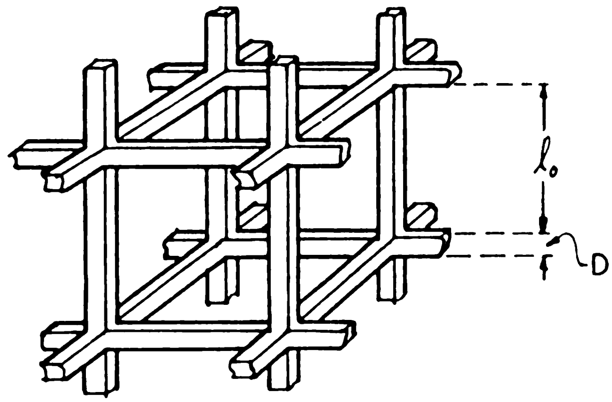


Fig. 3.1 A simple model of a foamed material (from Gent & Thomas, 1963)

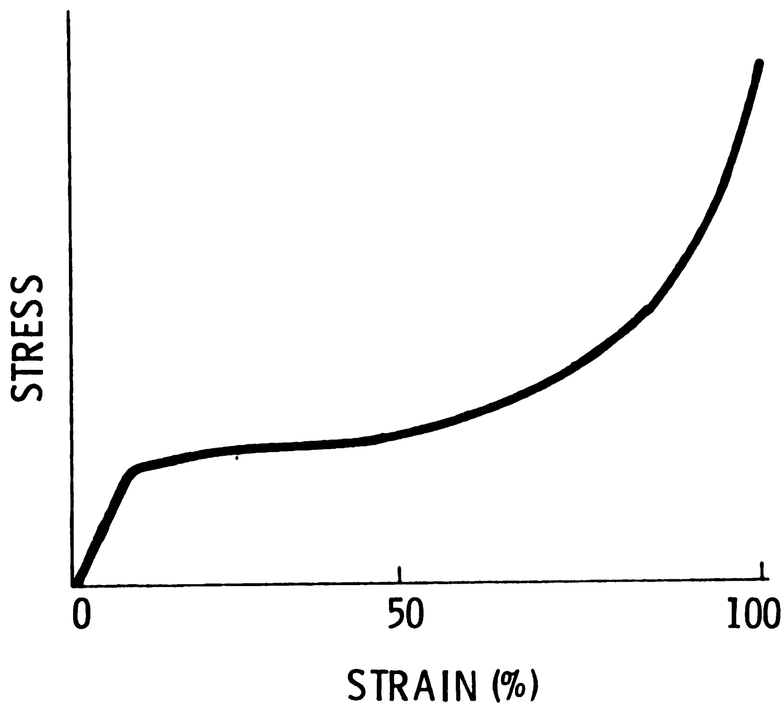


Fig. 3.2 Stress-strain behavior for a compressed polymeric foam. (from Schwaber, 1973)

then it increases very slowly with an increase in the compressive load. Since the bending stress is dependent on the third power of the thread's radius (Skochdopole and Rubens) the buckling effect would be more pronounced in a thicker thread (large cell).

Although the mechanics of foams can be better understood through the assessment of the changes in the microstructure, the actual mechanism of the response is extremely complex and depends on many variables such as the flexibility of polymer chains, molecular weight, and degree of crystallization. A rigorous examination of all these variables, the associated crystallographic features and their interactions is beyond the scope of this study. This study will consider only some of the microstructure variables which seem pertinent.

When a foam is being deformed, as under impact loading, energy is absorbed and dissipated by the foam, thus providing the desired cushioning effect. The mechanism of energy dissipation in foams is very complex and involves an energy loss in the strained polymer matrix, friction between units of the cellular matrix, loss due to viscous flow of fluids through the open pores of the foam (pneumatic damping), and thermal damping of gases in closed cells. Although the energy dissipation is governed primarily by the first two mechanisms, the other two may account for some of the discrepancies that sometimes exist between theoretical and experimental results. A distinction between open-cell and closed-cell foams is important since energy is dissipated by air flow through the pores in the former. Kosten and Zwikker (1939) postulated a model in which the dynamic mechanical properties of the foam-fluid system were related to the geometry and porosity of the sample. In closed-cell foams, the contained gas is compressed and expands rapidly as stress is removed. In addition to the visco-elastic behavior and stress softening of the matrix material, another mechanism was proposed by Otis (1970) that energy dissipation can occur because of heat transport between the compressed gas and the solid structure of the foam. Deformation of the foam compresses the gas in the voids, resulting in a temperature rise and an irreversible heat transport process from the hot gas to the cooler solid structure, manifested as a damping effect.

Energy dissipation during impact loading is associated primarily with straining the polymer matrix and the internal friction of the cellular matrix. It is generally accepted that impact loading can be predicted from stress-strain data obtained at constant strain rates. This method is valid only if we assume that impact velocity has no significant influence on the compressive stress-strain behavior. This assumption holds if the bulk material is in the glassy or rubbery plateau regions (Fig. 3.3) where its modulus is approximately rate independent. Materials in the transition region, however, are strongly rate dependent. The Urea-Formaldehyde foam used in this

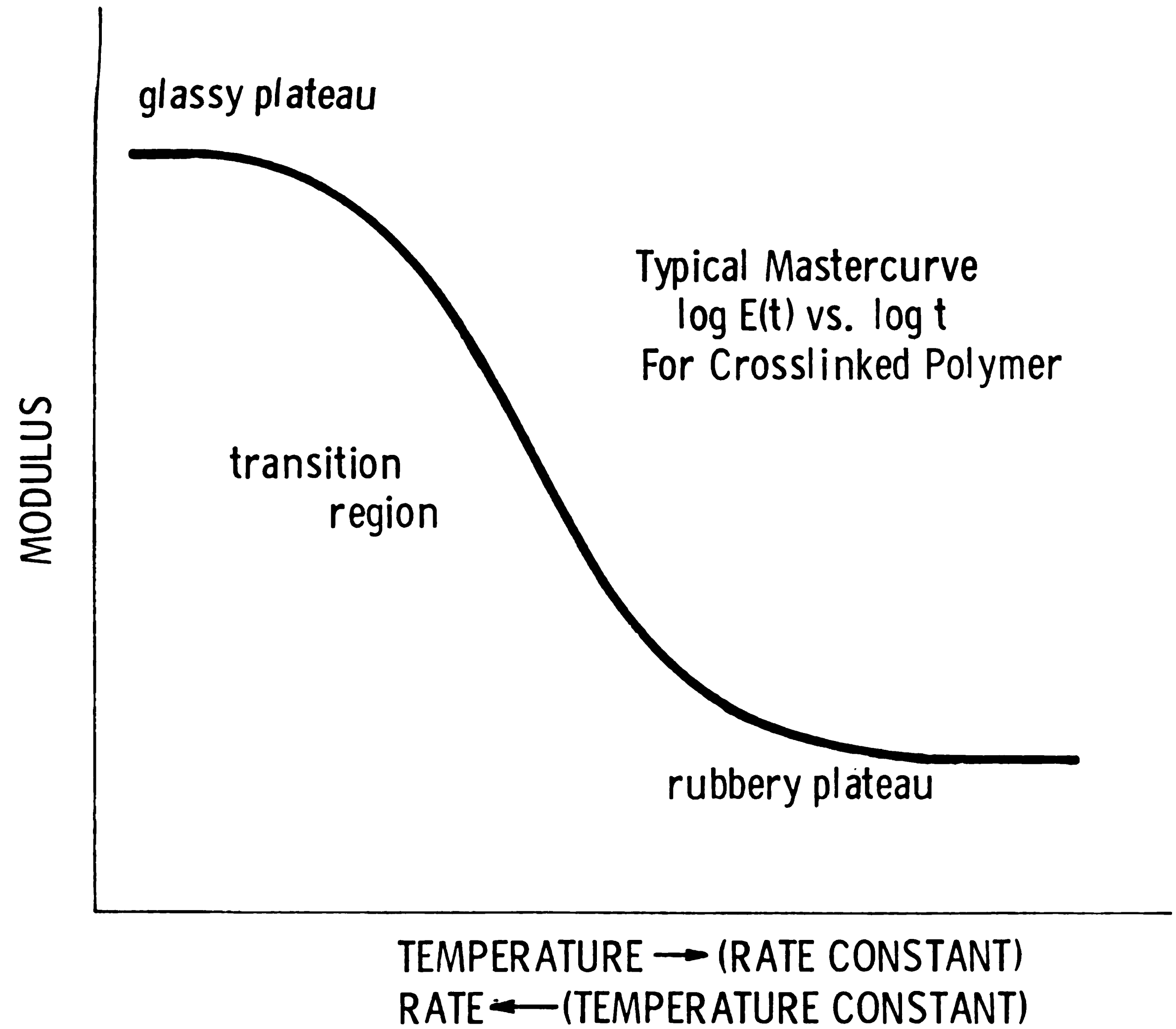


Fig. 3.3 Typeical mastercurve of modulus vs. rate and temperature for crosslinked polymer (from Schwaber, 1973).

investigation is a highly cross-linked polymer and has a low glassy transition temperature which makes it a typical rate-independent material. It is possible, therefore, to compare deformation energies determined at constant loading rates (e.g., Instron tests) with those obtained at different velocities (impact). Thus, the behavior of the foam during impact loading can be predicted from the area under the load-compression curve representing the energy absorption capacity of the foam (Meinecke and Schwaber 1970). It should be noted that the Urea-Formaldehyde foam exhibits a pneumatic damping effect which is a rate dependent parameter. This effect is usually of no significance compared to hysteresis in the strained solid phase, since even in a true closed-cell type polymer it is possible for the air to escape (Schwaber 1973). This is true with brittle foam, such as the U-F, where the pneumatic damping is ineffective once crushing of the cells is initiated. Consistent experimental results can be obtained by performing the load-deformation tests at a slow loading rate on a reasonably small sample, allowing the air to escape (Schwaber 1973). The experience of other investigators supports this practice. When considering brittle thermosetting materials, the impact properties may be so insensitive to speed of testing, that the area under a normal slow speed stress-strain curve gives a good estimate of the impact strength (Nielsen 1962, Rusch 1970a). Any contribution to the overall energy dissipation from the pneumatic damping effect can be considered as a bonus.

To model the dependence of the energy-absorption characteristics on the physical properties of the foam matrix, Rusch (1970b) proposed to factor the compressive stress ($\sigma$) into the product of three terms: $\sigma = \varepsilon E_f \Psi(\varepsilon)$. [$\Psi(\varepsilon)$] is a dimensionless function of the compressive strain ($\varepsilon$), ($E_f$) the apparent Young's modulus of the foam and ($\varepsilon$) the compressive strain. ($E_f$) depends primarily on the density of the polymer and on Young's modulus of the matrix polymer ($E_o$) and is largely independent of cell size or cell geometry. On the other hand, $\Psi(\varepsilon)$ reflects the buckling of the foam matrix and, therefore, is highly sensitive to the specific details of the matrix geometry. It is only moderately dependent on density of cell size, and independent of ($E_o$). Therefore [$\Psi(\varepsilon)$] is significantly affected by the brittleness of the foam matrix. A brittle matrix is broken rather than flexed during compression and the foam possesses a load-deformation curve with a flatter and wider plateau than that displayed by a ductile (flexible) foam of equivalent ($E_f$) and matrix geometry. This characteristic is particularly important in energy-absorbing applications. Rusch (1970a) has shown that in the region of maximum energy absorption, a brittle foam exhibits a higher energy-absorbing efficiency and a wider and more flat plateau in the maximum deceleration versus impact energy curve than a ductile foam of similar matrix geometry.

The energy absorbed by the foam is the area under the load compression curve:

$$\text{Energy} = \int_0^x F dx \tag{3.1}$$

Since $F = \sigma A$ and $x = \varepsilon l$ the above can be written as

$$\text{Energy} = \int_0^\varepsilon \sigma A l d\varepsilon \tag{3.2}$$

by incorporating the form of $(\sigma)$ as given by Rusch (1970b)

$$\text{Energy} = \int_0^\varepsilon \varepsilon E_f \Psi(\varepsilon) A l d\varepsilon \tag{3.3}$$

or

$$\text{Energy} = E_f A l \int_0^\varepsilon \varepsilon \Psi(\varepsilon) d\varepsilon \tag{3.4}$$

For a given foam, and a given strain history, the integral is constant. The two variables at our disposal, related to the energy absorbed, are the apparent modulus $(E_f)$ which is highly dependent on the density of the foam and the volume of the foam used in a particular application. Analysis of these two parameters should yield the desired foam characteristics for the absorption of the impact energy of the apple.

No attempt was made to evaluate the function $[\Psi(\varepsilon)]$

since for Urea-Formaldehyde very little change in the actual matrix geometry can occur. The above analysis, however, should be valuable in a possible future selection of other materials, which might be considered for the stated application.

### 3.2 Physical-Chemical Nature of Urea-Formaldehyde Foam

The proposed material for the apple encapsulation (Urea-Formaldehyde) possesses unique characteristics which make it an ideal medium for the given application. This does not rule out the possibility of a more suitable material in the future.

The material investigated is a 'Rapco-Foam'[1] which is a modified Urea-Formaldehyde resin formulated in accordance with the German patented Isoschaum process. It is a cold-setting resin which forms a low-density non-combustible resilient foam. The structure has a microscopic sized cell agglomeration interspersed with microscopic capillaries which are irregular and discontinuous (Fig. 3.4). The final form has 60 to 70 percent closed cells. The foam is generated in a continuous stream with a specially designed Isoschaum foam generator (Fig. 3.5) by mixing three components: air, foaming agent and foaming resin. Air foams up the foaming agent in the foaming cylinder and the

[1] Manufactured by Rapco Chemical, Inc., South Carolina, a subsidiary of Rapperswill Co., New York, N.Y.

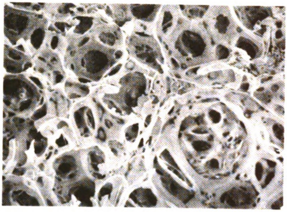

a. Density = 0.0064 gr/cm$^3$.

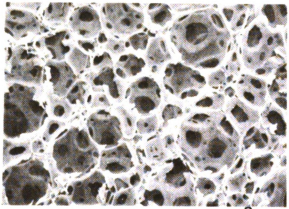

b. Density = 0.0112 gr/cm$^3$.

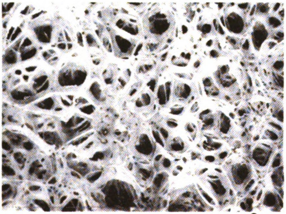

c. Density = 0.0192 gr/cm$^3$.

Fig. 3.4 Photomicrographs (Magnification = 100 X) showing the differences in cell geometry for different densities of Urea-Formaldehyde foam.

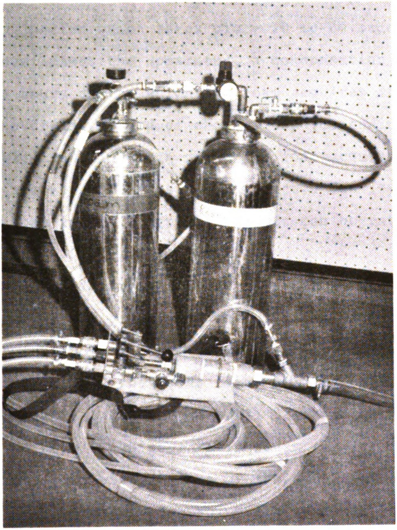

Fig. 3.5 Portable Isoschaum foam generator.

resin is then injected in the mixing chamber. The mixing and expansion is complete after the foam travels through the foam application hose and the formed gel is strong enough to bear its own weight until hardening has commenced. The curing process is comprised of a setting period which takes place 10 to 60 seconds after the foam leaves the apparatus, a condensation period of 2 to 4 hours during which the foam acquires its resilience, and the drying period of about 1 day (depending on climatic conditions) in which the foam acquires its final stable properties. The standard density of the Rapco-Foam is 0.0112 $gr/cm^3$, but it can be varied from 0.0064 to 0.0192 $gr/cm^3$.

The foaming resin should be water soluble to avoid blocking of the pipes and other difficulties in maintenance of the foaming device. The water-solubility of the resin is a function of the molar ratio of Urea to Formaldehyde, where a ratio exceeding 1 (Urea): 2(Formaldehyde) is water soluble. A higher ratio leads to free formaldehyde and causes unpleasant odors at the application site. A compromise between water solubility and elimination of air pollution leads to a ratio of 1 part Urea to 1.7 parts Formaldehyde making the resin a milky emulsion. As a surface active agent, a commercially available product was used, and as a catalyst, phosphoric acid. The pH should be neutral to avoid undesired effects when applied to the fruit.

## 3.3 Evaluation of the Mechanical Properties of Urea-Formaldehyde Foam

### 3.3.1 The test specimen

Blocks of U-F foam were generated in the laboratory utilizing the Isoschaum foam generator (Fig. 3.5) and cut into sheets. Density of the foam was regulated by changing the amount of flow of either of the three components to obtain two density groups: 0.0112 $gr/cm^3$ and 0.0192 $gr/cm^3$. A third group with a lower density (0.0064 $gr/cm^3$) was also attempted, but the generated foam would not sustain any forces and therefore was discarded. The foam attained its final characteristics after a curing period of 1-2 days and cylindrical test specimens were cut by driving a specially constructed cork borer through the sheets (Fig. 3.6). The microstructure was examined from photomicrographs taken of foam samples from the different density groups to illustrate the differences in cell structure and geometry (Fig. 3.4). The higher density has a more dense cell structure suggesting a higher potential for impact absorption.

The selection of suitable dimensions, length-diameter ratio (L/D) for the samples is very significant when considered from a theoretical point of view because of the requirement to satisfy the boundary conditions. Since the results of our tests are derived on a per unit volume basis, it is imperative to assume uniform distribution of

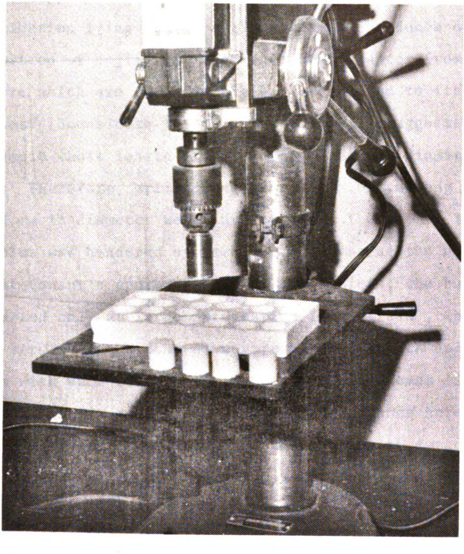

Fig. 3.6 Preparation of cylindrical samples of Urea-Formaldehyde foam. (Samples were 2.54 cm long and 2.54 cm diameter.)

the argument quantity in question (energy, stresses or displacement). The dimensions may be selected by the Saint-Venant's principle which (following Boussinesq's formulation) states: "An equilibrated system of external forces applied to an elastic body, all of the points of application lying within a given sphere, produces deformation of negligible magnitude at distances from the sphere which are sufficiently large compared to its radius" (Boussinesq 1885). This principle suggests using a sample whose length (L) is larger than its diameter (D). Therefore, cylindrical samples, 5.08 cm long and 2.54 cm in diameter were investigated The use of long samples was hindered by buckling, preventing the use of Saint-Venant's approximation. Nevertheless, the buckling occurred only at large deformation (85% strain), where the struts of the foam structure begin to touch and interfere with each other's movement (Gent and Thomas 1963). This region is of limited practical importance here since it is desired to remain in the plateau region for optimal energy absorption. The samples were compressed to the inflection point of the last two regions (45-50% strain), and it was hypothesized that in the region of interest the edge effects could be ignored, eliminating the need for long cylindrical samples. To test the hypothesis, cylinders, 5.08 cm long and 2.54 cm in diameter and cylinders 2.54 cm long and 2.54 cm in diameter were employed and the apparent modulus ($E_f$), measured as the initial slope of a stress-strain curve, was derived for the two regions. The results are given in Appendix 1. No significant difference was observed and it was concluded that it is valid in this case to use the short specimens (L/D = 1) and to assume uniform distribution of the stress. The final samples had a diameter of 2.54 cm ± 0.01 cm and length of 2.54 cm ± 0.1 cm.

### 3.3.2 Force-deformation tests

The objectives were to derive the apparent elastic modulus for the foam, to ascertain its dependence on the foam density and to assess the energy-absorption potential as a function of the foam density. Preliminary tests were performed at various loading rates with samples of constant density (0.0112 gr/cm$^3$) to verify the validity of the rate independence assumption, and to establish the appropriate loading rate for deriving the mechanical properties. The samples were compressed coaxial with the longer axis of the sample using the Instron Universal Testing Machine (Fig. 3.7). All tests were performed at ambient temperatures of 21 ± 1°C. The preliminary test compared five loading rates: 50.8 cm/min, 25.4 cm/min, 12.7 cm/min, 5.08 cm/min and 2.54 cm/min, using 10 samples per loading rate. The apparent modulus ($E_f$) was derived directly from the loading response by measuring the initial slope of the force-deformation curve. The

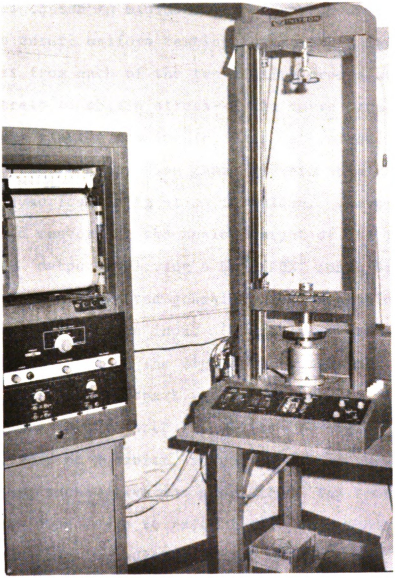


Fig. 3.7 Force-deformation test utilizing the Instron Universal Testing Machine.

results given in Appendix 2 confirm the assumption of rate independence, with only a slight deviation encountered at higher loading rates. The deviation was attributed to the pneumatic damping effect. A loading rate of 2.54 cm/min was chosen to minimize the pneumatic damping effect and to ensure uniform testing conditions. Twenty-five samples from each of the two density groups were loaded to 55% strain to obtain stress-strain curve from which the apparent elastic modulus ($E_f$) was determined. The values of the energy absorption capacity were obtained by performing a numerical integration technique. The procedure involved converting the analog output of the Instron to digital output utilizing a GRAF/PEN[1] sonic digitizing system which converted graphical representation into a digital data for the input of such data into a data processing system. The digitizing system consisted of a tracer which had a spark gap built into its point. When the tracer touched specific points of interest along the curve, laid on a tablet, a spark jumped across the gap and a hypersonic wave was generated. The time required for this sound wave to reach linear microphone sensors, mounted along two adjacent sides of the tablet, were analogous to the X and Y coordinates of the point from the sensors. The control unit of the system converted the times into binary representations of the X and Y

---

[1]Manufactured by Science Accessories Corporation, Southport, Conn.

coordinates. The numerical data were input into a CDC 6500 digital computer and the energy, determined as the area under the load-deformation curve, was calculated.

### 3.3.3 Measurements of Poisson's ratio

Poisson's ratio was determined using a method developed by Hughes and Segerlind (1972) which involved compressing two cylindrical cores of material. One sample was compressed axially while free to deform in the transverse direction. The second sample was compressed inside a rigid die to prevent lateral deformation (Fig. 3.8). The constitutive equation in cylindrical coordinates, when $\varepsilon_{\theta\theta}$ and $\varepsilon_{rr}$ are zero, is given by:

$$E_f\left(\frac{\varepsilon_{zz}}{\sigma_{zz}}\right) = \frac{(1 + \nu)(1 - 2\nu)}{(1 - \nu)} \qquad (3.6)$$

This equation relates the stress and strain in the direction of the applied load, $\left(\frac{\varepsilon_{zz}}{\sigma_{zz}}\right)$ to Poisson's ratio ($\nu$), provided the value of the elastic modulus ($E_f$) is known.

The experiments were performed on cylindrical samples of foam using twenty samples from each of the two density groups. All of the samples were 2.54 cm in diameter and 2.54 cm long. The samples were loaded using the Instron Universal Testing Machine at a loading rate of 2.54 cm/min and force deformation curves were obtained

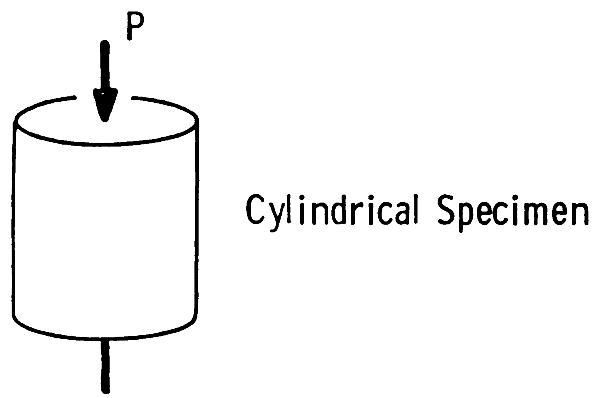


a. Uniaxial compression of unrestrained cylindrical specimen.

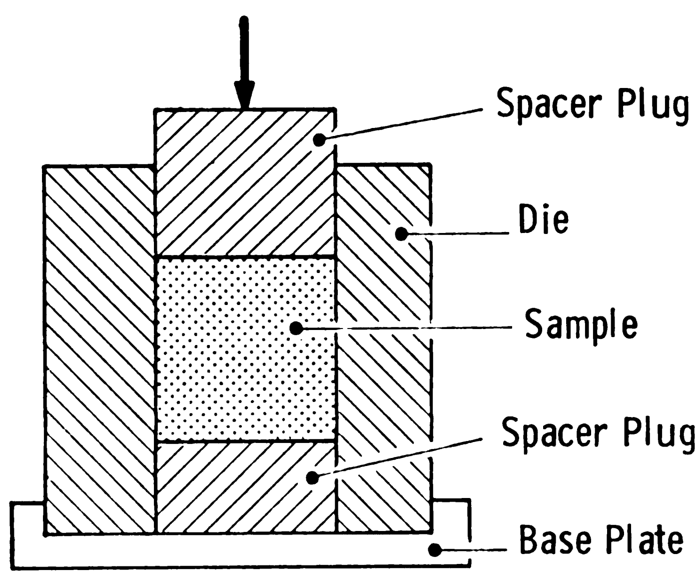


b. Compression of cylindrical sample in a rigid die.

Fig. 3.8 The method of loading used for deriving Poisson's ratio.

for both the unrestrained and the constrained tests. The initial slope of these curves yields the apparent modulus of elasticity ($E_f$) and $\sigma_{zz}/\varepsilon_{zz}$ for the unrestrained and the constrained samples, respectively.

### 3.3.4 Impact tests

Drop tests were performed to establish the loading conditions to which the encapsulated apple was subjected. This was necessary since the boundary conditions were specified in terms of the indentation resulting from the loading forces encountered in the free fall of the apples.

Heights of 5.08 cm, 15.2 cm, 30.5 cm and 38.1 cm were used to simulate actual dropping conditions of a detached apple impinging on lower branches. Ten 'Golden Delicious' apples were used for each of the drop heights. Mature fruit, free of defects, with an average diameter of 70 mm were carefully picked and tested on the day of picking at an ambient temperature of 21 $\pm$ 1°C.

A schematic diagram of the test set-up employed in the drop tests is given in Fig. 3.9. It consisted of a drop test apparatus (1) and a solenoid-activated release mechanism (2) to release the apple. The falling apple passed through a photocell sensor device (3) which triggered the oscilloscope (4) via a triggering circuit (5). The apple dropped onto a load cell (6) and the signal was recorded in the oscilloscope via a charge

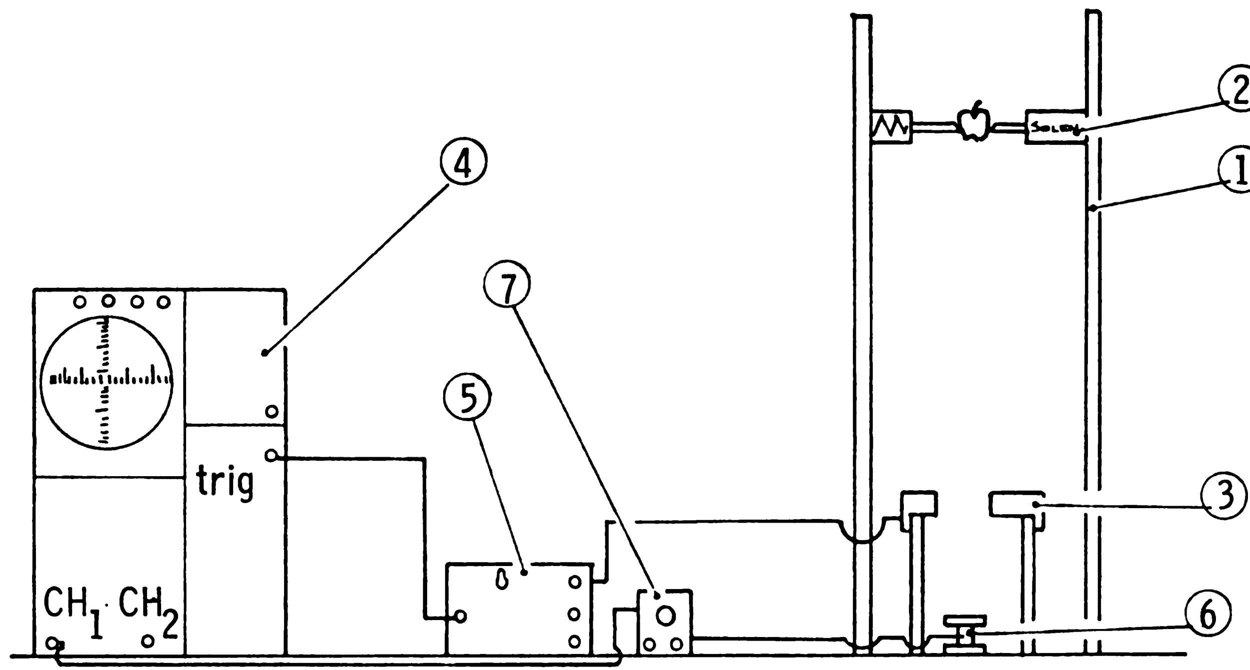


Fig. 3.9 Schematic diagram of the instrumentation set-up for drop tests.

1. Drop-test apparatus
2. Release (solenoid activated) mechanism
3. Photo-cell Sensors
4. Oscilloscope
5. Triggering circuit
6. Quartz washer type load cell
7. Charge amplifier

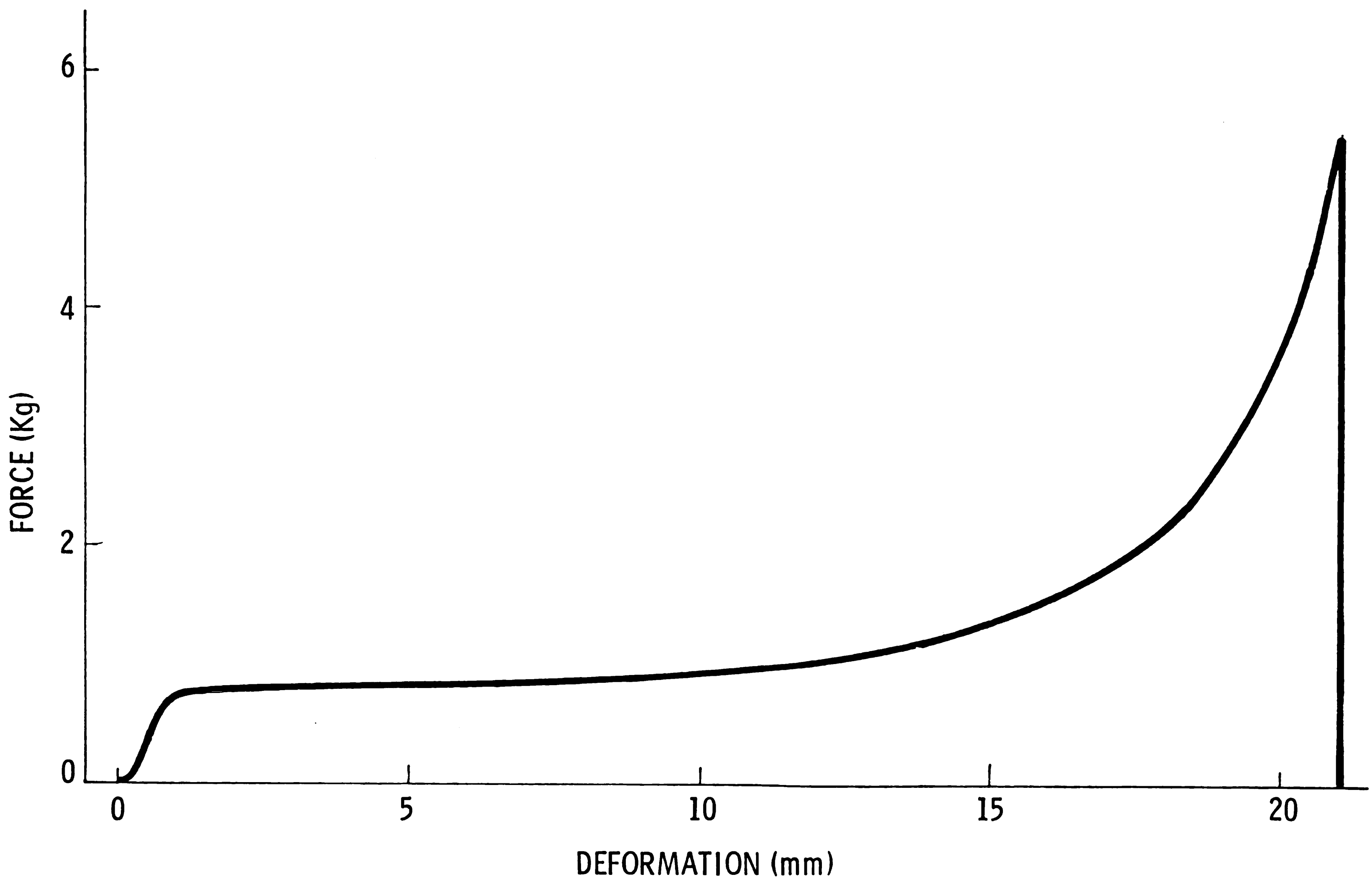


Fig. 3.1 Force-deformation curve of Urea-Formaldehyde foam subjected to a compression loading.

amplifier (7). A force-time trace was recorded with a storage oscilloscope to obtain a maximum force corresponding with the maximum indentation.

## 3.4 Results and Discussion

The response of Urea-Formaldehyde foam to a compression load is shown in Fig. 3.10. A nearly linear relationship existed at low strains until a critical value was reached where the modulus decreased and a semi-plateau region was encountered. The leveling was attributed to the buckling effect of the foam matrix at this point. The plateau region is maintained up to strain of 45-55%, at which point the modulus increased and approached the compressive modulus of the solid material. The last region was of limited practical value in this application and hence, stress-strain curves were obtained only for the instantaneous response and the plateau regions. Two representative curves for the two density groups are given in Fig. 3.11, a and b.

The apparent elastic modulus was measured as the slope of the stress ($\sigma$)-strain ($\varepsilon$) curve for $\varepsilon \to 0$. The results are given in Table 3.1 for two foam densities. The apparent elastic modulus ($E_f$) was found to be strongly dependent on the foam density. This result was expected, following previous studies by Rusch (1969, 1970b) on the load-compression behavior of brittle foams. Gent and Thomas (1963) also indicated that the resistance of

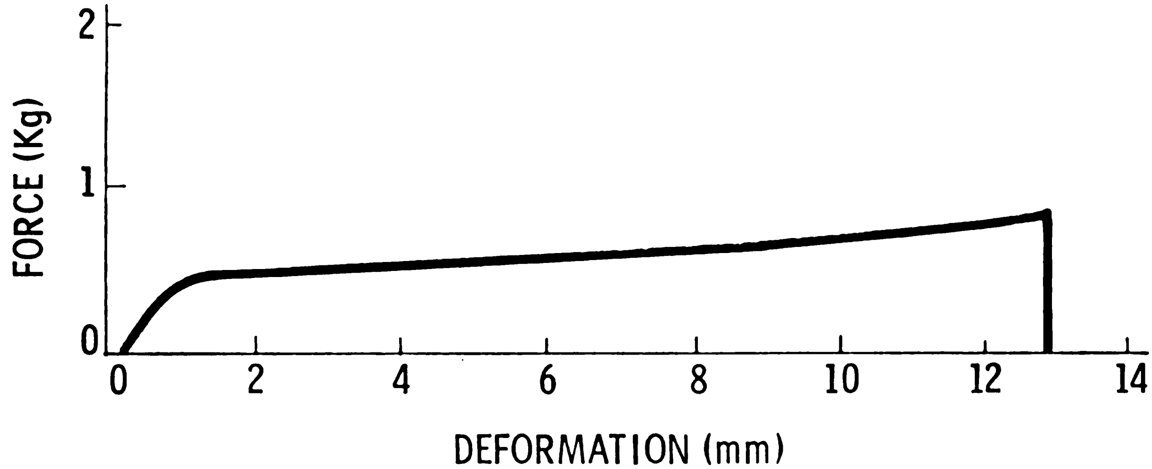


a. Foam Density = 0.0112 gr/cm$^2$

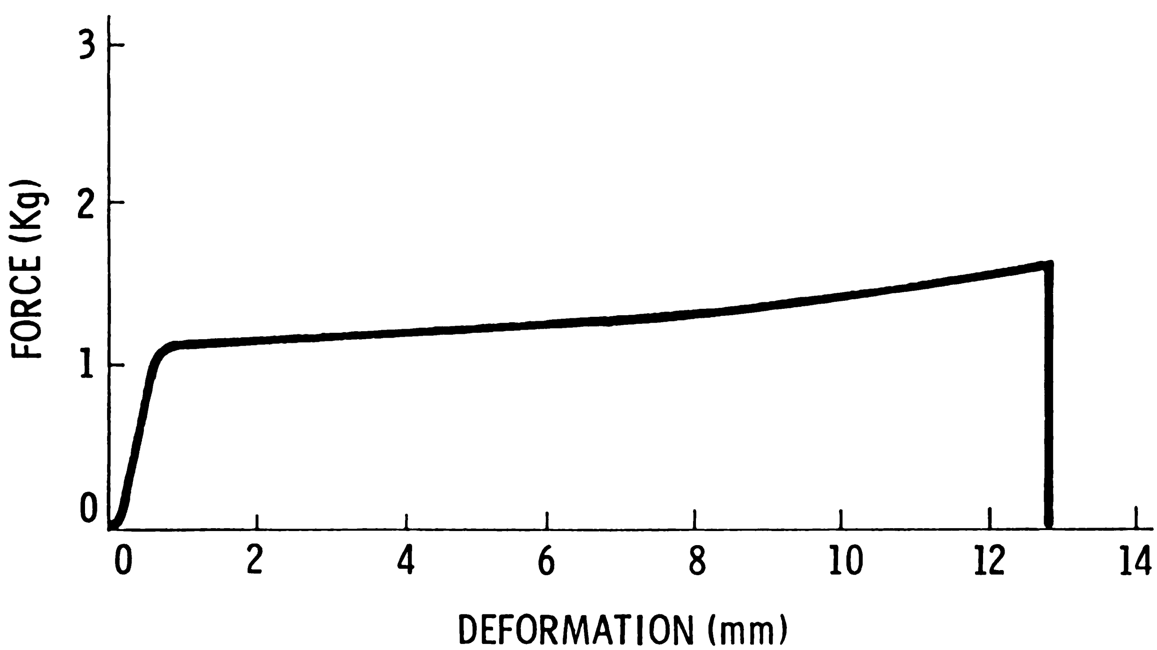


b. Foam Density = 0.0192 gr/cm$^2$

Fig. 3.11 Force-deformation curve of Urea-Formaldehyde foam of two densities subjected to uniaxial compressive load.

Table 3.1 Apparent elastic modulus values ($N/cm^2$) for Urea-Formaldehyde foam as a function of the foam density.

| Sample No. | Density | |
|---|---|---|
| | $0.0112\ gr/cm^3$ | $0.0192\ gr/cm^3$ |
| 1 | 97.31 | 106.67 |
| 2 | 95.70 | 97.31 |
| 3 | 87.66 | 150.49 |
| 4 | 65.40 | 133.70 |
| 5 | 72.55 | 139.96 |
| 6 | 83.36 | 117.86 |
| 7 | 78.19 | 148.65 |
| 8 | 62.55 | 123.16 |
| 9 | 83.60 | 138.43 |
| 10 | 92.19 | 155.86 |
| 11 | 88.10 | 145.97 |
| 12 | 73.09 | 150.49 |
| 13 | 74.44 | 100.62 |
| 14 | 77.27 | 121.48 |
| 15 | 65.41 | 127.64 |
| 16 | 71.25 | 131.84 |
| 17 | 86.15 | 105.94 |
| 18 | 79.12 | 160.04 |
| 19 | 82.99 | 103.87 |
| 20 | 88.63 | 101.03 |
| 21 | 79.46 | 157.61 |
| 22 | 82.14 | 162.08 |
| 23 | 87.37 | 136.77 |
| 24 | 90.50 | 138.06 |
| 25 | 89.10 | 154.66 |
| $\bar{x}$ | 83.53 | 132.41 |
| $\sigma$ | 14.80 | 20.83 |

polymeric foams to compression depends strongly on the foam density. The difference in the polymer matrix for different densities can also be observed from the photomicrographs (Fig. 3.4), obtained with a scanning electron microscope. The results show a distinct increase in the threads--which comprise the foam matrix--with an increase in density. We can relate these photographs to the theoretical model for a foam material, envisioned by Gent and Thomas and verified subsequently through experimentation, to be comprised of a system of n randomly-disposed threads. They established an almost linear relationship between a parameter associated with the threads' cross-sectional area and the foam density.

The validity of using the apparent elastic modulus of the foam as the mechanical property governing its behavior is subject to question since the material response in the plateau region is characterized by inelastic deformation. However, the studies of Rusch (1969, 1970b) have shown that the energy absorption capacity of polymeric foam is dictated by the initial modulus and that low modulus of the plateau region cannot be accounted for sustaining the impact forces. The same approach was used by Wilsea *et al.* (1975) who report values of Young's modulus, for low density forms, similar to those derived in this study. Nevertheless, it might be of value to explore this question in the future, treating the material as an elasto-plastic one. However, as a first approximation, it was considered adequate to use the apparent elastic modulus as the characteristic property.

Since the objective is to maximize energy absorption using a minimum thickness of cushioning, the relationship between energy-absorption potential and foam density needs to be ascertained. The energy values for the two density groups--derived from integration of the force-deformation curves--are given in Table 3.2. The data show that the energy-absorption potential was significantly greater for the higher foam density. This increase is attributed primarily to the increase in the apparent elastic modulus with increase of density as noted above. In addition, the energy-absorbing efficiency is dependent also on a dimensionless function [$\Psi(\varepsilon)$] of the compressive strain ($\varepsilon$) and the apparent Young's modulus (Rusch 1970a). This function, although it is primarily dependent on the buckling of the foam matrix, is also dependent on density of the material.

Increasing the density of the foam results in increased use of the resin, the most expensive component in the entire system. The optimal foam density can be assessed only in conjunction with the second parameter that governs the energy-absorption potential, foam thickness. A combined consideration of these two parameters will be discussed in Chapter 7.

The experimental values for Poisson's ratio given in Table 3.3 illustrate the influence of density on Poisson's

Table 3.2 Energy-absorption capacity (kg-cm) of Urea-Formaldehyde foam samples loaded to 55% strain.

| Sample No. | Density | |
|---|---|---|
| | 0.0112 $gr/cm^3$ | 0.0192 $gr/cm^3$ |
| 1 | 0.81 | 1.61 |
| 2 | 0.69 | 1.24 |
| 3 | 1.04 | 1.27 |
| 4 | 0.58 | 1.38 |
| 5 | 0.69 | 1.04 |
| 6 | 0.69 | 1.27 |
| 7 | 0.92 | 1.27 |
| 8 | 0.81 | 1.15 |
| 9 | 0.81 | 1.50 |
| 10 | 0.69 | 1.04 |
| 11 | 0.69 | 1.27 |
| 12 | 0.58 | 1.27 |
| 13 | 0.92 | 1.15 |
| 14 | 0.81 | 1.38 |
| 15 | 0.92 | 1.27 |
| 16 | 0.69 | 1.27 |
| 17 | 0.69 | 1.50 |
| 18 | 0.69 | 1.38 |
| 19 | 0.81 | 1.27 |
| 20 | 0.81 | 1.27 |
| 21 | 0.92 | 1.27 |
| 22 | 0.69 | 1.15 |
| 23 | 0.58 | 1.27 |
| 24 | 0.69 | 1.50 |
| 25 | 0.81 | 1.27 |
| $\bar{x}$ | 0.76 | 1.28 |
| $\sigma$ | 0.12 | 0.14 |

Table 3.3 Poisson's ratio for Urea-Formaldehyde foam as a function of foam density.

| Sample No. | Density | |
|---|---|---|
| | 0.0112 $gr/cm^3$ | 0.0192 $gr/cm^3$ |
| 1 | 0.362 | 0.431 |
| 2 | 0.342 | 0.402 |
| 3 | 0.351 | 0.368 |
| 4 | 0.339 | 0.345 |
| 5 | 0.413 | 0.379 |
| 6 | 0.343 | 0.384 |
| 7 | 0.331 | 0.412 |
| 8 | 0.403 | 0.351 |
| 9 | 0.336 | 0.335 |
| 10 | 0.386 | 0.331 |
| 11 | 0.354 | 0.361 |
| 12 | 0.394 | 0.370 |
| 13 | 0.363 | 0.340 |
| 14 | 0.391 | 0.348 |
| 15 | 0.330 | 0.369 |
| 16 | 0.329 | 0.364 |
| 17 | 0.362 | 0.392 |
| 18 | 0.358 | 0.329 |
| 19 | 0.376 | 0.339 |
| 20 | 0.384 | 0.391 |
| $\bar{x}$ | 0.362 | 0.367 |
| $\sigma$ | 0.025 | 0.028 |

ratio. No significant difference was found between the two density groups. These results are in agreement with studies made by Gent and Thomas (1963), on the mechanics of foamed elastic material, who report no systematic trend of Poisson's ratio with foam density. The average value found in these experiments ($\nu = 0.36$) is similar to the value reported by Gent and Thomas ($\nu = 0.33$) for polymeric foams with a density similar to Urea-Formaldehyde. The average is also in reasonable accord with their theoretically predicted value of 0.25 for a foam model with randomly disposed threads.

Examples of the impact force versus time trace on the oscilloscope are given in Fig. 3.12 (a-d) for drop heights of 5.08 cm, 15.2 cm, 30.5 cm and 38.1 cm. The effect of drop heights on the maximum deceleration forces is given in Fig. 3.13. As expected, impact forces increase with increased drop height. The results are slightly lower than those reported by Simpson (1971), the changes being attributed primarily to the different method of measurements. Similar results were also reported by Hamann (1967). As mentioned earlier, variation in testing results are conceivable and expected because of variations in testing equipment. However, since absolute values were not attempted, the range of these results is considered valid and will be used for deriving the associated indentation values of the apple.

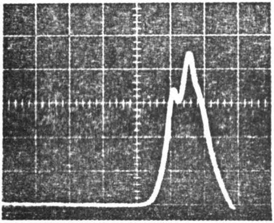

a. Impact force of 4.1 kg corresponding to a drop height of 5.09 cm (Scope sensitivity = 0.90 kg/cm)

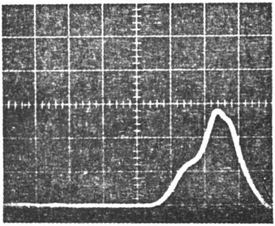

b. Impact force of 12.7 kg corresponding to a drop height of 15.2 cm (Scope sensitivity 4.5 kg/cm)

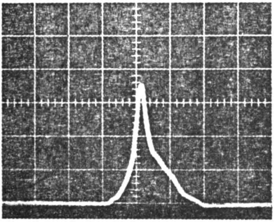

c. Impact force of 15.3 kg corresponding to a drop height of 30.5 cm (Scope sensitivity= 4.5 kg/cm)

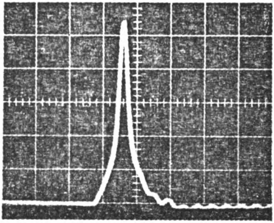

d. Impact force of 24.5 kg corresponding to a drop height of 38.1 cm (Scope sensitivity = 4.5 kg/cm)

Fig. 3.12 Impact forces vs. time of free fall 'Golden Delicious' apples.

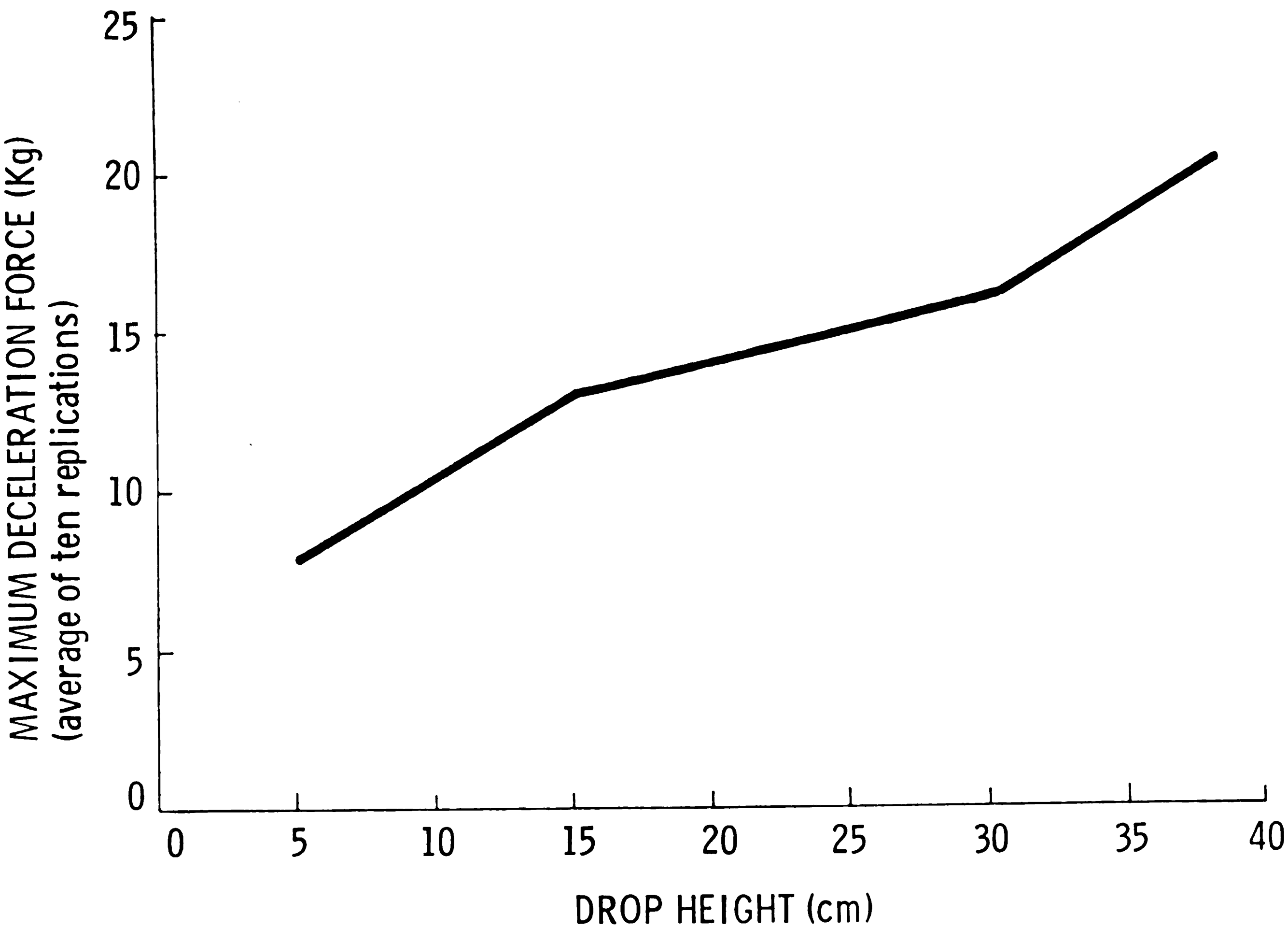


Fig. 3.13 Impact forces of apple as a function of drop heights.

# 4. EVALUATION OF APPLE DEFORMATION USING THE AXISYMMETRIC BOUSSINESQ METHOD

## 4.1 Theoretical Considerations

### 4.1.1 The mathematical model and basic assumptions

An exact solution of stress and strain problems in agricultural products cannot, in general, be obtained because the product, inherently, does not lend itself to a rigorous analytical treatment. Nevertheless, in order to obtain both qualitative and quantitative values, a mathematical model can be constructed simulating the actual physical system. The model is then assumed to be subjected to a given loading, and analyzed to obtain an approximation of the response (deformation) that would occur if the real materials were subjected to the same loading.

A foam-encapsulated apple being indented by the end of a limb with a circular cross-section was selected as a representative case of one of the various situations that typify a free-falling apple in the process of mechanical harvesting. The solution, however, should lend itself, with some modifications, to any other limb configurations. The mathematical model used to simulate the given case consists of an infinite linear elastic layer (foam), designated as region (1), resting on a linear elastic sub-space (apple), designated as region (2), as shown in Fig. 4.1. The elastic layer is bounded by the planes $z = 0$ and $z = -h$ of a cylindrical coordinate system $(r, \theta, z)$ where the z axis is directed downward. The elastic sub-space is in perfect contact with the elastic layer and is bounded by $z = 0$ and $z \to \infty$.

A vertical load (flat-ended rigid punch) is applied to the layer, over a circular area of radius (a). Some basic assumptions were made to facilitate the theoretical analysis and to obtain a tractable form of solution. Although this is a common practice, the validity of some of the assumptions may be debatable. Since most solutions of three-dimensional problems of elasticity have proven to be unattainable in simple form (Sneddon 1951), it seems both reasonable and practical to obtain a first approximated solution based on these assumptions.

The following assumptions were made: 1) The half-space (apple) was assumed to be an isotropic, homogeneous linear elastic solid. Some errors are introduced with these assumptions since the fruit flesh is composed of living cells, mainly of cellulose fibrils arranged in a random network. Moreover, part of the volume between the cells is occupied with intercellular middle lamella where pectic compounds bind the cells together (Mohsenin 1970).

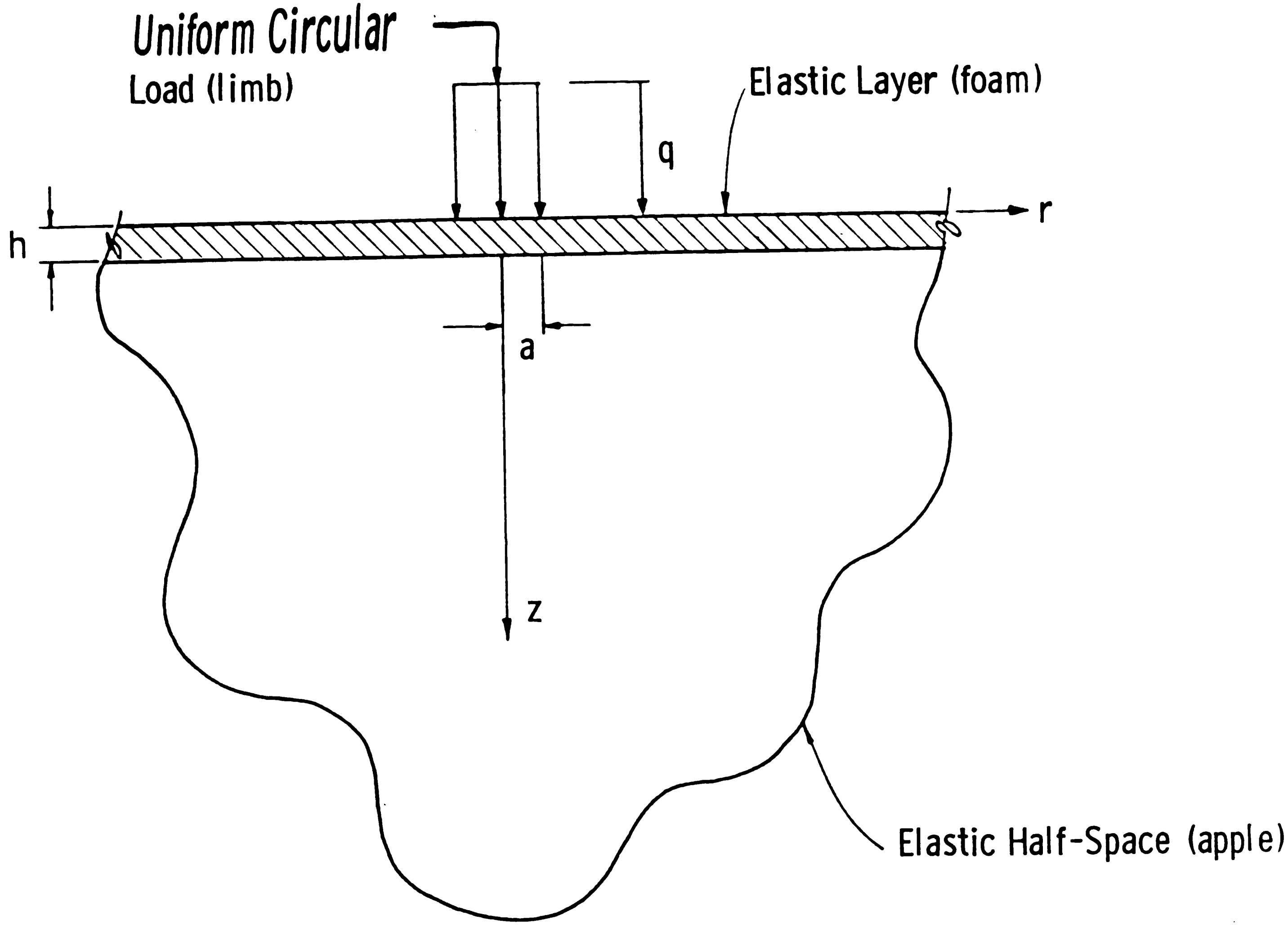


Fig. 4.1 Mathematical model of foam-encapsulated apple indented by a limb.

Studies by Hamann (1967), however, have shown that differences in material properties were not large if the apple was considered anisotropic. Although the apple definitely is not homogeneous, since the core, seed and skin regions are obviously different, the modulus values are of the same order of magnitude (Clevenger and Hamann 1966 and Chappell and Hamann 1968), and the error introduced is acceptable. In addition, the apple is not elastic but it is generally considered a viscoelastic material. The inaccuracy resulting from an assumption of elasticity is tolerable because the applied load occurs over a short time period. Specific values of the elastic modulus and Poisson's ratio of the apple were obtained from the work of Hamann (1967). 2) The layer of foam was assumed to be an isotropic, homogeneous linear elastic solid. It is recognized that the assumption of elastic behavior is questionable since the general characteristics of the foam is elasto-plastic. However, for the particular range of loading in this study it seems justified as a first approximation. Any distinct discrepancy would require incorporation of the true characteristics. 3) Body forces are neglected (a body force solution may be superimposed on the results obtained). 4) Since the study is concerned with only a short phase of the apple life-span, no thermal changes are considered. 5) Small deformation theory is assumed and its applicability seems valid since the major concern of the study is with small deformations (indentation) imparted to the apple by induced impacts. 6) The deformation of the model is assumed quasi-static, and the model is assumed to be at rest prior to application of the load. 7) Forces of friction are absent between the indenting punch (the limb) and the elastic layer (no shearing stress at the boundary).

## 4.1.2 Problem formulation and the solution procedure

### 4.1.2.1 The constitutive equations and boundary conditions

The suggested mathematical model pertains to a linear elastic material. The constitutive equation for such a material is:

$$\sigma_{ij} = C_{ijkl}E_{kl}{}^{1} \tag{4.1}$$

This equation is the generalized form of Hooke's law, where the second Piola-Kirchoff stress tensor is related to the Lagrangian strain tensor, $E_{kl}$.

Since the material in this model is isotropic, the number of independent coefficients in $C_{ijkl}$ is two.

---

[1]For conciseness the indicial notation is adopted, where letter indices, either subscripts or superscripts, are appended to the kernel letter representing the tensor quality of interest. Repeated indices imply summation.

Equation (4.1) can be rewritten as:

$$\sigma_{ij} = \{\lambda\delta_{ij}\delta_{kl} + \mu(\delta_{ik}\delta_{jl} + \delta_{il}\delta_{jk})\}E_{kl} \tag{4.2}$$

which may also be written as:

$$\sigma_{ij} = \lambda E_{kk}\delta_{ij} + 2\mu E_{ij} \tag{4.3}$$

where $\lambda$ and $\mu$ are the Lamé constants.

In the small deformation theory of linear elasticity no distinction is made between the Eulerian and the Lagrangian coordinates and the basic constitutive equation can be written as:

$$\sigma_{ij} = \lambda\varepsilon_{kk}\delta_{ij} + 2\mu\varepsilon_{ij} \tag{4.4}$$

The boundary conditions that usually appear in problems of elastostatics are either displacement and/or surface traction specified. Our problem is equivalent to a mixed boundary value problem where the displacement is specified over part of the boundary and the stress traction over the rest. Since stresses can also be stated in terms of derivatives of the displacements, we are motivated to seek a formulation in terms of displacements.

Substituting the definition of strain, symbolically defined as one-half the sum of the pre-gradient and the post-gradient of the displacement vector,

$$\bar{\varepsilon} = \frac{1}{2} (\bar{U} \overleftarrow{\nabla} + \vec{\nabla} \bar{U}) \tag{4.5}$$

where $\bar{\nabla}$ is a vector operator (the del operator) defined as

$$\bar{\nabla} = \hat{\imath}_{(k)} \frac{\partial}{\partial X_k} \tag{4.6}$$

in Cartesian coordinates.

Substitution of (4.5) into the stress-strain law yields:

$$\sigma_{ij} = \lambda \varepsilon_{kk} \delta_{ij} + \mu (\nabla_j U_i + \nabla_i U_j) \tag{4.7}$$

Substituting these equations into the Cauchy's equation of motion used in linear elasticity theory,

$$\bar{\nabla}_x \bar{\bar{\sigma}} + \rho \bar{b} = \rho \frac{\partial^2 U}{\partial t^2} \tag{4.8}$$

gives:

$$\nabla_i (\lambda \varepsilon_{kk}) \delta_{ij} + \nabla_i \{\mu (\nabla_j U_i + \nabla_i U_j)\} + \rho b_j = \rho \ddot{U}_j \tag{4.9}$$

If the material is homogeneous, body forces are neglected and the problem considered elastostatic (quasi-static), then (4.9) reduces to the Navier equations of elastostatics:

$$\mu\nabla^2 U_j + (\lambda + \mu)\nabla_j\nabla_i U_i = 0 \tag{4.10}$$

which can also be written symbolically as:

$$\mu\nabla^2\overline{U} + (\lambda + \mu)\overline{\nabla}(\overline{\nabla}\cdot\overline{U}) = 0 \tag{4.11}$$

In the case of axial symmetry (assumed in our model) the displacement vector $\overline{U}$ assumes the form $(U_r, 0, U_z)$ in a cylindrical coordinate system $(r, \theta, z)$.

$$\overline{U} = U_r\hat{i}_r + U_z\hat{i}_z \tag{4.12}$$

Substituting these expressions into the Navier equation yields:

$$(\nabla^2 - \frac{1}{r^2})U_r\hat{i}_r + \nabla^2 U_z\hat{i}_z + \frac{1}{1-2\nu}[\hat{i}_r\frac{\partial}{\partial r}(\frac{\partial U_r}{\partial r} + \frac{U_r}{r} + \frac{\partial U_z}{\partial z})$$

$$+ \hat{i}_z\frac{\partial}{\partial z}(\frac{\partial U_r}{\partial r} + \frac{U_r}{r} + \frac{\partial U_z}{\partial z})] = 0 \tag{4.13}$$

The above equation can be decomposed into

$$\nabla^2 U_r - \frac{1}{r^2}U_r + \frac{1}{1-2\nu}\frac{\partial}{\partial r}(\frac{\partial U_r}{\partial r} + \frac{U_r}{r} + \frac{\partial U_z}{\partial z}) = 0 \tag{4.14}$$

$$\nabla^2 U_z + \frac{1}{1-2\nu}\frac{\partial}{\partial z}\left(\frac{\partial U_r}{\partial r} + \frac{U_r}{r} + \frac{\partial U_z}{\partial z}\right) = 0 \qquad (4.15)$$

4.1.2.2 A solution

The solution[2] to Navier equations (4.14) and (4.15) is given by:

$$2\mu U_r(r, z) = \frac{\partial F}{\partial r} + z\frac{\partial G}{\partial r} \qquad (4.16)$$

$$2\mu U_z(r, z) = \frac{\partial F}{\partial z} + z\frac{\partial G}{\partial z} - (3-4\nu)G \qquad (4.17)$$

Where F(r, z) and G(r,z) are harmonic functions and $\nu$ is Poisson's ratio. Using the expression derived for the displacements, the stress components $\sigma_{zz}(r, z)$ and $\sigma_{rz}(r, z)$ may be expressed in terms of the harmonic functions F and G.

$$\sigma_{zz}(r, z) = (\lambda + 2\mu)\frac{\partial U_z}{\partial z} + \lambda\left\{\frac{\partial U_r}{\partial r} + \frac{U_r}{r}\right\} =$$

$$\frac{\partial^2 F}{\partial z} + z\frac{\partial^2 G}{\partial z} - 2(1-\nu)\frac{\partial G}{\partial z} \qquad (4.18)$$

---

[2] The basic equations and their solutions were derived from Dhaliwal's work on the axi-symmetric Boussinesq's method (Dhaliwal 1970).

$$\sigma_{rz}(r,\ z) = \mu\{\frac{\partial U_r}{\partial z} + \frac{\partial U_z}{\partial r}\} = \frac{\partial^2 F}{\partial r \partial z} + z\frac{\partial^2 G}{\partial r \partial z} -$$

$$(1 - 2\nu)\frac{\partial G}{\partial r} \qquad (4.19)$$

To facilitate the mathematical manipulation, the harmonic functions can be represented in their transformed form for each region of the domain:

$$\left.\begin{aligned} F^{(1)}(r,\ z) &= H_o[A(\xi)e^{-\xi z} + B(\xi)e^{\xi z};\ \xi \to r] \\ G^{(1)}(r,\ z) &= H_o[c(\xi)e^{-\xi z} + D(\xi)e^{\xi z};\ \xi \to r] \end{aligned}\right\} \quad h \leq z < 0 \qquad (4.20)$$

$$\left.\begin{aligned} F^{(2)}(r,z) &= H_o[E(\xi)e^{-\xi z};\ \xi \to r] \\ G^{(2)}(r,z) &= H_o[F(\xi)e^{-\xi z};\ \xi \to r] \end{aligned}\right\} \quad z > 0 \qquad (4.21)$$

Where $A(\xi)$, $B(\xi)$. . . $F(\xi)$ are arbitrary functions to be determined from the prescribed boundary and continuity conditions.

The quantity $H_n$ in the above equations denotes the Hankel transform of order n or a function (r) defined as:

$$\mathit{f}^{-n}(\xi) = H_n\{f(r);\ \xi\} = \int_0^\infty rf(r)J_n(\xi r)dr \qquad (4.22)$$

where $J_n$ is the Bessel function of order n of the first kind.

Substituting for $F^{(1)}$ and $G^{(1)}$ from (4.20) in (4.16), (4.17), (4.18) and (4.19) yields the expressions for the displacement and stress components for region 1:

$$2\mu_1 U_r^{(1)}(r,z) = \int_0^\infty \xi[(A+zC)e^{-\xi z} + (B+zD)e^{-\xi z}]J_1(\xi r)d\xi \quad (4.23)$$

$$2\mu_1 U_z^{(1)}(r,z) = \int_0^\infty [-\{\xi(A+zC) + (3-4\nu_1)C\ e^{-\xi z} +$$

$$\{\xi(B+zD) - (3-4\nu_1)D\}e^{\xi z}]J_0(\xi r)d\xi \quad (4.24)$$

$$\sigma_{zz}^{(1)}(r,z) = \int_0^\infty [\xi(A+zC) + 2(1-\nu_1)Ce^{-\xi z} +$$

$$\{\xi(B+zD) - 2(1-\nu_1)D\}e^{\xi z}]\xi J_0(\xi r)d\xi \quad (4.25)$$

$$\sigma_{rz}^{(1)}(r,z) = \int_0^\infty [-\{\xi(A+zC) + (1-2\nu_1)C\}e^{-\xi z}$$

$$+ \{\xi(B+zD) - (1-2\nu_1)D\}e^{\xi z}]J_1(\xi r)d\xi \quad (4.26)$$

The expressions for region 2 may be obtained by replacing A, C, $\mu$, $\nu$, by E, F, $\mu_2$, $\nu_2$ and setting B = D = 0.

When the elastic layer is indented by a rigid punch the following boundary conditions exist:

$$U_z^{(1)}(r,-h) = \delta - f(\tfrac{r}{a}), \quad 0 \le r \le a \quad (4.27)$$

$$\sigma_{zz}^{(1)}(r,-h) = 0 \qquad r > a \quad (4.28)$$

$$\sigma_{rz}^{(1)}(r,-h) = 0 \qquad r \geq 0 \qquad (4.29)$$

where the function $f(\frac{r}{a})$ is determined by the shape of the punch, (a) is the radius of the punch (for a cylindrical punch) and ($\delta$) is the depth the punch penetrates the elastic layer.

The assumption of perfect contact between the layer and the half-space implies the following continuity conditions at z = 0:

$$U_z^{(1)}(r,o) - U_z^{(2)}(r,o) = 0 \qquad r \geq 0 \qquad (4.30)$$

$$\sigma_{zz}^{(1)}(r,o) - \sigma_{zz}^{(2)}(r,o) = 0 \qquad r \geq 0 \qquad (4.31)$$

$$\sigma_{rz}^{(1)}(r,o) - \sigma_{rz}^{(2)}(r,o) = 0 \qquad r \geq 0 \qquad (4.32)$$

$$U_r^{(1)}(r,o) - U_r^{(2)}(r,o) = 0 \qquad r \geq 0 \qquad (4.33)$$

The continuity conditions will be satisfied if:

$$4\nu'A = k_3E - k_1\xi^{-1}F, \; 4\nu'B = \mu^1(3-4\nu_1)E - k_1\xi^{-1}F$$

$$4\nu'c = k_2F, \; 4\nu'd = 2\xi\mu'E + \mu'(3-4\sigma_2)F \qquad (4.34)$$

where $\mu = \mu_1/_{\mu 2}$; $\mu' = \mu - 1$, $\nu' = 1 - \nu$

$$k_1 = \mu(3-4\nu_2)(1-2\nu_1) - (1-2\nu_2)(3-4\nu_1)$$

$$k_2 = 1 + \mu(3-4\nu_2), \; k_3 = \mu + 3 - 4\nu_1$$

The boundary and continuity conditions lead to the following relationship between E and F

$$E = -\xi^{-1}F[G(\nu_1+\nu_2) - 4(1+2\nu_1\nu_2) + \xi h\, k_2 + \{2(\nu_2-\nu_1) - \xi h\mu'(3-4\nu_2)\}e^{-2\xi h}][-k_3+ \mu'(1-2\xi h)e^{-2\xi h}]^{-1} \tag{4.35}$$

Introducing new variables defined as

$$x = \frac{r}{a}, \; \zeta = \xi a$$

$$G(\zeta) = -\frac{k_2 k_3}{4\nu} \cdot \frac{\xi e^{\xi h}F(\xi)\chi(2\xi h)}{-k_3+\mu'(1-2\xi h)} e^{-2\xi h} \tag{4.36}$$

The boundary conditions are satisfied if $G(\zeta)$ is the solution of the dual integral equations

$$\int_0^\infty \zeta G(\zeta)J_o(\zeta x)d\zeta = 0 \qquad 1<\chi \tag{4.37}$$

$$\int_0^\infty [1+N(2\zeta\frac{h}{a}]G(\zeta)J_o(\zeta x)d\zeta = -\frac{\mu_1 a}{1-\nu_1}\{\delta - f(x)\} \qquad 0\leq x<1 \tag{4.38}$$

Where the functions $\chi(x)$ and $N(x)$ are defined by:

$$\chi(x) = 1 + [b + c(1+x^2)]e^{-x} + bce^{-2x}$$

$$N(x) = -e^{-x}[b + c(1+x)^2 + 2bce^{-x}][\chi(x)]^{-1} \quad (4.39)$$

$$\text{and } b = \frac{k_4}{k_2},\ c = \frac{-\mu'}{k_3},\ k_4 = (3-4\nu_1) - \mu(3-4\nu_2)$$

these dual integral equations have been considered by number of authors, primarily Sneddon (1951), and are solved by use of some relations between the Hankel and Fourier transforms.

The first boundary is satisfied if:

$$G(\zeta) = \frac{2}{\pi}\int_0^1 \phi(t)\cos(\zeta t)dt \quad (4.40)$$

and the second, if $\phi(t)$ satisfies the Fredholm integral equation

$$\phi(t) + \frac{a}{h\pi}\int_0^1 k(x,t)\phi(x)dx = -\frac{\mu_1 a}{1-\nu_1}\frac{d}{dt}\left[\int_0^1 \frac{\delta - f(x)}{\sqrt{t^2-x^2}}xdx\right] \quad (4.41)$$

$$0 \leq t < 1$$

$$\text{Where } K(x,t) = 2\int_0^\infty N(2U)\cos(\tfrac{a}{h}tU)\cos(\tfrac{a}{h}xU)\,dU \quad (4.42)$$

After solving the integral equation (4.41) numerically, the solutions for the displacement and stress components can be derived, using the expressions developed earlier.

## 4.2 Numerical Evaluation

The analytical solution presented at 4.1 is evaluated numerically for a specific example.

The mechanical properties for the elastic layer (foam), region one, were derived in section 3 and their averaged values are given in Table 4.1 for two foam densities. These values were used in the numerical calculations.

Table 4.1 Mechanical properties of Urea-Formaldehyde foam.

| Density ($gr/cm^3$) | Apparent Elastic Modulus - [$E_{f_1}$] ($N/cm^2$) | Apparent Modulus of Rigidity - [$\mu_1$] ($N/cm^2$) | Poisson's Ratio ($\nu_1$) |
|---|---|---|---|
| 0.0112 | 83.3 | 30.6 | 0.36 |
| 0.0192 | 132.2 | 48.6 | 0.36 |

The mechanical properties of the half-space (apple), region two, were derived from the works of Hamann (1967) and Mohsenin (1970)(See discussion in section 6.2) and are given in Table 4.2 for two varieties commonly available in fresh market.

Table 4.2 Mechanical properties of apples.

| Variety | Modulus of Elasticity - [$E_2$] ($N/cm^2$) | Modulus of Rigidity - [$\mu_2$] ($N/cm^2$) | Poisson's Ratio ($\nu_2$) |
|---|---|---|---|
| Golden Delicious | 378 | 155 | 0.218 |
| Red Delicious | 334 | 137 | 0.219 |

The prescribed displacement boundary conditions ($\delta$ - amount of indentation) were derived from the expression for the force (P) that must be applied to the punch to yield a known indentation. This expression has been worked out by Dhaliwal (1970) and is given in the form:

$$P = -2\pi \int_0^1 \sigma_{zz}^{(1)}(r,h)\ r dr = -4\int_0^1 \phi(t)dt \qquad (4.43)$$

The last integral has been programmed to yield numerical values of P vs. $\delta$. Thus for a known force, the corresponding value of indentation is derived utilizing the equation:

$$P/(\mu_1\delta) = P^* \Rightarrow \delta = \frac{P}{P^*\mu_1} \qquad (4.44)$$

where ($P^*$) is a function of (H)(Ratio of the layer thickness (h) to the punch radius (a) which is related to the normal stress and pressure under the punch, and is calculated in the computer program. The punch radius (a) (simulating a limb stub) was selected as 5 mm and (H) obtained for three values of foam thickness, h = 15 mm, the minimum effective thickness established in earlier studies (Sarig 1975), h = 20 mm and h = 25 mm.

Values of $P^*$, $\mu_1$, $\mu_2$, $\nu_1$, and $\nu_2$, as calculated by the program, are given in Table 4.3, and the corresponding value of indentation -($\delta$).

Table 4.3 Values of indentation ($\delta$) induced in a U-F foam layer as a function of the impact forces and the foam's modulus of rigidity.

| Foam Density [$gr/cm^3$] | Foam Modulus of Rigidity ($\mu_1$) [$N/cm^2$] | Apple Modulus of Rigidity ($\mu_2$) [$N/cm^2$] | $\frac{\mu_1}{\mu_2}$ | Foam Thickness (h) [mm] | H=h/a | Impact Forces - P [Kg] 4.5 | 9.0 | 18.0 | 27.0 | P* [mm] |
|---|---|---|---|---|---|---|---|---|---|---|
| | | | | | | Indentation - $\delta$ [mm] | | | | |
| 0.112 | 30.6 | 155 | 0.190 | 15 | 3 | 0.711 | 1.422 | 2.845 | 4.267 | 203.96 |
| 0.112 | 30.6 | 155 | 0.190 | 20 | 4 | 0.734 | 1.473 | 3.048 | 4.547 | 191.52 |
| 0.112 | 30.6 | 155 | 0.190 | 25 | 5 | 0.787 | 1.575 | 3.150 | 4.724 | 184.40 |
| 0.192 | 48.6 | 155 | 0.313 | 15 | 3 | 0.457 | 0.940 | 1.880 | 2.819 | 193.80 |
| 0.192 | 48.6 | 155 | 0.313 | 20 | 4 | 0.483 | 0.991 | 1.981 | 2.972 | 184.40 |
| 0.192 | 48.6 | 155 | 0.313 | 25 | 5 | 0.508 | 1.016 | 2.032 | 3.073 | 178.82 |
| 0.112 | 30.6 | 137 | 0.220 | 15 | 3 | 0.711 | 1.448 | 2.870 | 4.318 | 201.42 |
| 0.112 | 30.6 | 137 | 0.220 | 20 | 4 | 0.762 | 1.524 | 3.048 | 4.572 | 180.74 |
| 0.112 | 30.6 | 137 | 0.220 | 25 | 5 | 0.787 | 1.575 | 3.175 | 4.750 | 182.88 |
| 0.192 | 48.6 | 137 | 0.354 | 15 | 3 | 0.483 | 0.965 | 1.905 | 2.870 | 191.01 |
| 0.192 | 48.6 | 137 | 0.354 | 20 | 4 | 0.508 | 0.991 | 2.007 | 2.997 | 182.37 |
| 0.192 | 48.6 | 137 | 0.354 | 25 | 5 | 0.508 | 1.016 | 2.057 | 3.099 | 24.89 |

Since the main objective is evaluation of deformation induced in the encapsulated apple, the analysis will be restricted to that of deriving the displacement of the half-space--$U_z^{(2)}(r,z)$.

Recalling from (4.24), the corresponding expression for region 2 is:

$$2\mu_2 U_z^{(2)}(r,z) = \int_0^\infty [-\{\xi(E+zF) + (3-\nu_2)F\}e^{-\xi z}]J_o(\xi r)d\xi \qquad (4.45)$$

To facilitate the mathematical manipulation and the computer implementation, the following additional notations have been used:

$$k_4 = (3-4\nu_1) - \mu(3-4\nu_2), \ \xi = t/h$$

$$Z = Z' = \frac{z}{a}, \ H = h' = \frac{h}{a} \qquad r' = \frac{r}{a} \qquad (4.46)$$

where (a) is the punch radius and (h) is the layer thickness.

Incorporating the relations developed in Section 4.2 and the notations introduced here, we can write equation (4.45) in a form which lends itself to computer programming:

$$U_z^{(2)}(r',z') = \frac{2\nu'}{h'\mu k_2 k_3} \int_o^\infty e^{-t} FcTG \cdot \frac{e^{\frac{-z't}{h'}}[-k_3+\mu'(1-2t)e^{-2t}]}{1+\{b+c(1+4t^2)\}e^{-2t}+bce^{-4t}} \cdot J_o(\frac{tr'}{h'}) \cdot$$

$$[\frac{tz'}{h'} + 3-4\nu_2 - [\frac{6(\nu_1+\nu_2)-4(1+2\nu_1\nu_2)+k_2t+\{2(\nu_2-\nu_1)-\mu't(3-U\nu_2)\}e^{-2t}}{-k_3+\mu'(1-2t)e^{-2t}}]]dt \quad (4.47)$$

$$\text{where } FcTG = \frac{2}{\pi} \int_o^1 \phi'(U)\cos(\frac{tU}{h'})\, dU \quad (4.48)$$

$$\phi'(t) + \frac{1}{\pi h'} \int_o^1 K(x,t)\phi'(x)dx = -\frac{\mu_1}{1-\nu_1} R(t) \quad (4.49)$$

$$R(t) = \frac{d}{dt} \int_o^t \frac{\delta - f(x)}{\sqrt{t^2-x^2}}\, xdx \quad (4.50)$$

and

$$K(x,t) = -\int_o^\infty \frac{e^{-U}[b+c(1+U)^2+2bce^{-U}]}{1+[b+c(1+U^2)]e^{-U}+bce^{-2U}} \cos(\frac{tU}{2h'})\cos(\frac{xU}{2h'})dU \quad (4.51)$$

A computer program was written to determine the values of $U_z^{(2)}(r,z)$ for a given value of $\nu_1$, $\nu_2$, $\mu_1$, $\mu_2$ and H. Equation (4.49) is a Fredholm integral equation of the second kind of the form

$$\phi(x) - \lambda \int_a^b K(x,y)\phi(y)dy = (x) \quad (4.52)$$

where f(x) is an unknown function, K(x,y) is the kernel of the equation, (x) the free term and $\lambda$ a numerical parameter. This equation is often solved (Kantorovich and Krylov 1958) by replacing it with a finite system of linear algebraic equations. Such a system can be constructed if we replace the integral by a quadrature sum:

$$\phi(x) - \lambda \sum_{k=1}^{m} A_k K(x,x_k)\,\phi(x_k) = f(x) + R(x) \qquad (4.53)$$

If we substitute successively $x = x_1, x_2$ ---- $x_n$ in this equation we obtain a system of linear equations where the numbers $\phi(x_i)$, the values of the desired function at the points $x_i$, satisfy:

$$\phi(x_i) - \lambda \sum_{k=1}^{m} A_k K(x_i,x_k)\phi(x_k) = f(x_i) + R(x_i)(i=1,2,----n \qquad (4.54)$$

Neglecting the remainder term $R(x_i)$, we obtain a system of n equations in the n approximate values $\tilde{\phi}(x_1)$, $\tilde{\phi}(x_2)$---- $\tilde{\phi}(x_n)$:

$$\tilde{\phi}(x_1) - \lambda \sum_{k=1}^{m} A_k K(x_i,x_k)\tilde{\phi}(x_k) = f(x_i)(i = 1, 2,----n) \quad (4.55)$$

On solving this system of equations, we find approximations to the values of the desired function $\phi(x_1)$, $\phi(x_2)$---$\phi(x_n)$.

The integral in equation (4.49) was solved using the Simpson integration method with N = 19 points, and the system of equations by the method of elimination using the largest pivotal divisor.

The integrals with limits from zero to infinity can be solved by the method of 10 point Gaussian-Laguerre quadrature formula (Krylov 1962) where the integral of the form:

$$\int_0^\infty x^\alpha e^{-x} f(x)\, dx \tag{4.56}$$

is replaced by the quadrature formula

$$\int_0^\infty x^\alpha e^{-x} f(x) dx = \sum_{k=1}^{m} A_k f(x_k) + R(f) \tag{4.57}$$

The remainder term R(f) is usually ignored, and values of $x_k$ and $A_k$ have been tabulated (Krylov 1962) for various values of n.

The Bessel function $J_o(\frac{tr'}{h'})$ is calculated by a polynomial approximation given in the Handbook of Mathematical Functions (Abramowitz and Stegun, edit., 1965).

## 4.3 Results and Discussion

The deformation of the apple, under the given boundary conditions, $U_z^2(r,z)$ was derived from the computer program executed on a CDC 6500 digital computer. Four values of indentations were selected, associated with the four selected drop heights (Section 3). The deformation was calculated as a function of the z-axis for values of (r) from r = 0 to r = 35 (the radius of the apple in millimeters). A sample result of the output is given in

Tables 4.4-4.7 for apples of the 'Golden Delicious' variety encapsulated in U-F foam of 15 millimeters thickness and density of 0.0112 $gr/cm^3$ under impact forces of 4.5, 9, 18 and 27 kgs respectively. The effect of changing the thickness of the layer and changing the foam density is illustrated in Fig. 4.2 for the case of the same apple variety under an impact force of 4.5 kg. It can be clearly seen that changing the foam thickness has a more pronounced effect on reducing the apple deformation than changing the foam density. In all cases the deformation converges to an asymptotic value at the center of the apple, which for all practical purposes can be considered zero. Nevertheless, the deformation value at the interface between the foam layer and the apple ($z = 0$), is very small as can be seen from Table 4.8. Apples with this amount of deformation would classify as extra-fancy, using U.S. Grading standards (Burt 1959). We may therefore conclude that a foam thickness of 15 millimeters of standard density (0.0112 $gr/cm^3$) would be adequate to ensure minimal damage.

Table 4.4 Axial deformation (mm) of a 'Golden Delicious' apple encapsulated in Urea-Formaldehyde foam under impact force of 4.5 kg (foam density - 0.0112 $gr/cm^3$; foam thickness - 15 mm).

| Z-axis (mm) | Radius - r (mm) 0 | 5 | 10 | 15 | 20 | 25 | 30 | 35 |
|---|---|---|---|---|---|---|---|---|
| 0 | 0.097 | 0.074 | 0.059 | 0.044 | 0.034 | 0.027 | 0.023 | 0.019 |
| 5 | 0.061 | 0.058 | 0.050 | 0.040 | 0.033 | 0.027 | 0.022 | 0.019 |
| 10 | 0.049 | 0.046 | 0.042 | 0.036 | 0.030 | 0.026 | 0.022 | 0.019 |
| 15 | 0.040 | 0.039 | 0.036 | 0.032 | 0.028 | 0.024 | 0.021 | 0.019 |
| 20 | 0.034 | 0.033 | 0.031 | 0.029 | 0.026 | 0.023 | 0.020 | 0.018 |
| 25 | 0.029 | 0.029 | 0.028 | 0.026 | 0.024 | 0.022 | 0.020 | 0.018 |
| 30 | 0.026 | 0.026 | 0.025 | 0.023 | 0.022 | 0.020 | 0.019 | 0.017 |
| 35 | 0.023 | 0.023 | 0.022 | 0.021 | 0.020 | 0.019 | 0.018 | 0.016 |

Table 4.5 Axial deformation (mm) of a 'Golden Delicious' apple encapsulated in Urea-Formaldehyde foam under impact force of 9 kg (foam density - 0.0112 $gr/cm^3$; foam thickness - 15 mm)

| z-axis (mm) | Radius - r (mm) | | | | | | | |
|---|---|---|---|---|---|---|---|---|
| | 0 | 5 | 10 | 15 | 20 | 25 | 30 | 35 |
| 0 | 0.163 | 0.149 | 0.116 | 0.089 | 0.068 | 0.054 | 0.045 | 0.037 |
| 5 | 0.122 | 0.115 | 0.099 | 0.081 | 0.065 | 0.053 | 0.044 | 0.038 |
| 10 | 0.097 | 0.093 | 0.084 | 0.072 | 0.061 | 0.051 | 0.044 | 0.038 |
| 15 | 0.080 | 0.077 | 0.072 | 0.064 | 0.056 | 0.049 | 0.040 | 0.037 |
| 20 | 0.068 | 0.066 | 0.062 | 0.057 | 0.052 | 0.046 | 0.041 | 0.037 |
| 25 | 0.059 | 0.058 | 0.055 | 0.052 | 0.047 | 0.043 | 0.039 | 0.035 |
| 30 | 0.052 | 0.051 | 0.050 | 0.047 | 0.044 | 0.040 | 0.037 | 0.034 |
| 35 | 0.046 | 0.046 | 0.045 | 0.043 | 0.040 | 0.038 | 0.035 | 0.032 |

Table 4.6 Axial deformation (mm) of a 'Golden Delicious' apple encapsulated in Urea-Formaldehyde foam under impact force of 18 kg (foam density - 0.0112 $gr/cm^3$; foam thickness - 15 mm).

| z-axis (mm) | Radius - r (mm) | | | | | | | |
|---|---|---|---|---|---|---|---|---|
| | 0 | 5 | 10 | 15 | 20 | 25 | 30 | 35 |
| 0 | 0.326 | 0.298 | 0.236 | 0.178 | 0.135 | 0.108 | 0.090 | 0.074 |
| 5 | 0.244 | 0.231 | 0.198 | 0.161 | 0.130 | 0.106 | 0.089 | 0.075 |
| 10 | 0.194 | 0.186 | 0.167 | 0.144 | 0.121 | 0.102 | 0.087 | 0.076 |
| 15 | 0.160 | 0.155 | 0.144 | 0.128 | 0.112 | 0.098 | 0.085 | 0.075 |
| 20 | 0.135 | 0.133 | 0.125 | 0.115 | 0.103 | 0.192 | 0.084 | 0.073 |
| 25 | 0.117 | 0.116 | 0.110 | 0.103 | 0.095 | 0.086 | 0.078 | 0.071 |
| 30 | 0.104 | 0.102 | 0.099 | 0.093 | 0.087 | 0.081 | 0.074 | 0.068 |
| 35 | 0.093 | 0.092 | 0.089 | 0.085 | 0.081 | 0.075 | 0.070 | 0.065 |

Table 4.7 Axial deformation (mm) of a 'Golden Delicious' apple encapsulated in Urea-Formaldehyde foam under impact force of 27 kg (foam density - 0.0112 gr/cm$^3$; foam thickness - 15 mm).

| z-axis (mm) | Radius - r (mm) | | | | | | | |
|---|---|---|---|---|---|---|---|---|
| | 0 | 5 | 10 | 15 | 20 | 25 | 30 | 35 |
| 0 | 0.489 | 0.447 | 0.355 | 0.266 | 0.203 | 0.162 | 0.135 | 0.111 |
| 5 | 0.367 | 0.346 | 0.295 | 0.242 | 0.195 | 0.160 | 0.133 | 0.113 |
| 10 | 0.290 | 0.279 | 0.251 | 0.216 | 0.182 | 0.154 | 0.131 | 0.114 |
| 15 | 0.239 | 0.233 | 0.215 | 0.192 | 0.168 | 0.146 | 0.128 | 0.112 |
| 20 | 0.203 | 0.199 | 0.188 | 0.172 | 0.155 | 0.138 | 0.122 | 0.110 |
| 25 | 0.176 | 0.173 | 0.166 | 0.155 | 0.142 | 0.129 | 0.117 | 0.106 |
| 30 | 0.155 | 0.154 | 0.148 | 0.140 | 0.131 | 0.121 | 0.111 | 0.101 |
| 35 | 0.139 | 0.138 | 0.134 | 0.128 | 0.121 | 0.113 | 0.105 | 0.097 |

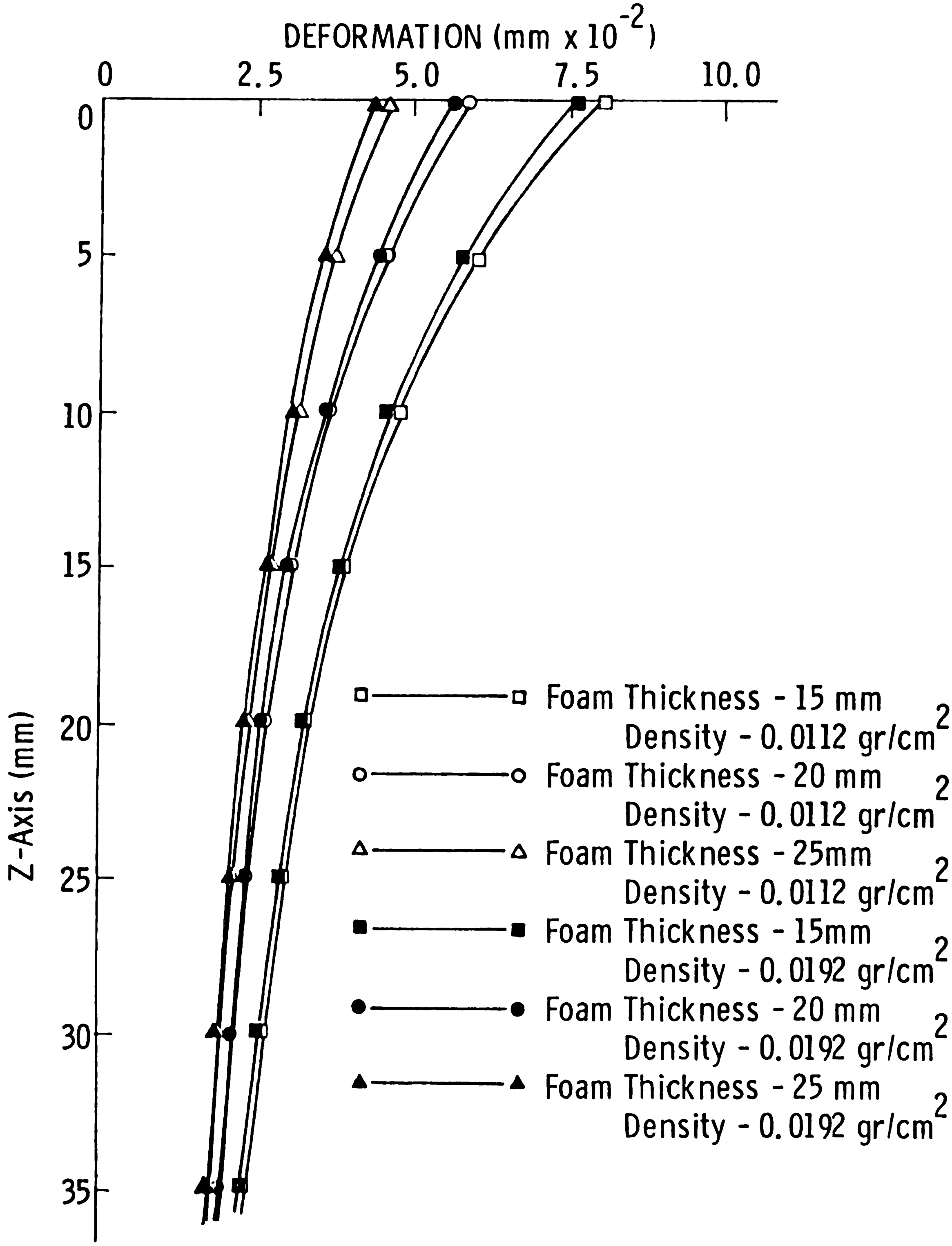


Fig. 4.2 Axial deformation of foam-encapsulated apple as a function of foam thickness and density (Boussinesq's method).

Table 4.8 Surface deformation (mm) at z = 0 of a 'Golden Delicious' apple encapsulated in Urea-Formaldehyde foam under various impact forces.

| Foam density ($gr/cm^3$) | Foam thickness (mm) | Impact Forces (Kg) | | | |
|---|---|---|---|---|---|
| | | 4.5 | 9.0 | 18.0 | 27.0 |
| 0.0112 | 15 | 0.081 | 0.163 | 0.326 | 0.489 |
| | 20 | 0.060 | 0.118 | 0.237 | 0.355 |
| | 25 | 0.046 | 0.092 | 0.185 | 0.277 |
| 0.0192 | 15 | 0.078 | 0.161 | 0.323 | 0.484 |
| | 20 | 0.058 | 0.119 | 0.237 | 0.356 |
| | 25 | 0.045 | 0.093 | 0.187 | 0.028 |

# 5. FINITE ELEMENT FORMULATION

As a result of the mathematical complexity involved in obtaining quantitative solutions to problems in three-dimensional elasticity, relatively few exact solutions to such problems appear in the literature. One such solution was employed in the preceding chapter after the appropriate assumptions were made including approximation of the continuum in study by a suitable model.

Because of the initial assumptions and the methods used to formulate the previous problem, numerical methods are used to evaluate the results. The solution, therefore, was approximated by a discrete process. A logical alternative to this classical approach is to represent the continuum by a consistent discrete model at the onset, then further idealization in either the formulation or the solution may be unnecessary. One such model is the finite element method. The use of the finite element method is especially motivated in the study of agricultural products which do not lend themselves to exact closed-form mathematical solutions.

The finite element method has already been successfully applied in the study of mechanical properties of agricultural products. Apaclla (1973) used the method to analyze the stresses in agricultural products that resemble axi-symmetric solids. Rumsey and Fridley (1974) solved standard contact and impact problems and presented a method for finding the shear relaxation function when the bulk modulus is assumed constant. DeBaerdemaeker (1975) used the finite element method to obtain numerical solutions to the viscoelastic boundary value problem of a viscoelastic sphere loaded by a rigid flat plate.

The present work attempts to utilize the finite element method for the solution of the contact problem involving a continuum composed of two different materials under quasi-static loading.

## 5.1 Finite Element Formulation for Elasticity

The finite element approximation, as outlined before, replaces a continuous function, defined by suitable governing differential equations and subjected to given boundary conditions by a set of piecewise continuous functions over a single element. These functions are defined in terms of values of the continuous function at the nodal points of the element and approximate the displacements over the entire domain. The best set of nodal values for the displacements are obtained by minimizing the potential energy of the domain. The potential energy is defined by a suitable integration of the unknown quantities over the whole domain and is known as a functional (Zienkiewicz 1971).

Let ($\chi$) be the functional defined as some integral over the domain (V) and part of its boundary (S) in which the unknown function $\{\phi\}$ or its derivatives appear, that is

$$\chi = \int_V f(\{\phi\}, \frac{\partial}{\partial x}\{\phi\}....)dv + \int_S g(\{\phi\}, \frac{\partial}{\partial x}\{\phi\}....)dS \quad (5.1)$$

Then the minimization process is equivalent to finding a stationary value of the functional ($\chi$). This value is, in general, at points at which all the derivatives of the function vanish.

If the functional ($\chi$) is denoted as the total potential energy, the following can be written (Zienkiewicz 1971)

$$d(\chi) = d\ (\Pi + W) = 0,$$

where the first term on the right is the variation of the strain energy (U) of the system and the second is the variation of the potential energy and the external loads (W).

The total strain energy ($\Pi$) is obtained by integrating the tensorial product between stress and strain over the volume of the body yielding:

$$\Pi = \int_V \frac{1}{2}\{\varepsilon\}^T\{\sigma\}dv \tag{5.2}$$

where $\{\varepsilon\}$ is a column vector of strain components and $\{\sigma\}$ is a column vector of stress components. The two are related by the elastic constants of the material

$$\{\sigma\} = [D]\{\varepsilon\} \tag{5.3}$$

where isothermic conditions are assumed.

Expressing the strain energy in terms of the prescribed displacement yields:

$$\Pi^{(e)} = \int_{V^{(e)}} \frac{1}{2}\{U\}^T[B^{(e)}]^T[D^{(e)}][B^{(e)}]\{U\}dv \tag{5.4}$$

where [B] defines the relationship between the strain and displacements.

$$\{\varepsilon^{(e)}\} = [B^{(e)}]\{U\} \tag{5.5}$$

and is obtained by differentiating the matrix of the shape functions [N] which relate the element displacements $[U^{(e)}]$ to the nodal displacements $\{U\}$.

$$\{U^{(e)}\} = [N^{(e)}]\{U\} \tag{5.6}$$

The potential energy of the external load is comprised of three parts: that due to the concentrated loads, that resulting from stress components acting on the outside surface and that related to body forces. In matrix form they are given as:

$$W = \{U\}^T\{P\} + \int_{S^{(e)}} \{U\}^T[N^{(e)}]^T\begin{Bmatrix} P_x^{(e)} \\ P_y^{(e)} \\ P_z^{(e)} \end{Bmatrix} dS + \int_{V^{(e)}} \{U\}^T[N^{(e)}]^T\begin{Bmatrix} x^{(e)} \\ y^{(e)} \\ z^{(e)} \end{Bmatrix} dV \tag{5.7}$$

Minimizing the functional ($\chi$) implies differentiating with respect to {U} and setting it equal to zero which yields:

$$\frac{\partial\chi^{(e)}}{\partial\{U\}} = \sum_{e=1}^{E} \int_{V^{(e)}} [B^{(e)}]^T[D^{(e)}][B^{(e)}]dV\{U\} - \int_{V^{(e)}} [N^{(e)}]^T \begin{Bmatrix} x^{(e)} \\ y^{(e)} \\ z^{(e)} \end{Bmatrix} dV$$

$$- \int_{S^{(e)}} [N^{(e)}]^T \begin{Bmatrix} P_x^{(e)} \\ P_y^{(e)} \\ P_z^{(e)} \end{Bmatrix} dS - \{P\} = 0 \tag{5.8}$$

The last equation can be written as:

$$\frac{\partial\chi^{(e)}}{\partial\{U\}} = [K^{(e)}]\{U\} + \{f^{(e)}\} = 0 \tag{5.9}$$

where $[K^{(e)}] = \int_{V^{(e)}} [B^{(e)}]^T[D^{(e)}][B^{(e)}]dV$ (5.10) and $\{f^{(e)}\}$ is an element force matrix which is the sum of the other integrals. Equation (5.10) is the well-known displacement formulation of the finite element equations of elasticity.

## 5.2 The Axi-symmetric Case

The composite body of this study can be classified within a special class of boundary value problems in the mathematical theory of elasticity which deals with axi-symmetric deformation of solids of revolutions (Fig. 5.1a). Since the deformation is symmetrical with respect to the axis of revolution, it is most convenient to employ orthogonal cylindrical coordinates r, $\theta$, z with the z axis along the axis of symmetry. The components of the displacement vector and of the stress tensor will be independant of the angle $\theta$, hence, only the radial and vertical components of the displacement need to be considered. Thus, from a mathematical point of view, this body is two-dimensional in nature and may be represented as shown in Fig. 5.1b. An appropriate idealization to this two-dimensional system, using triangular element configurations is shown in Fig. 51b. Each element is actually a complete ring in the third dimension (extending through the angle $\theta = 2\Pi$) and the nodal points at which they are connected are in reality circular lines in plain view as shown in Fig. 5.1c. The formulation is analogous to a finite element plane stress or plane strain problem. The

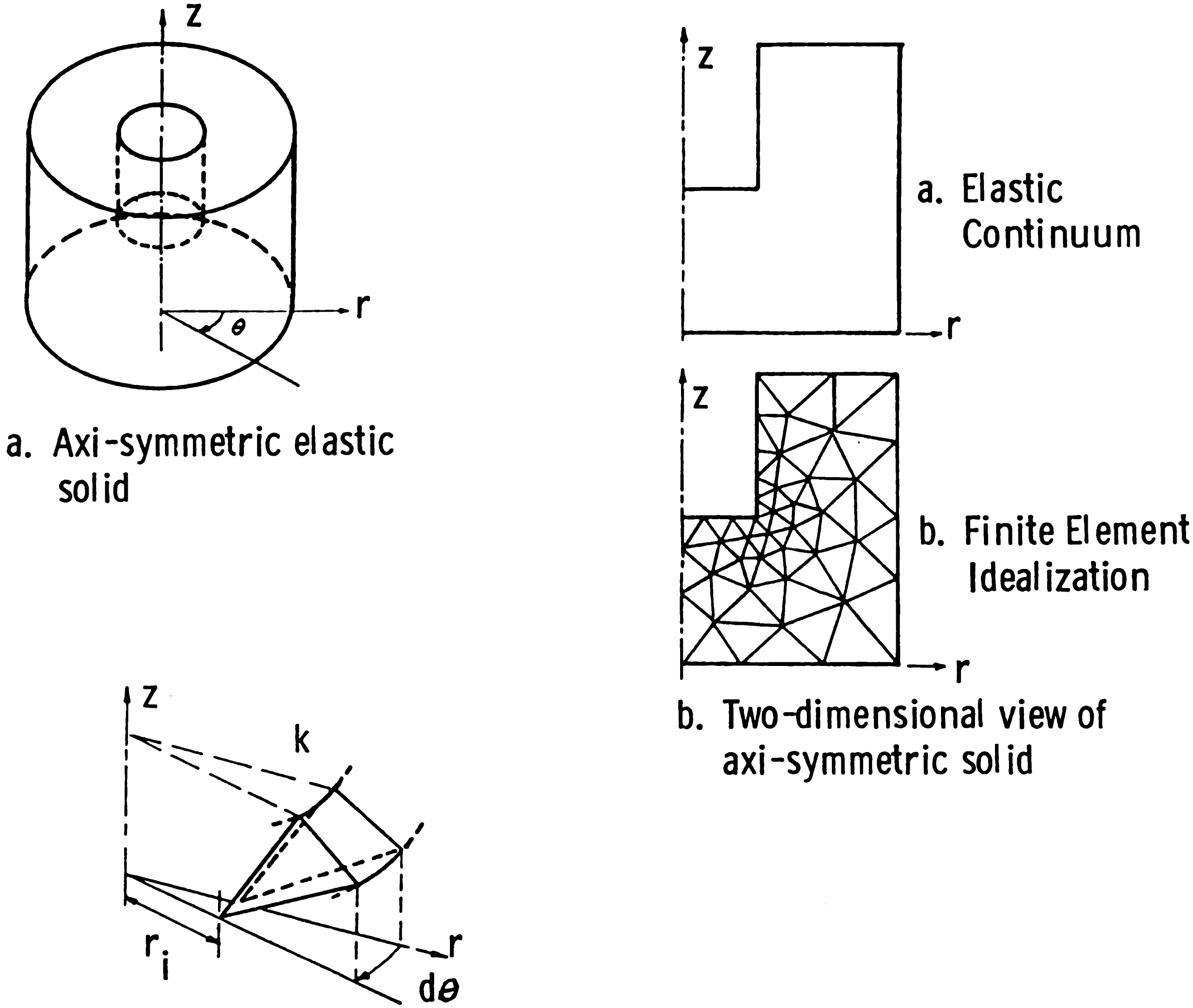


a. Axi-symmetric elastic solid

a. Elastic Continuum

b. Finite Element Idealization

b. Two-dimensional view of axi-symmetric solid

c. Typical triangular axi-symmetric element

Fig. 5.1 Finite element modeling of an axi-symmetric solid.
(from Clough & Rashid, 1965)

essential difference between these two types of problems is that in the axi-symmetric case the radial component of the displacement induces a strain in the circumferential direction and an associated stress component which have to be considered.

# 6. EVALUATION OF APPLE DEFORMATION USING FINITE ELEMENT METHODS

## 6.1 Discretization of the Domain

The domain consists of an elastic sphere encapsulated in an elastic shell under prescribed deformation on the boundary, depicting the behavior of foam-encapsulated apple being doubly indented by a limb (Fig. 6.1).

The finite element grids for the model are shown in Figs. 6.2-6.4. Because of the symmetry of the sphere and the axisymmetric loading, it is necessary to consider only one quadrant of the sphere. The radius of the sphere (apple) was chosen as 35 mm, and three (foam) layers of thickness were considered: 15 mm, 20 mm, and 25 mm.

The division of the regions into triangular elements was carried out with a grid generation computer program (Segerlind 1976) which incorporates an optimization sub-routine for labeling the nodes for minimum computer memory requirements. The elements' size in the grid were varied such that finer mesh was obtained for the regions near the applied loadings. The final grid consisted of 568 elements with 315 nodes.

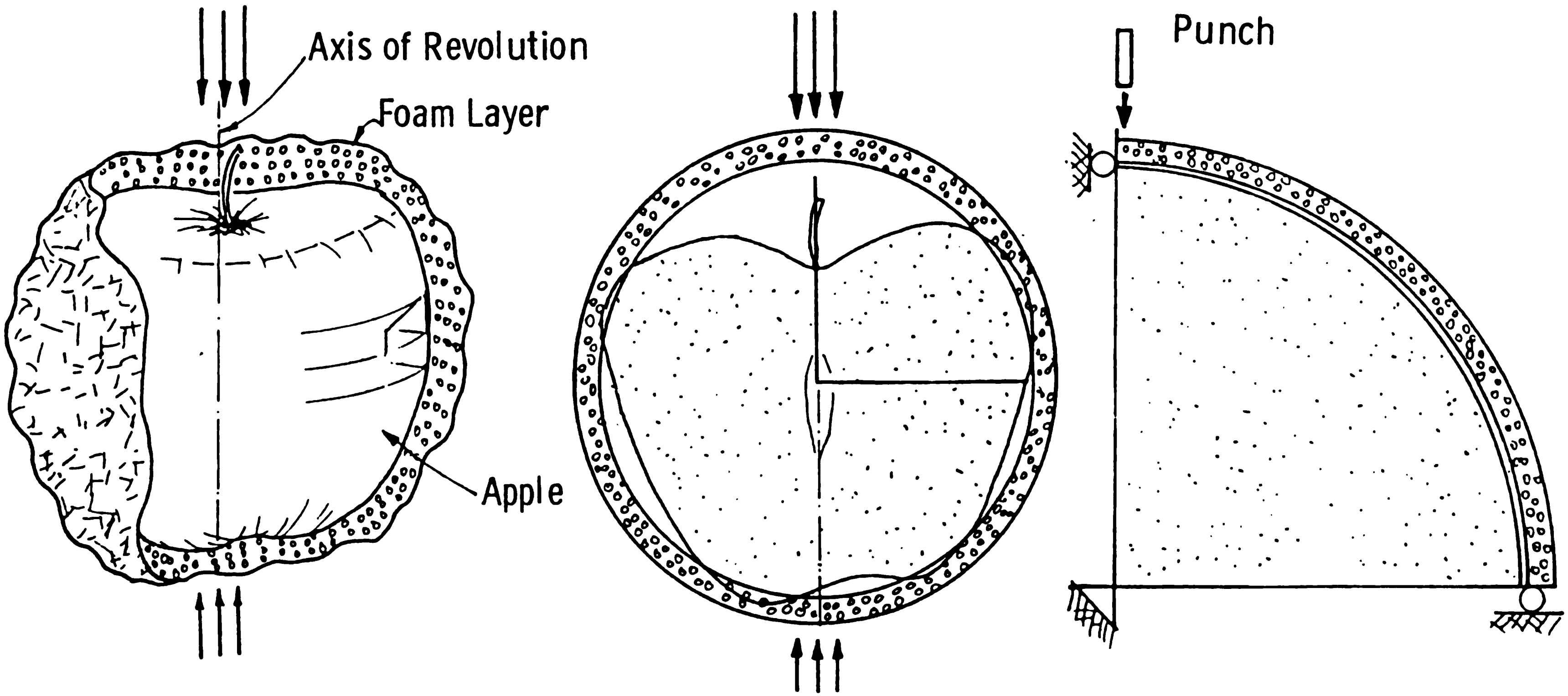


a. Axi-symmetric foam encapsulated apple

b. Two-dimensional view of the domain.

c. Final model with prescribed assumptions of the boundaries.

Fig. 6.1 Model of foam-encapsulated apple for the finite element analysis.

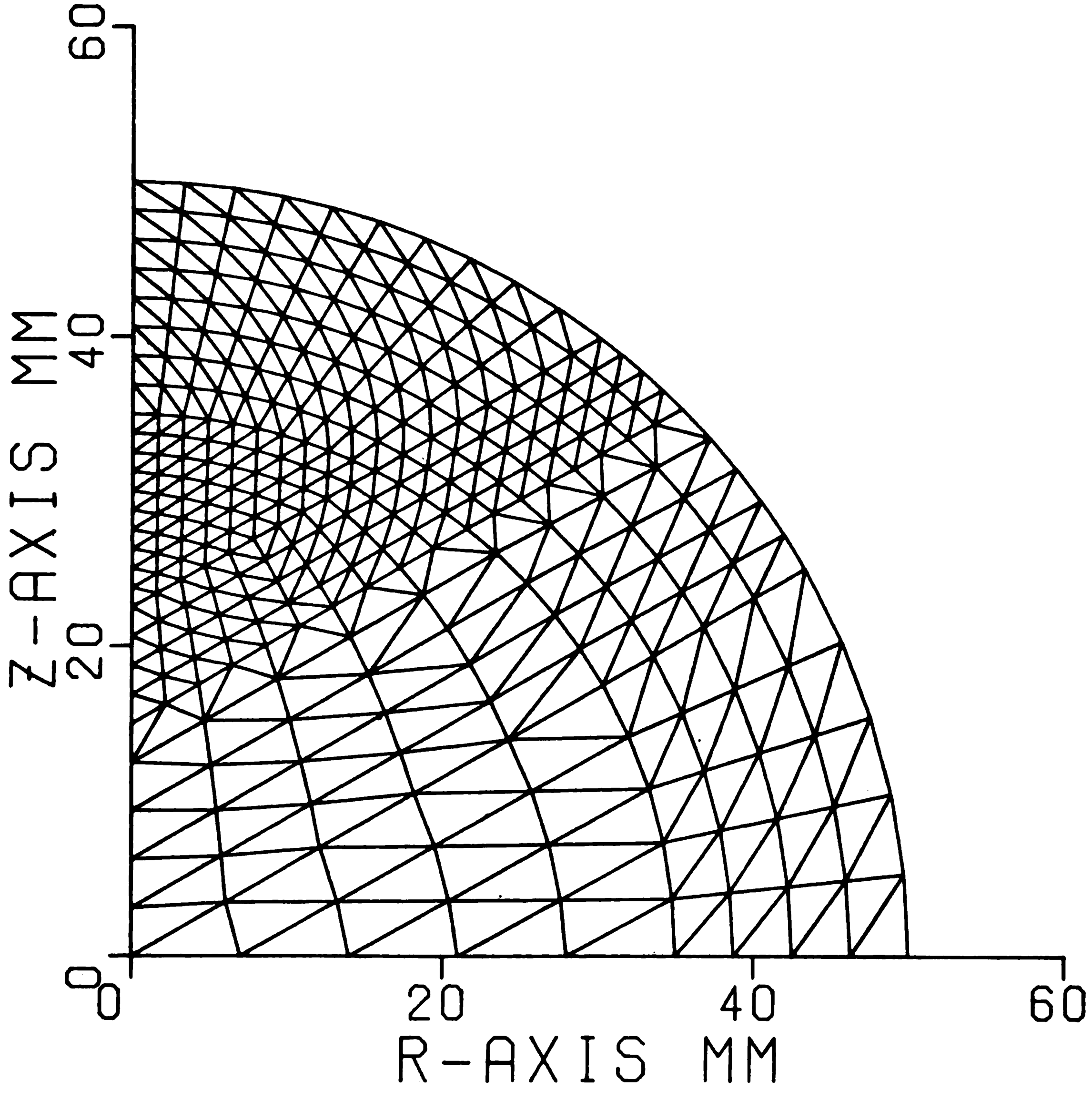


Fig. 6.2 Finite element grid for foam-encapsulated apple model. Foam thickness 15 mm.

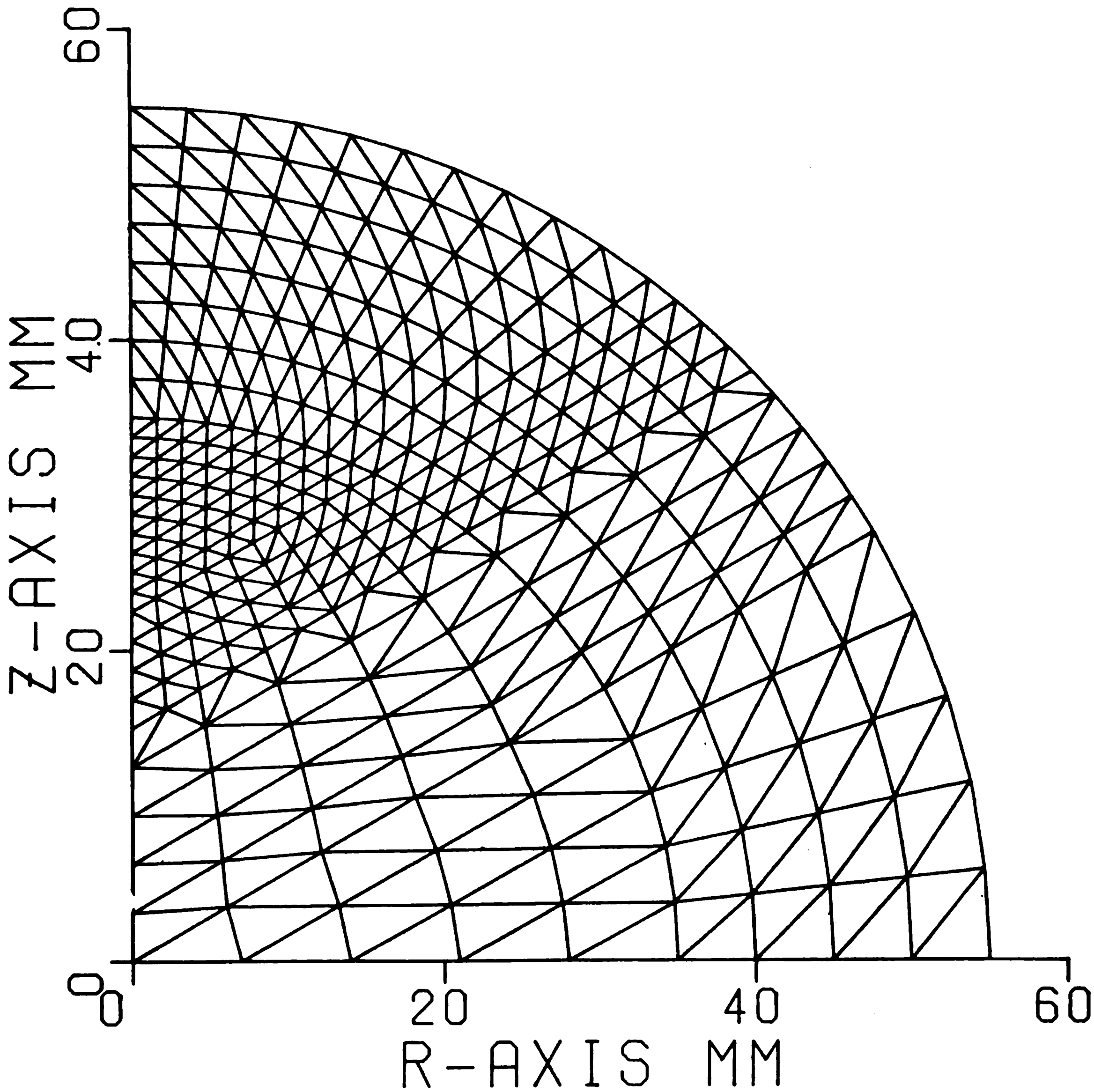


Fig. 6.3 Finite element grid for foam-encapsulated apple model.
model. Foam thickness 20 mm.

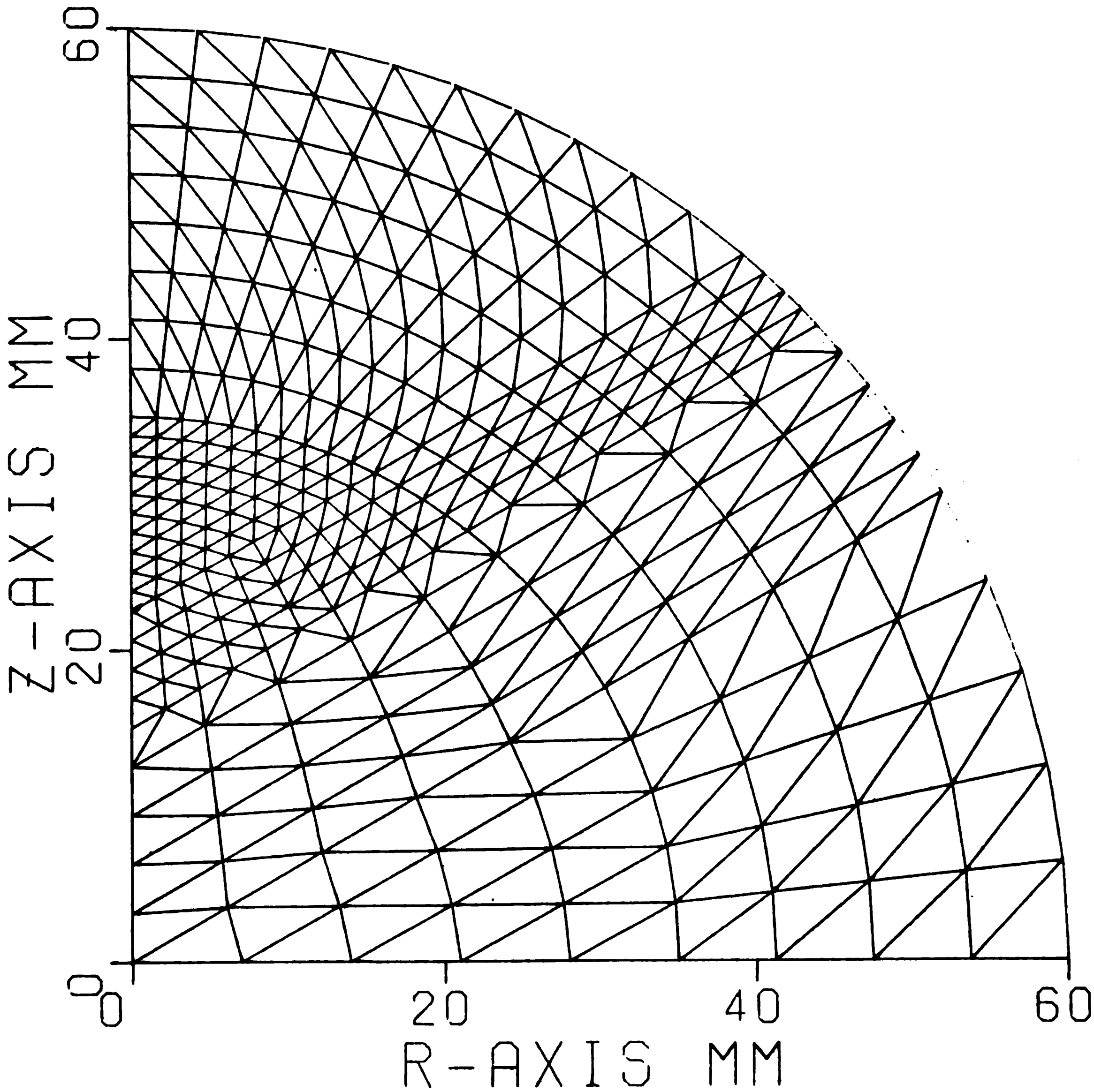


**Fig. 6.4 Finite element grid for foam-encapsulated apple model. (Foam thickness 25 mm.)**

## 6.2 Mechanical Properties of the Domain

An impressive amount of data has been accumulated in recent years pertaining to the mechanical properties of agricultural products and of apples in particular. Therefore, no attempt was made to evaluate these properties and available data was used.

Due to variation in growing practices, climatic conditions and experimental methods, a range of values exist for the apple fruit rather than a single, generally accepted one. Average values, based on the experimental works of Mohsenin (1970), Chappell and Hamann (1968), Hamann (1967), and Miles (1971) were used in this study. All the assumptions outlined in Chapter 4 were employed here too. In addition, no differentiation was made between the apple flesh and the skin. Rumsey and Fridley (1974) reported that no significant change in the internal stresses was observed when different constitutive relations were assigned to the flesh and the skin. Some discrepancy was found in the skin itself, but since interest is in the internal stress-strain relationship, only one value was used for the elastic modulus.

Most of the published work related to Poisson's ratio for the apple indicate a time dependency (Chappell and Hamann 1968, Hamann 1967, DeBaerdemaeker 1975). However, impact problems, such as the one considered in this work, require Poisson's ratio for very short loading times which cannot be derived from long time creep or stress relaxation curves. A reasonable assumption was made and verified by Hamann to use constants rather than time dependent relations. The values used for Poisson's ratio in the current study are based on Hamann's work related to the impact response of apples.

The mechanical properties of the Urea-Formaldehyde foam were those derived at Chapter 3 for different density values. The mechanical properties for both the foam and the apple are given in Table 6.1. It should be noted that the values for the apple correspond to data derived from experiments carried out on the day of harvest. At different stages of maturity a significant change was observed (Mohsenin 1970).

## 6.3 Calculation of the Deformation of the Encapsulated Apple

An available finite element program was modified for the axi-symmetric case of a domain composed of two different materials. The model was visualized as being doubly indented by a limb of a known radius similar to the physical characteristics assumed in the Boussinesq method formulation (Chapter 4). The same indentation values which were derived for the latter formulation were used as the boundary values in the finite element formulation. The program yields both the axial ($U_z$) and the radial ($U_r$) deformation in the entire domain for discrete nodal points.

Table 6.1 Mechanical properties of the foam/apple domain.

| Foam | | | Apple | | |
|---|---|---|---|---|---|
| Density ($gr/cm^3$) | Apparent elastic modulus ($N/cm^2$) | Poisson's ratio | Variety | Elastic modulus ($N/cm^2$) | Poisson's ratio |
| 0.0112 | 83.3 | 0.364 | 'Golden Delicious' | 378 | 0.218 |
| 0.0192 | 132.2 | 0.364 | 'Red Delicious' | 334 | 0.219 |

In addition, the program provided the values for the stresses which were not considered in the current study. To verify the reliability of the program, a simple cylinder, comprised of 100 elements under uniaxial fixed displacement on the upper surface, was analyzed and compared with a known analytical solution.

The calculations were carried out for two values of foam density with different elastic moduli, under four conditions of impact forces yielding the corresponding boundary values of indentation.

Examples of the deformed grids are given in Figs. 6.5-6.8 for the case of a 'Golden Delicious' apple encapsulated in U-F foam of different thicknesses and density of 0.0112 gr/cm$^3$, subjected to impact forces of 4.5, 9, 18 and 27 kg. The apple surface deformation is given in Table 6.2 for apples of 'Golden Delicious' variety encapsulated in U-F foam of different thicknesses and different densities subjected to different impact forces. It can be seen from this table that increasing the thickness of the foam is more effective than increasing the foam density, especially at higher impact forces. Since in practice (see Chapter 7) it would be hard to attain a thin layer of foams, we may conclude that thickness rather than density is more effective in terms of optimization of the method.

The variation of the axial deformation (along the z-axis) induced in the apple is given in Fig. 6.9 for the case of apple encapsulated in U-F foam of various densities

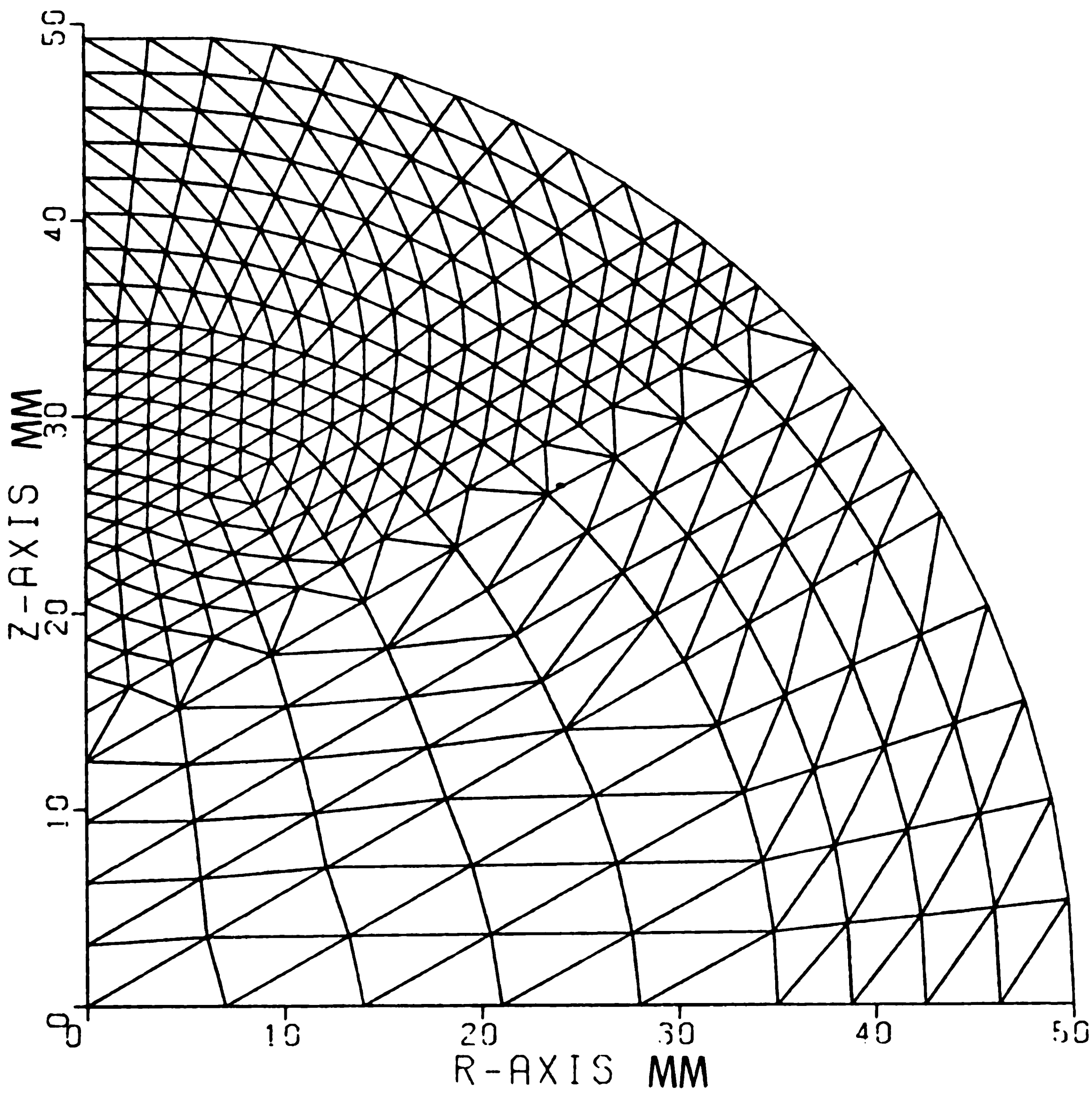


Fig. 6.5 Deformed grid for foam-encapsulated apple model under impact force of 4.5 kg. (Foam thickness 15 mm.)

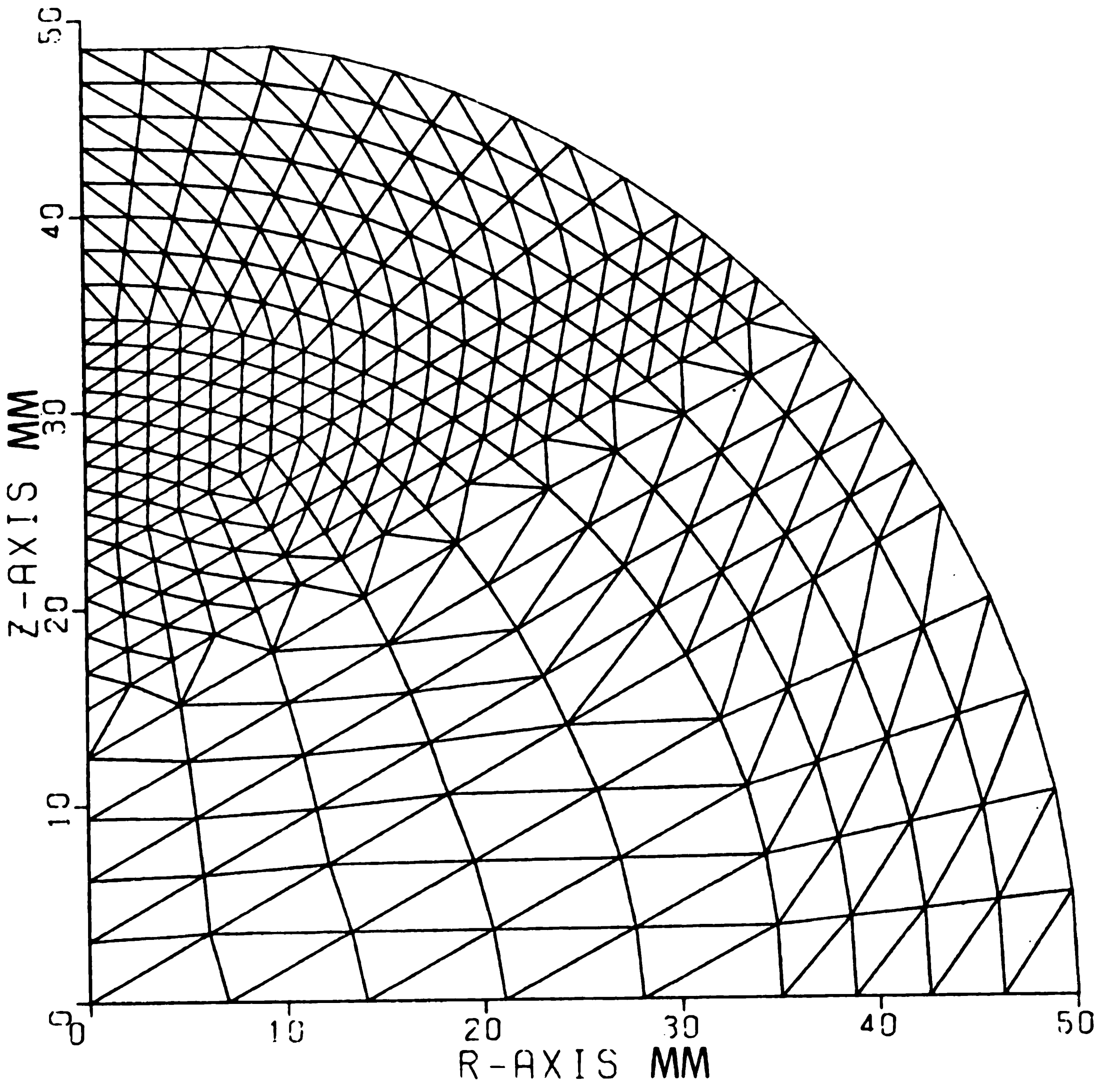


Fig. 6.6 Deformed grid for foam-encapsulated apple model under impact force of 9 kg.. (Foam thickness 15 mm.)

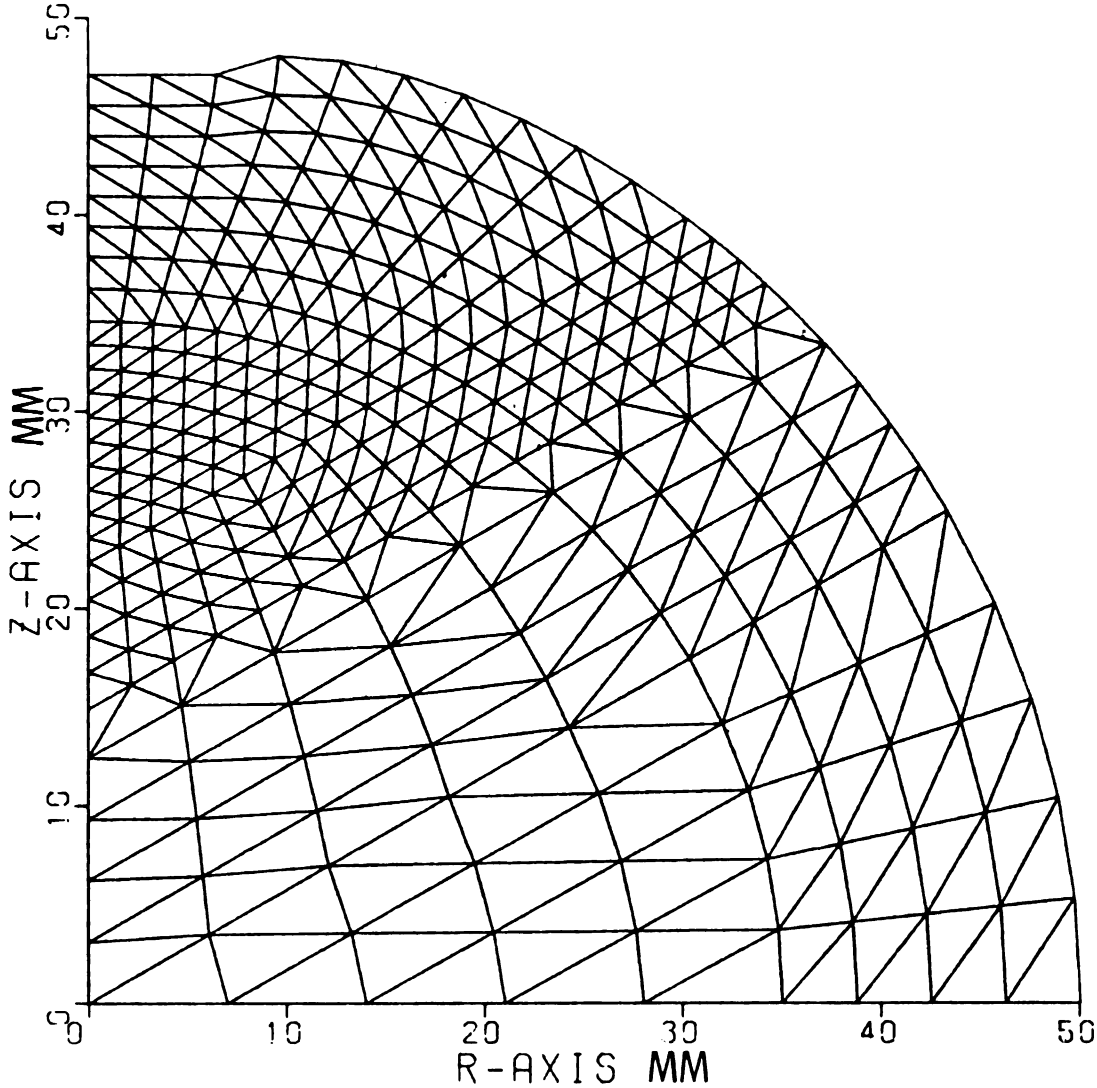


Fig. 6.7 Deformed grid for foam-encapsulated apple model under impact force of 18 kg. (Foam thickness 15 15 mm.)

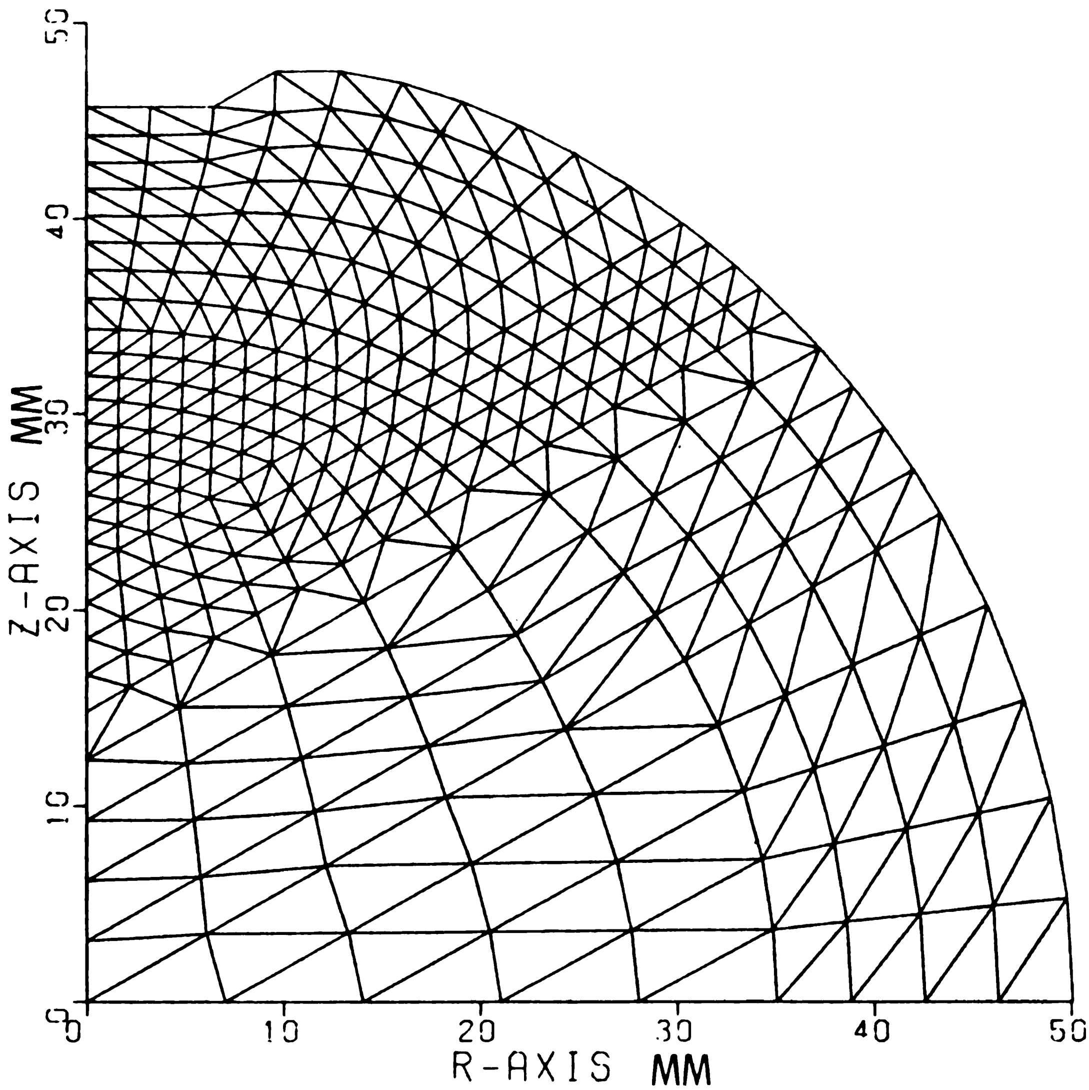


Fig. 6.8 Deformed grid for foam-encapsulated apple model under impact force of 27 kg. (Foam thickness 15 mm.)

Table 6.2 Surface deformation (mm), at $r = 0$, of a 'Golden Delicious' apple encapsulated in Urea-Formaldehyde foam under various impact forces (finite element method).

| Foam Density ($gr/cm^3$) | Foam Thickness (mm) | Impact Forces (Kg) | | | |
|---|---|---|---|---|---|
| | | 4.5 | 9.0 | 18.0 | 27.0 |
| 0.0112 | 15 | 0.063 | 0.180 | 0.414 | 0.648 |
| | 20 | 0.048 | 0.140 | 0.322 | 0.508 |
| | 25 | 0.043 | 0.127 | 0.295 | 0.465 |
| 0.0192 | 15 | 0.030 | 0.145 | 0.363 | 0.584 |
| | 20 | 0.020 | 0.112 | 0.287 | 0.460 |
| | 25 | 0.018 | 0.102 | 0.262 | 0.422 |

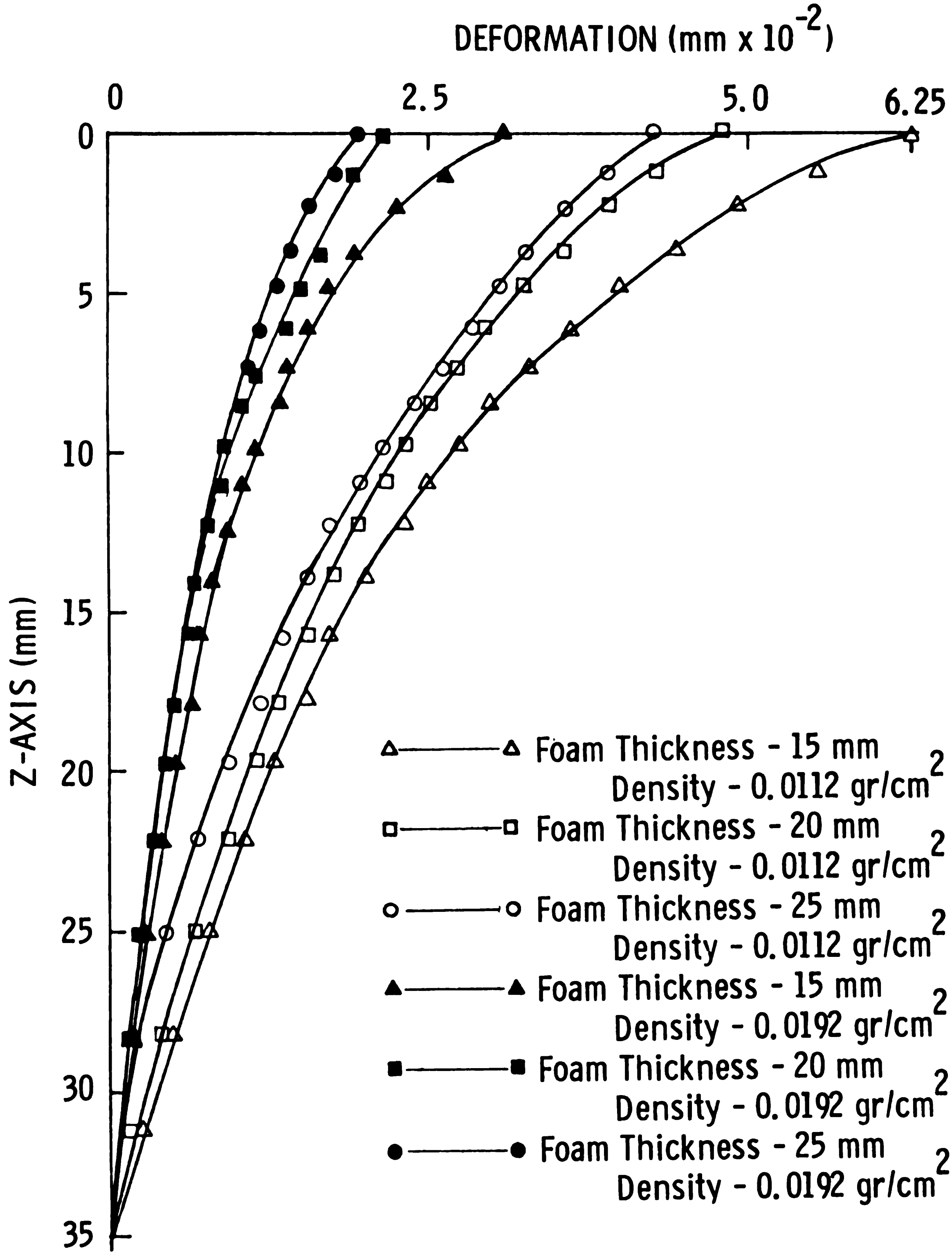


Fig. 6.9 Axial deformation of foam-encapsulated apple as a function of the z-axis.

and thicknesses. The values of the deformation converge to a zero value at a faster rate for the more dense foam.

It should be noted that the surface deformation of the apple is very small, showing even at the lower foam thickness values. Therefore we may conclude that a foam of standard density (0.0112 gr/cm$^3$) and a minimum thickness of 15 mm should provide adequate protection for free falling apples.

# 7. ASSESSMENT OF THE PROPOSED METHOD

The major objective of this study was to develop a theoretical method for analyzing the response of an encapsulated apple under given boundary conditions. Since the two methods presented in Chapters 4 and 6 offer an alternative analysis, their characteristic merits were compared. No attempt was made to carry out an in-depth study to analyze the various factors and their interactions, which govern the feasibility of a commercial application. Moreover, since the major thrust of the study is primarily of theoretical nature, it was considered premature to draw any final conclusions pertaining to its possible application. However, to get a feel for a possible future implementation of the method and to compare the simulated models with actual field conditions, a field experiment of a preliminary nature was conducted and the effect on fruit quality was evaluated. Based on the results of this experiment and the theoretical analysis, the economics of the proposed method was considered. The major objective of the proposed assessment was to establish the feasibility limits to be further explored in future studies.

## 7.1 Comparison of Apple Deformation Evaluation Method

The differences in the numerical results of both methods, presented in Chapter 4 and Chapter 6, are illustrated in Fig. 7.1. The analytical results of the two methods are compared for a foam thickness of 15 mm and density of 0.0112 gr/cm$^3$. Rigid body deformations have been equated at the center of the apple ($z$ = 35 mm) for the purpose of comparison. The Boussinesq method considers the radius of curvature to be infinite while a finite radius (35mm) was used in the finite element method. The good agreement obtained between the two methods signifies the reliability of the results and indicates that bruising is a local phenomena and that the overall geometry does not affect the results.

The prime merit of the finite element method is its capability to handle different shapes. Thus, for more accurate results the true shape of the apple can be considered, utilizing the finite element method, with minor changes made. The Boussinesq method would be very complicated when handling odd-shaped bodies. The main drawback of the finite element method is its dependency on access to a large computer. Moreover, for a more exact solution a finer grid is required which increases the high cost. The Boussinesq method is a more rigorous mathematical approach and as such, offers a better insight to the actual behavior of the domain under given boundary

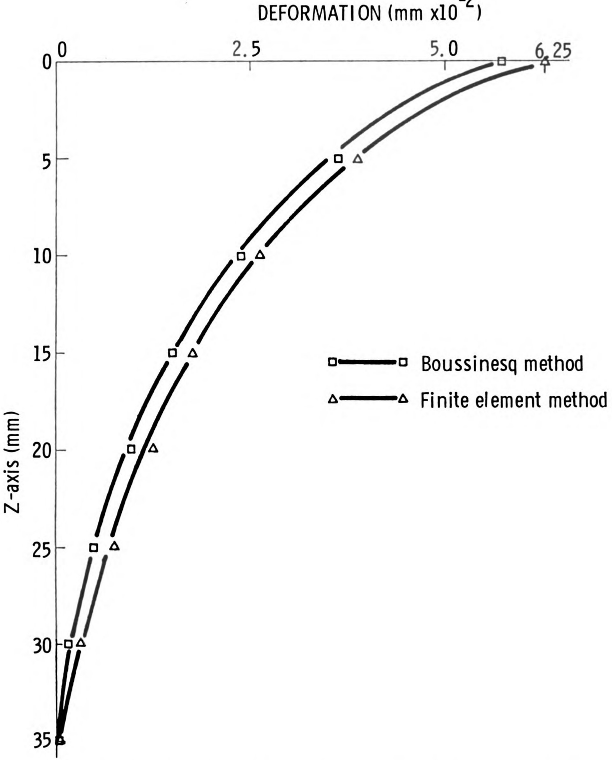


Fig. 7.1 Axial deformation of foam-encapsulated apple (foam thickness - 15 mm, foam density 0.0112 gr/cm$^3$.)

conditions. However, the complexity involved in obtaining a tracktable form for solution limits its utilization for well defined cases, where accurate results can be obtained.

## 7.2 Field Studies

Field experiments were carried out in a commercial apple orchard allocated for the processing industry. One tree of the 'Golden Delicious' variety was sprayed with the U-F foam utilizing a portable foam generator, and a second tree was used as a control. Average estimated yield of the trees was 8 to 10 bushel, and the tree's height was roughly 3.5 m. The treated tree was sprayed in a manner to obtain primarily fruit coverage, but in practice only one-half of the tree was sprayed and both fruit and branches were partially covered in different proportions (Fig. 7.2). After a curing period of one day, the trees were shaken using a Friday Tractor Shake and Catch system. Samples of the fruit from both trees were collected at the conveyor end and were transferred to the laboratory (distance of 106 km) for a final evaluation. The fruit were placed in room temperature of 21 ± 1°C for one day to allow the bruises to become more pronounced. Sixty-five fruit were taken at random from the two samples and evaluated for quality. The method comprised of examining each apple individually and counting the bruises per apple, recording both the diameter

Fig. 7.2 Experimental application of Urea-Formaldehyde foam to a 'Golden Delicious' apple tree.

and indentation of the bruise. In addition, punctures, cuts and scratches were identified and counted. The final bruise classification followed the criteria used by Burt (1959) in his study on bruising caused in a packing line, where bruises were classified as either slight, moderate, or severe, corresponding to the applicable U.S. Grade. The results are given in Table 7.1 for the evaluation of sixty-five fruit.

Table 7.1 Evaluation of foam-encapsulated and uncoated apples (percentage of apples bruised).

| Treatment | Quality Classification | | |
|---|---|---|---|
| | Slight Bruising (Apples to U.S. Extra-fancy Grade) | Moderate Bruising (Applies to U.S. Fancy and U.S. No.1 Grade) | Serious Bruising (Applies to U.S. Utility Grade) |
| Foam-encapsulated apples | 55 | 30 | 15 |
| Uncoated apples | 8 | 14 | 78 |

In general the number of bruises of the apples were small (averaged two bruises[1] per apple) and of slight depth (not over 3 mm by definition) compared with the uncoated apples which averaged five bruises[2] and indentations

[1]Bruise size averaged 10 mm.

[2]Bruise size averaged 15 mm.

that ranged between 3 mm and 6 mm. In addition the uncoated fruit had more scratches than the foam-sprayed apples.

It should be noted, however, that the results for the treated apples apply to fruit which was in practice only partially covered with the foam. Nevertheless, the most significant result was that the part of the fruit which was covered was bruise free! This result conforms to the results predicted from the theoretical analysis. Namely, the Urea-Formaldehyde encapsulation at a given thickness may provide an adequate protection for free drop apples impinging on the tree limbs.

## 7.3 Economic Considerations

The economic evaluation should be viewed only as a guideline for further future studies, since the experimental data derived from the current study was of a preliminary nature. The calculations are made on a per-tree basis, incorporating the quality evaluations data given in Table 7.1, assuming yield per tree of 226 kg, and utilizing the price per grade as given in Michigan Agricultural Statistics in June 1975. The results for the predicted return per tree are given in Table 7.2 incorporating data on percentage of sound fruit, prior to harvesting, for 'Golden Delicious' apple (Dewey and Schueneman 1972). Estimated cost of operating the

Table 7.2 Predicted return of foam-encapsulated vs. uncoated mechanically harvested apples.

| Treatment | Price Paid Per Quality Classification | | | Total Return per Tree |
|---|---|---|---|---|
| | U.S. Extra Fancy ($0.13/Kg) | U.S. Fancy & U.S. No. 1 ($0.044/Kg) | U.S. Utility ($0.0016/Kg) | (Dollars) |
| Foam-en-capsulated apple | 7.36[1] | 1.34 | 0.25 | 8.95 |
| Uncoated apple | 1.07 | 0.62 | 1.30 | 2.99 |

[1]Based on 44.6% sound fruit for 'Golden Delicious' apple prior to harvesting (Dewey and Scheuneman 1972).

Table 7.3 Estimated costs of encapsulating apple with a Urea-Formaldehyde foam.

| Factor | Cost (Dollars/tree) |
|---|---|
| Material[1] | 7.26 |
| Application labor[2] | .20 |
| Machine depreciation | .50 |
| | 8.00 |

[1]Based on the manufacturer quoted price of $200 per 208 l and experimental foam application of 7.5 l/tree.

[2]Based on estimated capacity of spraying 20 trees/hour and average payment of $4/hour.

proposed method are given in Table 7.3 based, in part, on information supplied by the foam manufacturer.

Comparing the net return per tree for the foam-encapsulated apple with that of the uncoated apple indicates an increase in the total return due to the enhanced fruit quality resulting from the foam coating. However, when compared with the cost of application the net return is marginal. Therefore, although the method provides a definite protection for the fruit the cost factor is a major deterrent for practical implementation at present. Nevertheless, it is conceivable that the method can be improved with further experimentation resulting in lower cost of application. Moreover, with continuation of the current trend of labor shortage and decrease in picking quality, mechanical harvesting of fresh market fruit would become mandatory. Thus, the proposed method which helps to maintain fruit quality would become imperative.

# 8. SUMMARY AND CONCLUSIONS

A new method was proposed for protecting apples in the process of mechanical harvesting. The method consisted of spraying the tree with a Urea-Formaldehyde foam prior to harvesting. The apple and branches were encapsulated in a layer of foam which absorbs the impact energy induced in a free-drop apple, thus minimizing the resulting deformation. The mechanical properties of the foam were derived through experimentation and were incorporated subsequently in the theoretical analysis.

Two analytical methods were utilized for predicting the apple deformation under given boundary conditions. In the Boussinesq-problem method the domain was modeled as an elastic layer depicting the foam, lying on an elastic sub-space (the apple). In the second--the finite element method--the domain was approximated by a discrete model composed of interconnected elements. The approximate solution for the entire domain is obtained through the combined solutions of the elements which constitute the domain. Very good agreement was obtained with the two proposed solutions, substantiating the validity of the results of almost negligible deformation resulting in foam-encapsulated apple. Either method should offer an alternative approach. The Boussinesq method is a more rigorous mathematically, but limited to cases of well-defined shapes. Any deviation from the 'standard' forms presents a mathematical complexity. The finite element method, although an approximation method, can handle oddly shaped bodies and provides an acceptable alternative.

The numerical analyses were followed by limited field experiments which conform to the numerical results. Based on both the theoretical and field analyses, it may be concluded that the proposed method is sound since it provides adequate protection to the fruit. An adequate parameters of the method were found to be a foam density of 0.0112 $gr/cm^3$ and thickness of 15 mm. Although a lower value for the foam thickness would have still provided the needed protection, it was considered hard to attain in practice. When the fruit was covered with the foam, no indentation occurred and the fruit was rated at prime quality. However, in practice only part of the fruit was covered (50% on the average). Nevertheless, it is conceivable that with the perfection of the method of application the coverage could be improved.

# 9. SUGGESTIONS FOR FURTHER STUDIES

It is recognized that both the analytical solution and the actual practical application are of a preliminary nature which leave much to be further explored. It is suggested that future studies should be in three major areas as follows:

1. The Mathematical Analysis (the analytical solution)

The loss of a more rigorous analysis was accepted in the course of this study as a possible sacrifice for obtaining a first approximation to the solution. Further studies should attempt to improve the solution by considering the true time effects associated with impact. A possible approach would be a finite element formulation for a transient dynamic response of the continuum or consideration of the dynamic Boussinesq problem. In addition, the true mechanical behavior of the apple is of a viscoelastic nature which should be considered in the more accurate analysis. Similarly, the proposed encapsulation, the Urea-Formaldehyde foam, is an elasto-plastic material and should be treated as such for a more rigorous analysis. Finally, since the impact encountered in the process of mechanical harvesting is not confined to cases of a well-defined punch configuration, other more realistic shapes should be considered.

## 2. The Proposed Material

The selection of the Urea-Formaldehyde foam, as the appropriate material for the proposed application, was the result of a suggestion by a group of scientists from the Weitzman Science Institute in Israel. It is conceivable that other materials may be found with even superior characteristics. However, since the U-F foam is the only one presently available, an attempt should be made to perfect its characteristics for possible reduced cost and better performance. One way of having some control of the process is through the introduction of carbon fillers to the resin which may result in a smoother layer and hence a more even coverage of the fruit (Bikermann 1953). The problem of free Formaldehyde, emanating during the process and resulting in some leaves burned, should be further studied. According to the manufacturer this factor is controllable and, therefore, needs to be investigated.

## 3. Application Methods

The mode of application utilized in the field study left much to be desired. Since more even coverage seems to bc a crucial factor, a great effort should be directed to develop a more efficient method of application. One possible approach that may be explored is the principle of a straddle sprayer moving continuously along the row. Such sprayers have already been conceived and are currently being investigated. This mode of application may result in a more economic and efficient utilization of the material and more complete coverage. Finally, the method was evaluated for its adaptability to apples. Since all soft fruit destined for fresh market encounter similar problems of bruising, it sould be worthwhile to evaluate the potential of the method for other fruit crops.

REFERENCES

## REFERENCES


Abramowitz, M. and Stegun, I. A. (edit.), 1965. Handbook of Mathematical Functions. Ch. 9.4, Dover Publications, Inc., New York, N.Y. 1046 p.

Apaclla, R. 1973. Stress analysis in agricultural products using the finite element method. Unpublished M.S. thesis, Department of Agricultural Engineering, Michigan State University, East Lansing, Mich.

Berlage, A. G., and R. D. Langmo. 1974. Trunk shaker harvesting of apples surrounded by plastic spheres. ASAE Paper 74-1522.

Bernshausen, F. 1970. Method of harvesting fruit. U.S. Patent No. 3,545,182. December 8.

Bikerman, J. J. 1953. Foams--theory and industrial applications. Reinhold Publishing Co., New York. 352 p.

Bittner, D. R., H. B. Manbeck, and N. N. Mohsenin. 1967. A method of evaluating cushioning material used in mechanical harvesting and handling of fruits and vegetables. Trans. of the ASAE 10(6):711-714.

Boussinesq, J. 1885. Application des Potential a l'Equilibre et du Mouvement des Solides Elastiques. Gauthier-Villars Paris.

Brown, G. K. and L. J. Segerlind. 1975. The location probabilities of surface injuries for some mechanically harvested apples. Trans. of the ASAE 18(1):57-59.

Burkhardt, T. H. and B. A. Stout. 1971. A high-velocity, high momentum impact testing device for agricultural materials. Trans. of the ASAE 14(3):455-457.

Burmister, D. M. 1945. The general theory of the stresses and displacements in layered systems. J. Appl. Phys. 16:89-94, 120-127; 296-302.

Burt, S. W. 1959. An experimental packing line for McIntosh. An interim report. U.S.D.A., Agricultural Marketing Service, Marketing Research Division, AMS No. 330, Washington, D.C. 28 p.

Chappell, T. W. and D. D. Hamann. 1968. Poisson's ratio and Young's modulus for apple under compressive loading. Trans. of the ASAE 11(5):608-610, 612.

Chen, W. T. 1971. Computation of stresses and displacements in a layered elastic medium. Int. J. Engng. Sci. 9:775-800.

Clevenger, J. H., Jr. and D. D. Hamann. 1968. The behavior of apple skin under tensile loading. Trans. of the ASAE 11(1):34-37.

Clough, R. W. and Y. Rashid. 1965. Finite element analysis of axi-symmetric solids. J. Eng. Mech. Div. Proc. Amer. Soc. Civ. Engrs. 91:71-85.

Davis, D. C. and G. E. Rehkugler. 1971. A theoretical and experimental analysis of the apple-limb impact problem. Trans. of the ASAE 14(2):234-239.

DeBaerdemaker, J. G. 1975. Experimental and numerical techniques related to the stress analysis of apples under static loads. Unpublished Ph.D. thesis, Dept. of Agricultural Engineering, Michigan State University, East Lansing, Mich.

Dedolph, R. R. and M. E. Austin. 1961. The evaluation of impact bruises on apple fruit. Proc. Amer. Soc. Hort. Sci. 80:125-129.

Despain, C. C. 1968. Fruit harvesting technique. U.S. Patent No. 3,630,758. December 28.

Dewey, D. H. and T. J. Schueneman. 1972. Quality and packout of storage apples. Agricultural Experiment Station Research Report No. 147. Michigan State University, East Lansing, Michigan. 6 p.

Dhaliwal, R. R. 1970. Punch problem for an elastic layer overlying an elastic foundation. Int. J. Engng. Sci. 8:273-288.

Dhaliwal, R. S. and I. S. Rau. 1970. The axisymmetric Boussinesq problem for a thick elastic layer under a punch of arbitrary profile. Int. J. Engng. Sci. 8:843-856.

Fletcher, S. W., N. N. Mohsenin, J. R. Hammerle, and L. D. Tukey. 1965. Mechanical behavior of selected fruits and vegetables under fast rates of loading. Trans. of the ASAE 8(3):324-326, 331.

Fluck, R. C., and E. M. Ahmed. 1973. Impact testing of fruit and vegetables. Trans. of the ASAE 16(4):660-666.

Fridley, R. B., H. Gohlich, L. L. Claypool, and P. A. Adrian. 1964. Factors affecting impact injury to mechanically harvested fruit. Trans. of the ASAE 7(4):408-411.

Fridley, R. B. and P. A. Adrian. 1966. Mechanical properties of peaches, pears, apricots, and apples. Trans. of the ASAE 8(1):135-138.

Fridley, R. B., L. L. Claypool, J. H. Mehlschau. 1973. A new approach to tree fruit collection. ASAE Paper 73-1522.

Galin, L. A. 1961. Contact problems in the theory of elasticity. Department of Mathematics, School of Physical Sciences and Applied Mathematics, North Carolina State College. 233 p.

Gaston, H. P. and J. H. Levin. 1951. How to reduce apple bruising. Mich. State Univ., Agric. Exp. Stat. Special Bull. No. 374. East Lansing, Mich. 30 p.

Gent, A. N. and A. G. Thomas. 1963. Mechanics of foamed elastic materials. 7th Annual Technical Conference Proceedings. The Society of the Plastic Industry, Cellular Plastic Division. Section 2-A:p.1-8.

Gillespshe, F. L. and R. C. Scott. 1950. Bruising and apples. Ohio Agr. Exp. Sta. Res. Cir. 6, 8p.

Goldsmith, W. 1960. Impact--the theory and physical behavior of colliding solids. Edward Arnold Publishers. London. 369 p.

Green, H. C. 1962. The resistance of apples to bruising. J. Agric. Engng. Res. 7(2):155-157.

Hamann, D. D. 1967. Some dynamic mechanical properties of apple fruits and their use in the solution of an impacting contact problem of spherical fruit. Unpublished Ph.D. thesis. Dept. of Engineering Mechanics, Virginia Polytechnic Institute, Blacksburg, Virginia.

Hammerle, J. R. and N. N. Mohsenin. 1966. Some dynamic aspects of fruits impacting hard and soft materials. Trans. of the ASAE 9(4):484-488.

Hertz, H. 1896. Miscellaneous papers. MacMillan and Company, New York, N.Y.

Horsfield, B. L., R. B. Fridley, and L. L. Claypool. 1972. Application of theory of elasticity to the design of fruit harvesting and handling equipment for minimum bruising. Trans. of the ASAE 15:746-750.

Hughes, H. and L. J. Segerlind. 1972. A rapid mechanical method for determining Poisson's ratio in biological materials. ASAE Paper 72-310.

Kantorovich, L. V. and V. I. Krylov. 1958. Approximate Methods of Higher Analysis. Interscience Publishers, Inc., New York, N.Y. 681 p.

Keer, L. M. 1964. The contact stress problem for an elastic sphere indenting an elastic layer. J. Mech. Appl. Math. 4,423.

Kosten, C. W. and C. Zwikker. 1939 Mededelingen van de Rubber - stichting. Rubber Chem. Tech., 12:105.

Krylov, V. I. 1962. Approximate calculation of integrals. The MacMillan Co., New York, N.Y. p. 130-132, 347-352. 357 p.

Lebedev, N. N. and Ia. S. Ufliand. 1958. Axisymmetric contact problem for an elastic layer. Appl. Math. and Mech. 22:442-450.

Levin, J. H. 1970. Mechanization of fruit harvest--progress and impact. Proc. 18th Int. Hort. Cong. 4:387-393.

Ling, C. Y. and L. F. Whitney. 1975. Appendix. Analysis of spherical shell acted on by two concentric forces in opposite directions. Theory, Determination and control of physical properties of food materials. Chokyun Rha (ed.) Ch. 9, p. 189-196. D. Reidel Publishing Co., Dordecht, Holland.

Little, R. W. 1973. Elasticity. Prentice-Hall, Inc., Englewood Cliffs, N. J. 431 p.

Luré, A. I. 1964. Three-dimensional problems of the theory of elasticity. Interscience Publishers, New York, N.Y. 493 p.

Megilley, B. W., H. P. Rasmussen, and D. H. Dewey. 1968. Fruit characteristics affecting apple orientation in water. Quart. Bull. Mich. Agric. Exp. Station 50(4): 527-537. East Lansing, Michigan.

Meinecke, E. A. and D. M. Schwaber. 1970. Energy absorption in polymeric foams. I. Prediction of impact behavior from Instron data for foams with rate-dependent modulus. J. Appl. Polym. Sci. 14:2239-2248.

Miles, J. A. 1971. The development of a failure criterion for apple flesh. Unpublished Ph.D. thesis. Dept. of Agricultural Engineering, Cornell University, Ithaca, N.Y.

Millier, W. F., G. E. Rehkugler, R. O. Pellerin, J. A. Thorp, and R. B. Bradley. 1973. A tree fruit harvester with an insertable multi-level catching system. Trans. of the ASAE 16(5):844-850.

Mohsenin, N. N. and H. Göhlich. 1962. Techniques for determination of mechanical properties of fruits and vegetables as related to design and development of harvesting and processing machinery. J. Agric. Eng. Res. 7(4):300-304.

Mohsenin, N. N. 1970. Mechanical properties of plant and animal materials. Vol. 1. Gordon and Breach Science Publishers, New York, N.Y. 734 p.

Mohsenin, N. N. 1971. Mechanical properties of fruits and vegetables. Review of a decade of research, applications and future needs. ASAE Paper 71-849.

Mohsenin, N. N., C. T. Morrow and L. D. Tukey. 1974. Design considerations for selection of cushioning materials. Unpublished Annual Report of Cooperative Regional Projects. The Pennsylvania State University, Agri. Exp. Sta., College Park, PA.

Muki, R. 1960. Progress in Solid Mechanics. Vol. 1. North-Holland, Amsterdam, Holland.

Nelson, C. W. and N. N. Mohsenin. 1968. Maximum allowable static and dynamic loads and effects of temperature for mechanical injury in apples. J. Agric. Engng. Res. 13(4):305-315.

Nielson, L. E. 1962. Mechanical properties of polymers. Reinhold Publishing Company, New York, N.Y. 274 p.

Otis, D. R. 1970. Thermal damping in gas-filled composite materials during impact loading. J. Appl. Mech. 37,38-43.

Perrelli, J. 1970. Method of harvesting fruit. U.S. Patent No. 3,496,705. February 24.

Rau, I. S. and R. S. Dhaliwal. 1972. Further considerations on the axisymmetric Boussinesq problem. Int. J. Engng. Sci. 10:659-553.

Rehkugler, G. E. 1968. Mechanical harvest of tender apple varieties. Unpublished paper. Annual Meeting of Maine State Pomology Society.

Rehkugler, G. E. and E. D. Markwardt. 1971.. An evaluation of limb padding to reduce damage in mechanical harvesting. Trans. of the ASAE 14(2):734-737, 741.

Rehkugler, G. E. and J. E. Throop. 1973. An optical-Mechanical bruised apple sorter. ASAE Paper 73-1526.

Rider, R. B. Fridley and M. O'Brien. 1973. Elastic behavior of a pseudo fruit for determining bruise damage to fruit during mechanized handling. Trans. of the ASAE 16(2):241-244.

Roberts, O. C. 1959. Causes and effects of mechanical injuries to McIntosh apples. Mass. Agr. Exp. Sta. Bull. 520. 39 p.

Rumsey, T. R. and R. B. Fridley. 1974. Analysis of viscoelastic contact stresses in agricultural products using a finite element method. ASAE Paper No. 74-3513.

Rusch, K. C. 1969. Load-compression behavior of flexible foams. J. of Appl. Polym. Sci. 13:2297-2311.

Rusch, K. C. 1970a. Load-compression behavior of brittle foams. J. of Appl. Polym. Sci. 14:1263-1276.

Rusch, K. C. 1970b. Energy absorbing characteristics of foamed polymers. J. of Appl. Polym. Sci. 14:1433-1477.

Sarig, Y. 1975. Bruise reduction potential for foam-encapsulated fruit as related to mechanical harvesting. ASAE Paper 75-6506.

Schertz, C. C. and G. K. Brown. 1966. Fundamental considerations in citrus harvest mechanization. ASAE Paper 66-131.

Schmidt, E. D. 1962. Apparatus for the dynamic evaluation of cushioning materials. ASAE Paper 62-322.

Schomer, H. A. 1957. Bruising of apples: where does it occur and how can it be minimized? Wash. State Hort. Assoc. Proc. 53:129-131.

Schwaber, D. M. and E. A. Meineke. 1971. Energy absorption in polymeric foams. II Prediction of impact behavior from Instron data for foams with rate dependent modulus. J. of Appl. Polym. Sci. 15:2381-2393.

Schwaber, D. M. 1973. Impact behavior of polymeric foams: A review. Polym. Plast. Technol. Eng. 2(2):231-249.

Segerlind, L. J. 1976. Applied Finite Element Analysis. John Wiley and Sons, Inc. New York, N.Y. (in press).

Simpson, J. B. 1971. Forces, pressures, and apple damage during cushioned impact. Unpublished Ph.D. thesis. Department of Agricultural Engineering, Cornell University, Ithaca, N.Y.

Skochdopole, R. E. and L. C. Rubens. 1965. Prediction of stress-strain behavior for closed-cell foams. J. Cellular Plast. 1:95.

Sneddon, I. N. 1951. Fourier transforms. McGraw-Hill Book Company, Inc., New York, N.Y. 542 p.

Stern, R. K. 1953. The FPL dynamic compression testing equipment for testing package cushioning materials. U.S.D.A., Forest Service, Forest Products Laboratory, Madison 5, Wisconsin. Report No. 2120.

Tene, Y., D. Hial, and M. Nivon. 1973. Mechanical harvesting of apples in a damped medium. Unpublished Comprehensive Report. The Agricultural Engineering Institute, Bet-Dagan, Israel. 18 p.

Tennes, B. R. and J. H. Levin. 1972. Feasibility study on mechanical apple harvesting in Michigan. Trans. of the ASAE 15(5):890-893.

Tennes, B. R., L. J. Segerlind, and C. Burton. 1974. How handling and storage affect processing quality and yield of mechanically damaged apples. Trans. of the ASAE 17(1):49-51.

Timoshenko, S. P. and J. N. Goodier. 1970. Theory of elasticity. 3rd Edition, McGraw-Hill Book Co., New York, N.Y. 567 p.

Wennergren, B. E. and W. A. Lee. 1961. The economic aspects of bruising in the apple processing industry. Penn. Agr. Exp. Sta. Bull. 675. 20 p.

Whitney, J. D., N. N. Mohsenin, and L. D. Tukey. 1963. An elevating mechanical harvester for apple trees trained to the plateau system. Proc. Amer. Soc. Hort. Sci. 83:175-184.

Whitney, L. F. 1971. Evaluation of foam plastic globules as an energy absorbent for harvesting fruit. Proc. Nat. Agric. Plastics Conference. Chicago, Ill. 206-213.

Whitney, L. F. 1975. Alteration of apparent physical properties of fruit for harvest. Theory, Determination and Control of Physical Properties of Food Materials, ChoKyun Rha (ed.), Ch. 9, p. 181-189. D. Reidel Publishing Co., Dordecht-Holland.

Wilsea, M., K. L. Johnson and M. F. Achby. 1975. Indentation of foamed plastics. Int. J. Mech. Sci. 17: 457-461.

Wright, R. S. and W. E. Splinter. 1967. The mechanical behavior of the sweet potato under slow loading rates and impact loading. Trans. of the ASAE 12(5):765-770.

Zienkiewicz, O. C. 1971. The finite element method in engineering science. McGraw-Hill Book Company, New York, N.Y. 521 p.

# APPENDICES

Appendix 1. Apparent elastic modulus ($E_f$)[$N/cm^2$] of cylindrical samples of U-F foam[1] samples[2] subjected to a compressive load as a function of (L/D) ratio.

| Sample No. | Apparent elastic modulus $N/cm^2$ | |
|---|---|---|
| | L/D = 2 | L/D =1 |
| 1 | 83.13 | 97.33 |
| 2 | 78.12 | 95.70 |
| 3 | 102.51 | 87.66 |
| 4 | 90.68 | 65.40 |
| 5 | 92.22 | 72.55 |
| 6 | 84.31 | 83.66 |
| 7 | 104.23 | 78.19 |
| 8 | 69.45 | 62.55 |
| 9 | 73.48 | 92.19 |
| 10 | 69.31 | 88.10 |
| 11 | 89.71 | 99.51 |
| 12 | 93.68 | 103.24 |
| 13 | 95.42 | 89.10 |
| 14 | 82.78 | 90.50 |
| 15 | 70.50 | 84.14 |
| 16 | 68.41 | 79.46 |
| 17 | 77.73 | 78.31 |
| 18 | 84.39 | 87.37 |
| 19 | 66.91 | 100.54 |
| 20 | 100.00 | 73.09 |
| 21 | 82.91 | 74.44 |
| 22 | 71.49 | 91.78 |
| 23 | 91.11 | 86.29 |
| 24 | 81.44 | 99.62 |
| 25 | 30.33 | 88.63 |
| $\bar{x}$ | 83.37 | 85.95 |
| $\sigma$ | 11.04 | 10.88 |

A t-test incorporating the given data confirmed the null hypothesis of no significant (at a 95% significance level) difference between the two samples.

[1]Foam density - 0.0112 $gr/cm^3$.

[2]Radius of the sample (R) - 2.54 cm.

Appendix 2. Apparent elastic modulus ($E_f$)[N/cm$^2$] of U-F foam samples subjected to a compressive load, as a function of the loading rate.

| Sample No. | Loading Rate (cm/min) | | | | |
|---|---|---|---|---|---|
| | 2.54 | 5.08 | 12.7 | 25.4 | 50.8 |
| 1 | 81.48 | 77.63 | 91.43 | 82.45 | 105.42 |
| 2 | 75.63 | 89.54 | 79.81 | 72.44 | 93.41 |
| 3 | 77.88 | 71.55 | 88.84 | 98.55 | 89.45 |
| 4 | 84.93 | 70.88 | 70.51 | 71.41 | 100.33 |
| 5 | 100.15 | 85.55 | 98.43 | 75.93 | 95.42 |
| 6 | 87.60 | 94.33 | 87.55 | 90.41 | 82.32 |
| 7 | 91.54 | 87.51 | 90.43 | 81.34 | 84.38 |
| 8 | 76.42 | 79.38 | 74.32 | 77.76 | 91.43 |
| 9 | 79.90 | 90.11 | 89.90 | 89.19 | 81.12 |
| 10 | 69.53 | 74.58 | 72.11 | 70.49 | 78.41 |
| $\bar{x}$ | 82.51 | 82.11 | 84.34 | 80.99 | 90.17 |
| $\sigma$ | 8.86 | 8.37 | 9.49 | 9.30 | 8.76 |

Incorporating Duncan's new Multiple-Range test for comparing each loading rate mean with every other loading rate mean.

For the 5% significance level only the high loading rate (50.8 cm/min) was found different from the other loading rates.